MITIGATING BIOFILM GROWTH THROUGH THE MODIFICATION OF CONCRETE DESIGN AND PRACTICE

A Thesis
Presented to
The Academic Faculty

By

Jonah C. Kurth

In Partial Fulfillment
of the Requirements for the Degree
Master of Science in Civil Engineering in the
School of Civil & Environmental Engineering

Georgia Institute of Technology

May 2008

MITIGATING BIOFILM GROWTH THROUGH THE MODIFICATION OF CONCRETE DESIGN AND PRACTICE

Approved by:

Dr. Kimberly Kurtis, Advisor
School of Civil & Environmental Engineering
Georgia Institute of Technology

Dr. Patricia Sobecky
School of Biology
Georgia Institute of Technology

Dr. Lawrence Kahn
School of Civil & Environmental Engineering
Georgia Institute of Technology

Date Approved: April 1, 2008

ACKNOWLEDGEMENTS

I would like to thank my fiancée, Betsy, who was willing to travel with me to Atlanta so I could pursue a degree in "moldy concrete". I must thank my advisor, Dr. Kurtis, without whom none of this work would have been accomplished. She was the best advisor possible for me as a graduate student, letting me run with the project but keeping me on course. Dr. Sobecky was a great biology co-advisor, willing to try out our crazy concrete ideas on the world of microbes. I would also like to thank Dr. Kahn for reading this thesis and offering his advice on field investigations.

David Giannantonio was the entire student bio-half on the project. With as little as I knew about biology (and he knew about concrete), this thesis could not have been completed without his work. Thanks to him, I have used more bleach and ethanol in the last few months than I have (or will) in my entire life. Frédéric Allain was an invaluable help in the summer, casting hundreds of tiny mortar tiles with me (and bringing a French perspective on our work). I would especially like to thank him for hosting me in Paris on the way to a photocatalytic conference. I would like to thank Robert Moser for traveling across the state in various Jeeps, just to drill tiny holes in the side of GDOT structures. I would also like to thank Dr. David Scott from GT-Savannah for taking Robert and I on a boat to survey the oceans around Savannah. Andrea Mezencevova was a great help at the close of this project, helping wrap up XRD, TGA, and (2686!) Rockwell Hardness measurements. I would like to acknowledge all the friends I've made during my short time at Georgia Tech, especially my office mates in Mason 508.

Parts of this thesis are based upon work supported by the National Science Foundation under Grant No. DMR-0115691.

TABLE OF CONTENTS

LIST OF TABLES

LIST OF FIGURES

LIST OF SYMBOLS AND ABBREVIATIONS

ASTM	American Society for Testing and Materials
DNA	deoxyribonucleic acid
ESEM	environmental scanning electron micrography
f_c'	compressive strength
FOV	field of view
GDOT	Georgia Department of Transportation
OPC	ordinary Portland cement
OTU	operational taxonomic units
RFLP	restriction fragment length polymorphism
RH	relative humidity
SCM	supplementary cementitious material
TG/DTA	thermogravimetric / differential thermal analysis
UV	ultraviolet
w/cm	water-to-cementitious materials ratio
XRD	X-ray diffractometry
λ	wavelength
σ	standard deviation

SUMMARY

Biological growth, or biofilm formation, on concrete is often overlooked in structural design and evaluation. These living colonies, which look like dirt or discoloration, are found growing on a multitude of surfaces in Georgia. This research project sampled a variety of biofilms to determine the type of organisms through both DNA and cultural analysis techniques. The primary components in all biofilms sampled were fungi and bacteria, with the variety and number of different species changing between geographic locations.

An experimental program was devised with two goals: develop a laboratory test that simulates natural growth conditions, and determine what properties of concrete affect biofilm formation. Rapid biofilm growth was best achieved by a nutrient rich "rain", which represents a potential source of nutrients for microbes in field conditions. Small mortar tiles, varying in w/cm, surface roughness, cement type, and air content, were selected to represent concrete surface. In addition, a cement with TiO_2 was tested under simulated daylight for a photocatalytic effect.

The results of the experimental program showed that many concrete properties affected biofilm formation. Biofilm formation was found to correlate positively with w/cm and surface roughness. Photocatalytic cement greatly decreased biofilm formation when exposed to UV light. Changing cement source, air content, and adding supplementary cements produced little change in growth levels. This research showed that biofilm growth occurs naturally on concrete surfaces, but can likely not be prevented. However, lowering w/cm, decreasing surface roughness, and adding photocatalytic cements are all ways to mitigate biofilm formation.

CHAPTER 1:

INTRODUCTION

1.1. Motivation

Biodeterioration of concrete is an important concern for the global construction industry, which demands longer service life due to the increasing initial cost of construction. As recently as 10 years ago, aesthetic deterioration (i.e. biodeterioration, biofilm formation) in the form of dark discolorations was not seen on the surface of concrete highway bridges in Georgia. Compare the beam in the center of Figure 1.1, photographed in 1997, to the same beam in Figure 1.2, photographed in 2007. This bridge structure was built in 1983, less than 25 years ago. This aesthetic deterioration could be either rapid or slowly progressing with an unknown initiating event. Furthermore, the agents and mechanism of deterioration are unknown and any structural impact on the concrete beneath the coating is uncertain.

Figure 1.1– Bridge for I-85 over Buford Highway (1997)

Figure 1.2 - Bridge for I-85 over Buford Highway (2007). White area on left span has been repainted.

The past 50 years saw an explosion of infrastructure construction across the country. The next 50 years will see the need for maintenance and upkeep of this now aging infrastructure. For example, capital outlays for the construction of transportation structures constituted 75% of the Georgia Department of Transportation (GDOT)'s annual budget in 2004. Structural concrete can be more attractive for structural costs than steel due to its lower life cycle costs [23]. Unlike steel, it does not require regular painting, and, with proper mixture design and construction practices, is assumed to last for its intended service life with minimal maintenance.

1.2. Purpose

The objectives of this investigation are to determine the character (chemical, physical, or biological) of the deterioration on concrete highway infrastructure, to determine its effects on durability and service life, and to prevent discoloration on future construction. To this end, multiple sites were surveyed for material and environmental factors, biological samples were collected and identified, and accelerated laboratory tests were performed to examine the susceptibility of concrete to biofilm formation. Research

was undertaken to determine the microbes present throughout the state's stained concrete infrastructures, to better understand the processes involved in microbial colonization and biofilm growth on concrete, to investigate the effect of the microbial activity (when found) on performance, and to identify methods involving materials selection, proportioning, and construction practices which reduce the susceptibility of concrete structures to biofilm formation and growth.

1.3. Organization

Chapter 2 of this thesis is a literature review of existing research on identification of biofilm on concrete and any results on its effect on concrete properties. Chapter 3 details the initial investigation and exploration of the occurrence of discoloration and how it relates to both concrete properties and environmental conditions. Chapter 4 details the growth pathway of the biological entities ultimately found to be responsible for the discoloration. Chapter 5 details the results of the laboratory tests used to determine the relation between concrete properties, environmental conditions, and biological growth. Chapter 6 presents the conclusion of the research project and gives recommendations to mitigate future biofilm growth.

CHAPTER 2: LITERATURE REVIEW

2.1. Investigating Concrete Biodeterioration

The first published research on concrete biodeterioration appears to have been done by the Australian researcher Parker in 1945, who investigated the influence of microbes on the corrosion of reinforced concrete sewer pipes [49]. This research was the first to propose that sulfuric acid formation in sewers was due to biological processes. The microbial strains found in this research were shown to deteriorate concrete rapidly in a hydrogen sulfide atmosphere [50] and were shown to oxidize elementary sulfur, thiosulfate, and hydrogen sulfide to produce sulfide, sulfuric acid, and tetrathionate [51]. Published research in concrete biodeterioration almost ceased until the early 1980s. It was suggested the 1972 National Pollution Discharge Elimination System (NPDES) regulation of toxic compounds stopped the inhibition of microbial growth in sewers [22]. Research by Milde et al. in Germany in 1983 showed that a hydrogen sulfide atmosphere was necessary for the metabolism of *Thiobacilli spp.* previously identified. Supplying oxygen to the sewer resulted in an increase of the concrete pH and a decrease in the number of *T. thiooxidans* [42]. A subsequent review by Boon in 1995 indicated that aerating sewers was one of the best ways to mitigate H_2S formation and subsequent biodeterioration [7].

The first research to examine microbial deterioration of concrete outside of a sewer environment was performed around 1991 by Sand and Bock [54]. They identified nitrifying bacteria, such as *Nitrosomas* or *Nitrobacter* spp., which are able to reduce ammonia or nitrite to nitric acid, that had been discovered on concrete structures and natural stone buildings. Tests performed by these researchers indicated material weight

loss of 3% in 12 months from nitric acid production under optimum growing conditions. This research also hypothesized that reducing ammonia and nitric oxide emissions would minimize deterioration caused by these microbes [54].

Fungi were not examined in published research as biodeterioration agents for concrete until research by Gu et al. in 1998. Although the *Fusarium* fungus they tested was a contaminant in a project meant to examine *Thiobacillus intermedius*, they showed that the *Fusarium* sp. caused greater material weight loss and more Ca^{2+} release than the bacteria [22]. A review of available literature by Gaylarde and Morton in 1999 agreed that very little research had been done on fungal corrosion of concrete and aggregated the results with biodeterioration of stone surfaces [17]. The same types of stone investigated (limestones and sandstones) are present in concrete as aggregate, but this compilation of results does not give an accurate picture of the importance of cement paste to concrete as a material. For example, an investigation by Housewright et al. attempted to show differences in aggregate content to bioreceptivity but instead concluded that the majority of fungal growth occurred on the cement paste [24].

In 2000, Kawai et al. presented research that tested the deterioration potential of two aerobic fungi (*Penicillum expansum* and *Aureobasidium pullulans*) and aerobic bacteria (*Bacillus subtilis* and *Escherichia coli*), microbes which were not selected from actual concrete specimens. The same year, research by Shirakawa et al. suggested that heterotrophic microbes could use hydrocarbons, such as diesel fuel, as an energy and carbon source and degrade concrete by their metabolic processes, which included possible sulfuric acid production from sulphur oxidizing bacteria [56]. The first research that tested the relationship of w/cm to biofilm coverage was done by Dubosc et al. in

France [15]. Using algae and *Cyanobacteria* isolated from concrete walls, they determined that a lower w/cm led to a decreased amount of surface coverage [15]. A review by Gaylarde et al. in 2003 pointed out that biofilm formation on stone and concrete building materials in aerobic environments was not fully investigated. Acid production by some environmental microbes had been shown, but their effect on actual materials had not been shown. Similarly, a colonization sequence of phototroph to heterotroph has been proposed, but not observed either in nature or in the lab [19].

Research published by Pinhiero and Silva in 2003 tested biodeterioration by the fungus *Cladosporidium sphaerospermum*. They inoculated carbonated mortar tiles with media containing fungus and found that gypsum had formed and that some calcium carbonates had solubilized. Shirakawa reported on the development of a test method to assess the bioreceptivity of mortars to fungus. The research indicated that high water activity, which is a measure of moisture content, low pH (< 9) and additional nutrients in the form of Saboraud Dextrose media were necessary for fungal growth [55]. A study by Pinheiro and Silva in 2004 showed images of concrete biodeterioration that are aesthetically similar to the biodeterioration seen for some of this investigation, as compared in Figure 2.1 and Figure 2.2 [53]. Their research also compared surface roughness for mortars and determined that a smoother mortar was less susceptible to growth; however, the surface roughness was unquantified and left as an aesthetic comparison.

Research on material degradation has shown that microbes' growth or metabolic activities can result in deterioration of concrete. The most typical form of degradation occurs by acid production as a natural part of microbial metabolism. However, much of

the aerobic environment research on concrete biodeterioration has focused on culturing and mostly morphological descriptions of microbes present and has assessed deterioration only by single species. Identification of microbes on concrete by DNA methods, the life cycle of microbes on concrete and the influence of multiple microbial species on biodeterioration have not been researched.

Figure 2.1 - Biodeterioration in Brasilia, Brazil [53]

Figure 2.2 - Biodeterioration on concrete abutment near LaGrange, GA

2.2. Weathering

Biofilm growth is an important factor to consider in the service life of concrete structures. It is estimated that as much as 30% of weathering of concrete and stone construction materials is due to biological sources [14]. Weathering of concrete can either be increased or initiated by biological sources. As a result of the presence of microbes on the surface of the concrete, their weathering effects, including production of acids, chelating compounds, and physical penetration are concentrated and localized [12]. In general, a multitude of organisms live together on a concrete surface and obtain nutrients from either the substrate or other microbial sources within the community [52].

2.3. Biofilm Diversity

Biofilms on concrete are typically composed of *cyanobacteria*, algae, fungi, heterotrophic bacteria, and occasionally protozoa [19]. *Cyanobacteria* are typically more prevalent than algae in drier conditions. Phototrophic algae typically need moisture conditions of a surface to be high and constant because they are less resistant to desiccation. Research by Crispim, Gaylarde, and Gaylarde demonstrated that the number and type of species present in a biofilm colony depends more on the specific building sampled than the annual variation in temperature and precipitation [12]. Typically a wide variety of organisms is found growing on stone and concrete buildings, of which only some have biodeterioration potential. For example, 71 bacterial isolates alone were obtained from five buildings, both unpainted and painted stone, over the course of three sampling periods in a study by Kiel and Gaylarde [28]. However, only three of these isolates were considered to have strong biodeterioration potential, due to these isolates' acid and surfactant production on media.

This review considers three types of microorganisms typically implicated in concrete biodeterioration, cyanobacteria, heterotrophic bacteria, and fungi. DNA analysis revealed the presence of all of these microbes at the sites examined for this research project. Other microbes, such as algaes, which have been implemented in biodeterioration were not found at any site and therefore will not be covered.

2.3.1. Cyanobacteria

Two orders of cyanobacteria, *Chamaesiphonales* and *Pleurocapsales*, reproduce through production. These spores help the species in these orders resist long periods of desiccation and/or high heat, by remaining dormant until better environmental conditions prevail [66]. *Cyanobacteria* are also resistant to high levels of UV radiation due to the dark pigment they produce. Unlike heterotrophic bacteria, they do not require an organic source for energy or growth, because they are able to use sunlight and atmospheric CO_2. Their desiccation resistance enables them to grow in very difficult locations, such as the high, hot desert of Arches National Park, Utah [11].

Cyanobacteria could contribute to the biodeterioration of concrete in three different ways. Sand and Bock postulated that the increase in water content near a biofilm colony, due to its hydrophilic compounds, result in additional weathering, due to effects such as freeze-thaw and uneven salt concentrations [54]. Second, microbes deposit $CaCO_3$ when exposed to light and solubilize it in the dark, creating crystals of calcium salts which causes expansive pressure. However, their primary role may be as a food source for heterotrophic organisms that produce acid as they decompose cyanobacteria [11]. For this reason, cyanobacteria are sometimes considered primary colonizers, or the first microbes to successfully grow on a surface. *Cyanobacteria* were

detected by DNA extraction at all sites in this research, but their detection alone is not proof of their role as a primary colonizer.

2.3.2. Heterotrophic Bacteria

Heterotrophic bacteria are chemolithotrophs (reducing carbon, sulfur or nitrogen for energy and inorganic carbon for growth) or chemoorganotrophs (using organic carbon for both energy and growth). The necessity of organic, sulfurous, or nitrogen compounds requires that they obtain these resources from places other than the concrete itself, which contains primarily inorganic calcium and silicon compounds. For example, if a heterotrophic bacteria is a nitrogen fixer, they could get sulfur and nitrogen compounds from the air.

Heterotrophic microbes affect concrete through chemical and physical means. Chemical attack of concrete occurs through metabolic processes in the microorganisms. Hydrolytic enzymes and chelating produced by fungi or bacteria break down mineral structures, such as calcium carbonate, monosulfates, and calcium-alumino-ferrite compounds which are components in concrete. Cells can produce agents called siderophores that aggressively bind to iron to bring it into the cell, of which one common siderophore is hydroxamic acid. These acids are used primarily to retrieve micronutrients for the cell, such as iron, calcium, and trace heavy metals needed for metabolic processes [36]. According to research by Perry et al., exopolysaccharides released by alkaphilic (pH range 8.5-10) bacteria aggressively bind calcite components, contributing to early deterioration of fresh limestone [60]. Additional acid production by fungi and bacteria as results of cellular respiration can dissolve $Ca(OH)_2$ and other parts of cement paste, promoting deterioration of concrete microstructure [19].

2.3.3. Fungi

Like heterotrophic bacteria, fungi are either chemolithotrophs or chemoorganotrophs. Fungi have been shown to be some of the more destructive microbes to concrete. Similarly to cyanobacteria, they are resistant to low moisture and high heat conditions, and also have been shown to be tolerate saline environments. An experiment by Kiel and Gaylarde showed that a variety of unidentified bacteria and fungi from buildings fared poorly in a medium of 15% salt (seawater is 3.5% salt), with the exception of a brown pigmented fungus, morphologically identified as a *Cladosporidium* sp. [29]. In a study on concrete specimens, Gu et al. showed that fungi caused more damage in terms of material loss than bacteria under the same environmental conditions [22]. It was hypothesized that the hyphae of the fungi grow into the pore structure of the cement paste, widening the pores and increasing the ability of deleterious components to migrate inward. However, no quantification of this effect has been demonstrated.

2.4. Mitigation

Many mitigation strategies exist for biofilm growth on buildings. However, few have shown good long term performance. Mitigation methods can be split into two methods, active and passive. Active measures include biocides that disrupt growth, but often lose effectiveness over time due to leaching and chemical degradation. Passive measures include physical changes that can only make growth less likely to occur.

2.4.1. Active measures

Biocides and physical cleaning are two active ways to reduce biofilm growth. However, these active treatments are not long term solutions, as both often require reapplication to remain effective. In a study of a painted masonry building in Brazil by

Shirakawa et al, the side was soaked with 2% hypochlorite and then pressure washed to remove existing biofilm. The building was then covered with two paints, one containing a biocide, carbendazin, N-octyl-2H-isothiazolin-3-one and N-(3,4-dichlorophenyl)N,N-dimethyl urea at 0.25% by wt., and another without. Tests showed that the building remained relatively free from microbial growth for both methods for approximately 35 weeks. After that time, microbial growth increased on both types of paint [57].

Photocatalysts are a third type of active measure that can be used to mitigate growth. A photocatalyst works by absorbing light energy to produce an excited electrical state. This charge then reacts with other compounds that approach it, often breaking down and modifying the chemical structure. The photocatalyst remains unchanged by the reaction, and is free again to absorb light energy and regain an excited state [34].

The most commonly studied photocatalyst for binding with Portland cement is titanium dioxide (TiO_2) in its anatase form. Other photocatalysts, such as tungsten oxide (WO_3), exist but are less suited to use for microbial growth mitigation. TiO_2 is well suited to applications with concrete for several reasons. TiO_2 particles can be ground very finely (<30 nm), leading to good dispersion in a cement mix. TiO_2 affects hydration behavior of Portland cement in a few ways. In concentrations of less than 2% of cement by weight, early hydration is inhibited. Later hydration, after approximately 2 days, proceeds more rapidly and is higher than that of cement alone. The inclusion of more than 2% TiO_2 accelerates all periods of hydration [26]. It has also been shown that the inclusion of TiO_2 in cement paste increases the compressive strength by about 20% [32].

2.4.2. Passive measures

Architectural considerations play a large role in the appearance of biofilm growth. Runoff patterns from rain or driplines caused by poor drainage are just two examples that greatly influence growth patterns. A study by Shirakawa that tested the effectiveness of washing and bleaching a building concluded that the architectural details played a larger role in final appearance than the biocide. They found that grooves in the façade harbored dirt and fungal spores, and runoff patterns beneath windows increased localized growth [57].

Material and surface changes are two more possible passive measures. Research by Pinheiro and Silva indicated that smoother mortar surfaces lead to reduced fungal growth; however, this effect was not quantified [53]. Decreasing the w/cm in concrete has also been shown to be effective for reducing algal colonization [15].

CHAPTER 3:

SAMPLE COLLECTION AND ANALYSIS

3.1. Introduction

Visual evidence, generally in the form of gray to black surface staining, suggests that biofilm and microbial growth occur commonly on the concrete infrastructure, including (but not limited to) bridges and retaining walls, throughout the state of Georgia, USA. These biological communities reduce the aesthetics of public structures and, as a result, affect public perception regarding the quality of construction and the maintenance on such structures. While researchers have previously examined staining caused by microbial growth on concrete structures, less information is available on the site conditions and materials characteristics required for colonization and sustained growth or on economical and robust methods for avoidance and mitigation [12],[15].

Affected bridges and concrete structures part of the Georgia highway system were sampled; sites were selected to assess the influence of different regions (e.g., rural vs. urban, coastal vs. mountainous) and growing conditions (e.g., variations in moisture, sunlight, pollution etc.) throughout the state. Sites were identified by visual inspection for growth in a location of interest. Characteristics of the concrete, including compressive strength, permeability, moisture content, and reflectance, were assessed in situ. Samples of microbial biofilm were obtained for identification by polymerase chain reaction (PCR) amplification and DNA sequencing. Samples of concrete powder were collected for further analysis by X-ray diffraction (XRD) and thermogravimetric / differential thermal analysis (TG/DTA).

3.2. Site Selection, investigation, and analysis

After visiting over twenty potential sites for sampling, and after obtaining preliminary data from ten sites, four sample sites were selected for an initial in-depth study based on geographic and climatic characteristics. These four sites were located near the cities of Atlanta, Gainesville, LaGrange, and Savannah, Georgia. Concrete at each of the sites exhibited dark and heavy coatings. A negative control site with no biofilm coverage was selected in Atlanta, GA.

3.2.1. Atlanta Site

The Atlanta site is located on GA-13 in Fulton County approximately 1000 ft south of GDOT bridge #121-0556-0. The concrete sampled was the south side of the barrier between GA-13 and Monroe Dr, as seen in Figure 3.1. A paint-like construction coating appeared to be covering the barrier. Figure 3.2 shows the uneven color and streaky nature of the biofilm. The biofilm could be removed easily by hand with a wire brush to reveal the concrete surface beneath.

Figure 3.1 - Overview of Atlanta Site

Figure 3.2 - Closeup of sampling location. Light color in the center of the picture is where biofilm has been removed by a wire brush

3.2.2. Gainesville Site

The Gainesville site is Brown's Bridge, GDOT bridge #117-0022-0, located on GA-369 and crossing Lake Lanier on the border of Hall County and Forsyth County. The biofilm sampled was on the concrete barrier on the east end of the bridge. The concrete was not covered by any painted coating. The biofilm coverage was heavier near the shore and dissipated as the bridge extended over the lake, as seen in Figure 3.3. The coverage on the south side of the bridge was generally lighter and streakier than the north side, as seen in Figure 3.4.

Figure 3.3 - Overview of Gainesville site, looking west over Lake Lanier

Figure 3.4 - Closeup of south side of bridge. Note streaky appearance of biofilm

3.2.3. LaGrange Site

The LaGrange site is located in Troup County on the bridge for the northbound lanes of I-185 to southbound I-85, GDOT bridge #285-0027-0. This site had the darkest and most uniform coverage of biofilm of all the sites visited, as seen in Figure 3.5. The concrete barriers appeared to be coated with a paint-like construction coating. The coating on the top of the concrete barrier appeared eroded but was not easily removed by a wire brush, as seen in Figure 3.6. The biofilm had a purplish hue and was easily removed with a wire brush.

Figure 3.5 - Overview of LaGrange site, looking south at the west barrier of the bridge

Figure 3.6 - Closeup of barrier. The light area has been scraped by a wire brush. Notice the deterioration of coating in the top right of the picture

3.2.4. Savannah Site

The Savannah site is located in Bulloch County, on the bridge for Ash Branch Church Rd over I-16, GDOT bridge #031-0089-0. The concrete for the abutment on the south side of the bridge was sampled at this site and was covered with a paint-like construction coating. The coating on this bridge showed the worst deterioration of all sites visited. Large portions of the coating were delaminating and flaking off the abutment. The concrete beneath the delaminated coating was covered in biofilm but did not appear to be deteriorated.

Figure 3.7 - Overview of Savannah site. The abutment sampled is immediately to the left of the image

Figure 3.8 - Closeup of abutment. Notice deteriorated coating

3.2.5. Atlanta Negative Control

The site chosen for negative control is the concrete barrier, shown in Figure 3.9, and is located in Cobb County, on the southbound lanes for I-75 for exit 259A to Cumberland Blvd. This ramp was constructed in 1999, and shows the very beginnings of biofilm growth, as seen in Figure 3.10 [69]. No construction coating is covering the concrete. Samples were taken from both the parts of the wall that showed the beginnings of growth as well as the parts that were clean.

Figure 3.9 - Negative control site in Atlanta. Sample area was the unpainted concrete at the base of the wall.

Figure 3.10 – Sample area of concrete wall with no biofilm present

3.2.6. Environmental Characteristics

The map in Figure 3.11 shows the location of all the sampling sites selected for analysis. Figure 3.12 is a topographic overlay for the state, showing that the site selection ranges from the north Georgia mountains to the Atlantic coastal plain below the Fall Line. Figure 3.13, Figure 3.14, and Figure 3.15 are overlays of precipitation, growing degree days, and annual mean temperature, respectively. Figure 3.16 is an overlay of hazardous air pollution and its relation to cancer risk. Accurate air emissions data is spotty for the state, so the cancer risk map was used as an indication of likely air pollution.

The climatic characteristics are listed in Table 3.1; the sites chosen represented close to the climatic extremes associated with the entire sample set of ten sites. In addition, hazardous air pollution as a measure of added cancer risk was examined for the county for each site.

Table 3.1: Summary of typical climate at sampling sites

Site	Growing Degree Days (C)[1]	Annual Precipitation (cm)	Elevation (m)	Air Pollution Index
Atlanta	2878	130	257	1000
Gainesville	2778	145	326	560
LaGrange	2948	135	226	380
Savannah	3192	122	27	300
Min. in Georgia	2455	117	0	240
Max. in Georgia	3681	218	1458	1100

1. Measure of cumulative annual temperature above 10 C. GDD for one day = $(T_{high} - T_{low}) / 2 - 10$

Figure 3.11 - Geographic map of Georgia

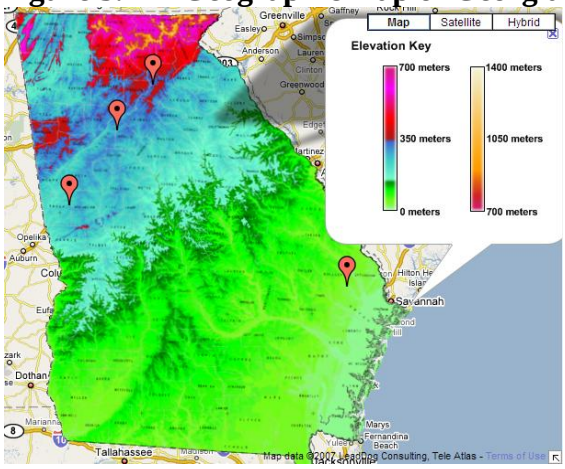

Figure 3.12 - Topographic map of Georgia

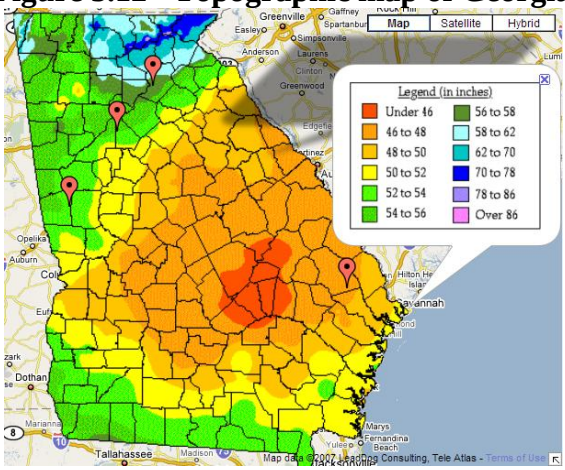

Figure 3.13 - Precipitation Map of Georgia

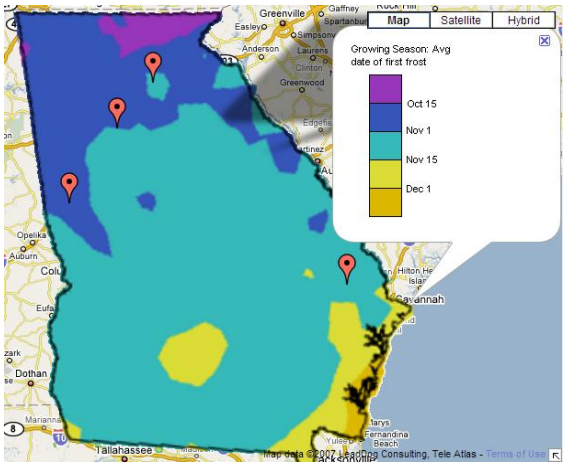

Figure 3.14 - Growing Degree Days Map of Georgia

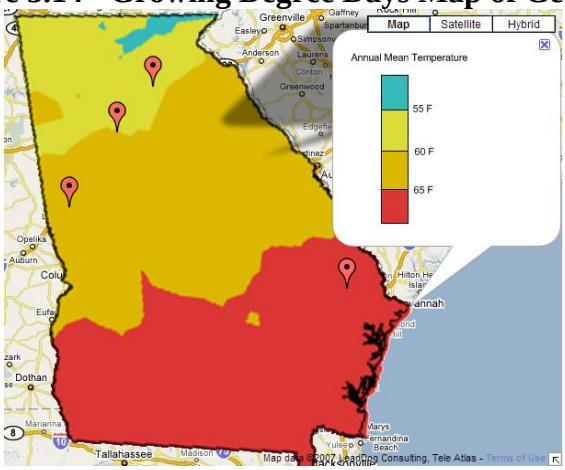

Figure 3.15 - Annual mean temperature map of Georgia

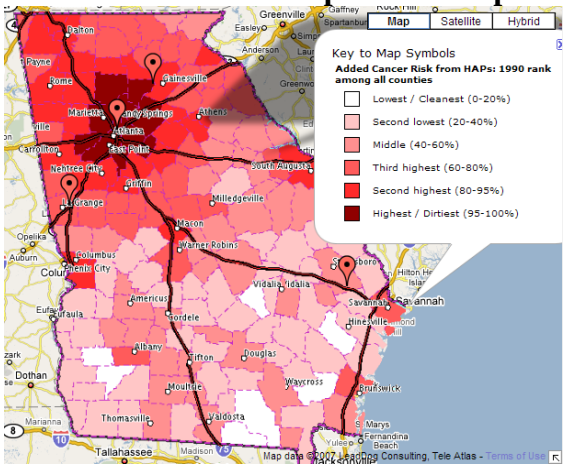

Figure 3.16 - Hazardous Air Pollution Map of Georgia

3.2.7. In situ concrete testing

Five different tests were carried out on each sampling site: reflectance, permeability, strength, moisture, and pH measurements. The test method used to measure reflectance is a modification of the ratio method employed in ASTM E 809-02, "Standard Practice for Measuring Photometric Characteristics of Retroreflectors". Light measurements were taken with a broad range lux meter, capable of measuring from 0 to 400,000 lux. Readings were first taken with the sensor facing the surface from a distance of less than 12". The second set of readings were obtained by placing the sensor near the surface and orienting toward the lighting source; for all cases tested, the light source was the sun. The reflectance (in %) was determined by the ratio of the average of the surface to the average of the source.

Concrete permeability was measured using the air permeability capability of a James Instruments P-6050 Poroscope Plus. The test method recommended by the manufacturer was used:

1. Drill at least three 3/8" holes to a depth of 1 ½" in the concrete.
2. Blow the loose dust out of the hole
3. Insert a specialized rubber plug into the hole
4. Insert a hypodermic needle through the rubber plug into the void between the plug and the concrete

The permeability of the material is measured by drawing a vacuum with the instrument in the space behind the rubber plug and measuring the time for the pressure to increase from 55 kPa to 50 kPa below atmospheric pressure. Additionally, the concrete powder from the holes drilled for the permeability measurement was collected in two stages. The first 10 mm of material from the hole was collected separately from the rest of the powder,

which was collected up to a depth of 40 mm, in order to gather samples both from the "exterior" and from the "interior" of the concrete.

Compressive strength was assessed non-destructively using a rebound hammer in general accordance with the procedure outlined in ASTM C 805-02, "Standard Test Method for Rebound Number of Hardened Concrete", with a minimum of 5 tests per site. It was not possible to take concrete cores for calibration from any of the sites, and, as a result, this data may not reflect the true compressive strength. Combined with the permeability measurements, the measurement was designed to be an overall indicator of concrete quality, not as a quantitative assessment of compressive strength.

Moisture content readings (in %) were taken with a James Instruments M-70 Aquameter from the surface. This instrument uses electromagnetic fields to detect water contents in non-metallic solids in a volume approximately 460 mm x 670 mm x 25 mm (LxWxD). It is calibrated specifically for concrete of standard density and was assumed that none of the surfaces tested were lightweight concrete.

A mixture of 1% phenolphthalein, 20% water, and 80% ethanol, was used to test freshly exposed concrete surfaces for carbonation. This mixture was sprayed onto the recently exposed surfaces created by performing the other tests were run and after the biological samples were taken. It was recorded if any parts of the surface turned pink, indicating a surface pH greater than 9 or whether they remained clear, indicating a pH less than 9 and a carbonated microstructure. Figure 3.17 shows the depth of carbonation for the concrete at the site in Atlanta, GA.

3.2.8. Microbial biofilm sampling

Surface samples of the biofilm at each site were collected by adhering various growth media to the concrete surfaces. Three types of media, sabouraud dextrose, malt extract, and nutrient agar were used. Samples were obtained by aseptically pressing strips of agar against the surfaces of the sites which were stored at 4ºC until DNA extraction and analysis was performed. Figure 3.18 shows an example of the material collected by this method.

Figure 3.17: Phenolphthalein indicator on freshly chipped surface (field of view ~10 cm)

Figure 3.18: Microbial sample on agar strip

3.3. Analysis of Samples

3.3.1. Concrete powder analysis

Samples of concrete powders obtained from each site were subjected to two additional types of analyses to characterize and contrast the composition of the material at the surface to a depth of 10 mm (exterior) with the material at a depth from 10 mm to 40 mm (interior). This was done to examine the influence of the microbial activity on composition and also to assess if particular compositions are more susceptible to microbial activity. First, x-ray diffractometry (XRD) was performed, using Cu-Kα radiation between 5 and 85 2θ°, on each powder sample to qualitatively identify crystalline compounds present. The powder samples were ground with an agate mortar and pestle prior to measurements. The finely ground powder was placed on a measuring

slide using a "side-loading" technique to limit bias and improve the randomness of crystal face orientation.

Thermogravimetric / differential thermal analysis (TG/DTA) was also performed on the collected concrete powders over a temperature range from 25 to 900^{o} C to determine the amounts of calcium hydroxide ($Ca(OH)_2$) and calcium carbonate ($CaCO_3$) present. Measurements were made using aluminum oxide ceramic crucibles. The percentage of carbonated $Ca(OH)_2$ was calculated for each site, using procedures and the model outlined by Bhatty [6] and shown in Equation (3.1).

$$Free\ Ca(OH)_2 = 4.11 * (Loss\ Ca(OH)_2\ peak) + 1.68 * (Loss\ CaCO_3\ peak) \quad \textbf{(3.1)}$$

An estimated age of the concrete was determined based upon the relative amount of $CaCO_3$ present at the surface. This was then compared to the actual age of the structure from construction records, both to determine if the biofilm was significantly increasing the degradation rate of $Ca(OH)_2$, and also to determine the influence of carbonation on the propensity for microbial activity.

3.3.2. Microbial analysis

The exposed sections of the agar strips were subsequently transferred to sterile microcentrifuge tubes for DNA extraction and purification using a soil DNA isolation kit (Mo Bio Laboratories, Inc.). Purified DNA was subsequently subjected to polymerase chain reaction (PCR) in order to amplify bacterial and fungal genes appropriate for phylogenetic analysis. The small subunit (16S) ribosomal DNA, since its initial use and analysis by Woese and colleagues [71] has long been the "gold standard" taxonomic

marker for bacteria despite the recent use of new genes [9]. The primers 27F and 1522R for 16S rDNA were used to identify and analyze bacteria in this study [38]. To identify the fungi diversity present in the microbial community the internal transcribed spacer (ITS) regions of fungal rRNA genes was targeted, using ITS1 and ITS4 primers [67]. The ITS region is an increasingly used region for identification of fungal species [62], [41].

Following their amplification, the genes chosen for phylogenetic analysis were inserted into a plasmid vector for transformation into electrocompetent *Escherichia coli* (Invitrogen), which were then separated out by individual colonies. This allowed for individual organisms' genes to be separated from the pooled DNA, as each clone (represented by a colony) should only contain one copy of the cloned rRNA gene. The DNA cloned into each colony (200 colonies for each gene, 50 per site) was then amplified for subsequent digestion by restriction enzymes. The resulting DNA fragments were then separated by size via electrophoresis on 2.0% agarose gels. 16S rRNA was double digested with HhaI/MspI, and ITS rRNA were double digested with HaeIII/RsaI (Promega). The restriction fragment length polymorphism (RFLP) patterns generated were used to group the cloned genes into operational taxonomic units (OTUs) [43],[44]. Representatives from each OTU were then sequenced at the University of Nevada Genomics Center (Reno, Nevada) using a Prism 3730 DNA Analyzer (Applied Biosystems) and the Georgia Tech Genomics Core facility (Atlanta, GA) using a Prism 3100 Gene Analyzer (Applied Biosystems). Sequences were subjected to a BLAST (Basic Local Alignment Search Tool) search against the National Center for

Biotechnology Information (www.ncbi.nlm.nih.gov) online gene database to determine taxonomic classification.

3.4. Results and Discussion

3.4.1. Visual appearance and concrete properties

Linear correlations between visible growth, measured concrete properties, (compressive strength, moisture content, permeability, and reflectance), and climatic factors (annual precipitation, growing degree days, air pollution, and elevation) were examined. Sites were ranked on a scale from 0 to 5, with 0 representing no visible biofilm and 5 representing dark and uniform coverage. This method is similar to ASTM D-3274, "Standard Test Method for Evaluating Degree of Surface Disfigurement of Paint Films by Microbial (Fungal or Algal) Growth or Soil and Dirt Accumulation." A summary of correlation coefficients and R^2 values can be seen in Table 3.2 along with the significance level at which the coefficient is not rejected as zero.

Table 3.2. Biofilm and concrete property correlation

	Correl. Coef.	R^2	*P-value*
Surface Factors			
Reflectance	-0.54	0.30	*0.01*
Moisture	-0.49	0.24	*0.01*
Strength	-0.42	0.18	*0.08*
Permeability	0.003	0.00	*0.99*
Environmental Factors			
Annual Precipitation	-0.18	0.03	*0.38*
AADT (2004)	-0.13	0.017	*0.55*
Elevation	0.08	0.01	*0.71*
Growing Degree Days	-0.057	0.003	*0.787*
Annual Mean Temp	*-0.02*	*0.00*	*0.93*

Negative correlations indicate that as a measured property decreases, the visible amount of biofilm increases. It was found that reflectance, moisture, and strength show the significant anti-correlation. All other measurements were found to be statistically insignificant. Reflectance measurements are likely indicators of the growth already present, because a darker surface will reflect less light than a lighter surface. Moisture measurements are both an indicator and a predictor of biofilm growth. Extremely low moisture will result in little growth, as seen on the negative control site. High moisture contents may indicate a smaller less permeable pore structure able to retain more water. A better pore structure would be consistent with a lower w/cm, which should be less susceptible to growth, as indicated by Dubosc et al. [15]. Z-scores, or a standardized score, are created by dividing each measures value by its standard deviation. Figure 3.19 and Figure 3.20 show the variations in z-scores of the data gathered from all sites visited, with a higher biofilm rating indicating more biofilm coverage.

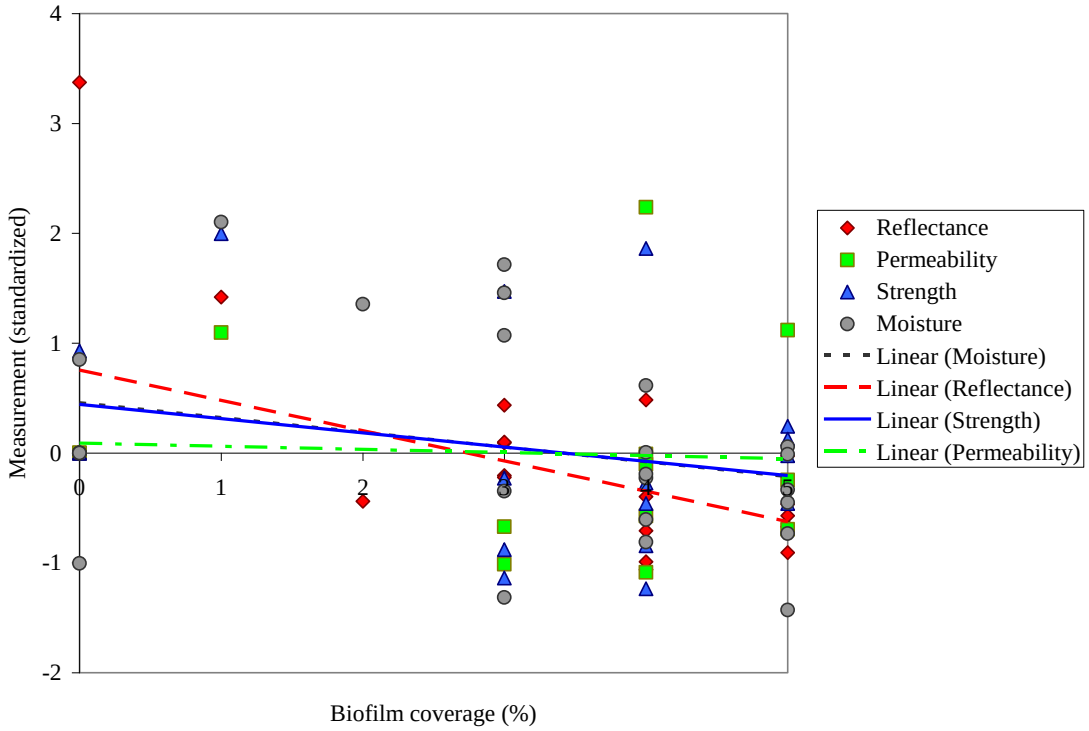

Figure 3.19 - Surface Factors

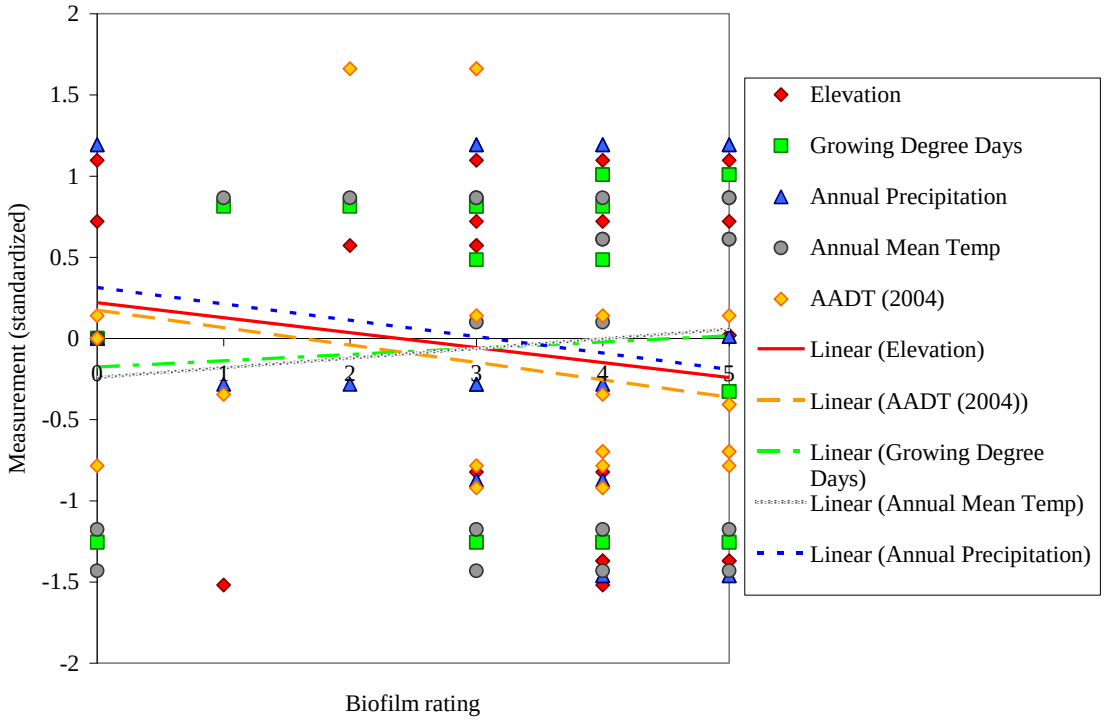

Figure 3.20 - Environmental Factors

Since microbes typically grow better in moist conditions, it may seem counterintuitive that the visible level of biofilm increases for drier surfaces. However, the author hypothesizes that this is likely due to the biofilm absorbing and removing water at the concrete surface. An example of this effect can be seen in Figure 3.21, noting that areas of dark growth produced drier moisture readings. Although the fits for reflectance and strength are low, a negative correlation is found as expected, since more growth should reduce the light reflectance of the surface.

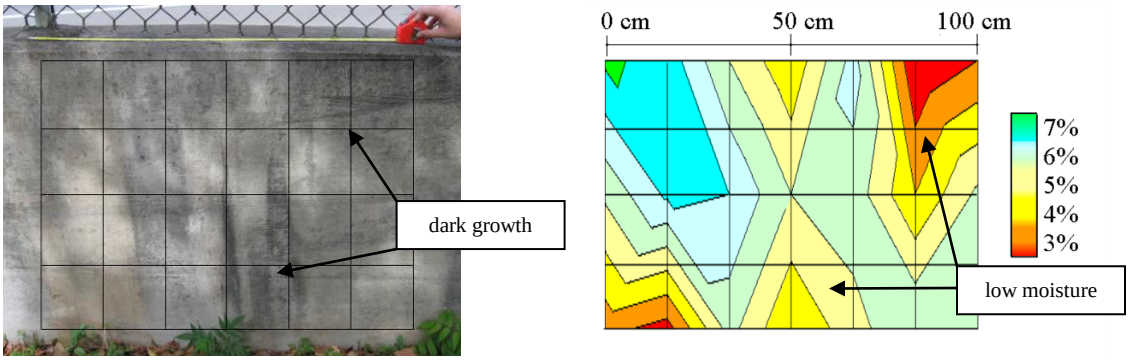

Figure 3.21: Picture of Atlanta biofilm growth and related moisture contours

Contrary to expected results, permeability showed no correlation with growth. This may be due to the fact that permeability measurements were taken from an area in the concrete 30-40 mm below the surface. Consequently, any change in permeability either caused or preferred by microbes living on the surface may not have been captured.

None of the climatic factors considered, including elevation, growing degree days, annual precipitation, or air pollution, were found to be statistically significant in determining the extent of growth. This may be due to two factors. All the sites were limited to Georgia, and it is possible that the microbial species responsible for discoloration are able to thrive in all the climates found at the sample sites. Additionally,

the number of sites sampled was limited, resulting in a small sample set for comparisons, allowing site-specific materials to overwhelm the relatively smaller variations in climatic conditions.

3.4.2. Biological identification

A wide variety of fungi and bacteria were found to colonize the surfaces of all four sites, as shown in Table 3.3. Fungi previously identified as growing on Portland cement materials were found at some of the sites, including *Cladosporidium* spp. Some *Cladosporidium* species have shown the capability to produce organic acids and chelating agents to leach micronutrients, such as iron, calcium, and traces of other heavy metals, from the concrete. Many other genera of fungi, including *Udeniomyces, Alternaria* and *Hypocrea* spp., were found on concrete surfaces in Georgia which have not been discussed previously in the literature on this topic. The bacteria found include the genera *Pseudomonas,* of which some species have previously been found to metabolize hydrocarbons and produce organic acids as waste products [56].

Table 3.3 - Biofilm species identified by DNA analysis

No. related clones	Site acquired	Nearest relative [accession no.]	Phylogenetic group	Similarity (%)
Bacteria (16S)				
41	A, G, S	ASC clone ctg_CGOF104 [DQ395781]	γ-Proteobacteria	99
30	L	SAC clone JSC2-A6 [DQ532167]	Cyanobacteria	93
15	S	*Pantoea ananatis* BD 561 [DQ133546]	γ-Proteobacteria	99
14	G	OCS clone OCS7 [AF001645]	β-Proteobacteria	93

Table 3.3 (continued)

11	S	*Pedobacter steynii* WB2.3-45T [AM491372]	Sphingobacteria	99
7	A	RS bacterium m5 [DQ453814]	γ-Proteobacteria	96
7	A, S	*Pseudomonas lutea* OK2 [AY364537]	γ-Proteobacteria	98
6	A, G, S	GW clone 005C-B03 [AY661994]	γ-Proteobacteria	93
5	G, L, S	*Janthinobacterium lividium* GA01 [DQ473538]	β-Proteobacteria	93
4	A	ID clone BF0002D02 [AM697512]	β-Proteobacteria	92
4	A, L	ARV clone AYRV1-102 [DQ990927]	Cyanobacteria	98
3	L	SAC clone KSC6-17 [DQ532358]	Acidobacteria	95
3	L	ID clone BF0001B010 [AM696984]	β-Proteobacteria	97
2	L	ocean margin clone ODP1230B22.23 [AB177177]	Cyanobacteria	98
2	S	*Rhodococcus erythropolis* EPWF [AY822047]	Actinobacteria	99
2	S	SAC clone JSC9-A3 [DQ532271]	Cyanobacteria	87
		Fungi (ITS)		
35	G, S	*Cladosporium* sp. B5B [EF432298]	Capnodiales	100
33	L	*Udeniomyces pseudopyricola* [AY841862]	Cystofilobasidiales	98
27	A, G	*Alternaria* sp. CID62 [EF589849]	Pleosporales	100
20	L, S	*Epicoccum* sp. G7A [EF432273]	Pleosporales	99
17	A	*Hypocrea lixii* [AJ608956]	Hypocreales	99
13	S	*Cladosporium cladosporoides* [DQ810182]	Capnodiales	100
6	G	*Trichosporon pullulans* CBS 2541 [AF444418]	Cystofilobasidiales	100

Table 3.3 (continued)

5	A	*Aspergillus niger* 16888 [AY373852]	Eurotiales	99
3	G	soil fungus clone 164-21 [DQ420945]	Pleosporales	100
3	G	*Mucor recamosus* UWFP 1053 [AY213661]	Mucorales	99
3	G	*Udeniomyces megalosporus* CBS 7236 [AF444408]	Cystofilobasidiales	100
3	G	*Davidiella tassiana* cla063 [EF589965]	Capnodiales	99

Analysis of the species of bacteria and fungi present at each site shows that the composition of the microbial colonies varies. Although sites show certain similarities, such as a predominance of *Cladosporidium* spp. in Gainesville and Savannah, the composition of bacterial clones is different. Furthermore, this variation shows that a single species is likely not the sole cause of the visible component of the biofilm. For example, *Udeniomyces pseudopyricola* is the dominant fungal species at the LaGrange site and was not found at most other sites. However, the aesthetic degradation is similar, suggesting a versatile mitigation strategy may be required, given the variety of microbes present at various locations within this state.

3.4.3. Microbial growth and concrete composition

3.4.3.1. XRD Analysis

XRD was performed to look for crystalline evidence of microbial deterioration. For example, evidence of gypsum could indicate an acidic deterioration of ettringite or monosulfate. Unfortunately, results from XRD were largely inconclusive for comparing

composition between internal and external powder samples, primarily due to the overwhelming presence of crystalline phases from the aggregate. For the four sites examined, most of the crystalline mineral components are found in aggregates, such as quartz, albite, biotite, and microcline. Some sites had small variations in the aggregate mineralogy, such as including cordierite or not having microcline. Some exterior samples contained $CaCO_3$ as calcite, which would be expected due to natural carbonation processes.

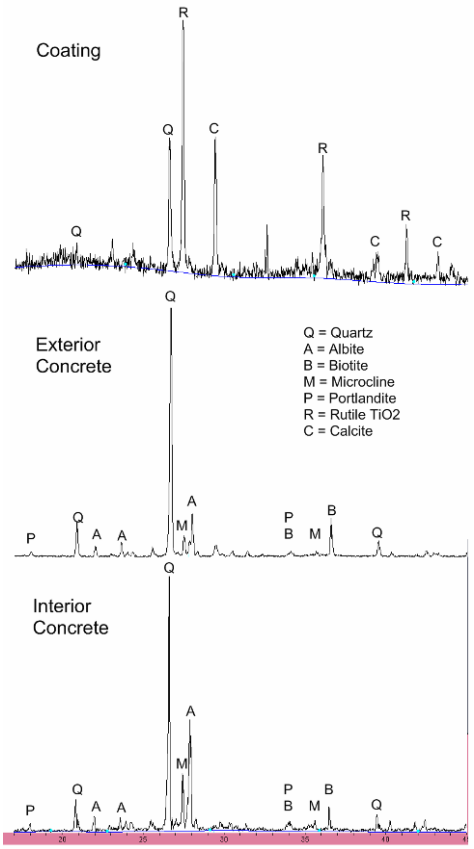

Figure 3.22: XRD pattern from Savannah

The coating found on the Savannah site is very different in its composition. As can be seen in the XRD graph in Figure 3.22, showing counts between 17 and 45 2θ°,

rutile (TiO_2), quartz, and calcite were the primary crystalline components. This demonstrates that established construction techniques may be modified to include an active anti-microbial coating based on anatase TiO_2.

Table 3.4 - Summary of Crystalline Components found by XRD

	Atlanta	Gainesville	LaGrange	Savannah
Albite	X	X	X	X
Biotite	X	X	X	X
Calcite				X
Calcium Aluminum Silicate	X			X
Cordierite	X			
Microcline	X	X	X	X
Portlandite	X	X	X	X
Quartz	X	X	X	X
Rutile TiO_2				X

Results from the analysis of concrete powder by TG/DTA showed that carbonation of the exterior concrete was not occurring at a rate faster than expected by atmospheric processes. Using the model developed by Papadakis [47] and shown in Equations (3.2) and (3.3), aggressive estimates were made for the depth of carbonation using estimated values of 0.45 for w/cm and 70% for relative humidity.

$$x_c = \sqrt{\frac{2D_{e,CO_2}(CO_2/100)t}{0.33CH + 0.214CSH}} \qquad \textbf{(3.2)}$$

x_c: carbonation depth(m)
CO_2: ambient atmosphere (%)
t: time (seconds)
CH and CSH: concentrations (kg/m^3)

$$D_{e,CO_2} = A\left(\frac{\varepsilon_c}{\frac{C}{\rho_C}+\frac{P}{\rho_P}+\frac{W}{\rho_W}}\right)^a\left(1-\frac{RH}{100}\right)^b \quad \textbf{(3.3)}$$

A: $6.1*10^{-6}$
a: 3
b: 2.2
ε_c: total porosity
C,P,W: cement, SCM, and water (kg/m^3)
ρ_C, ρ_P, ρ_W: density of cement, SCM, and water (kg/m^3)

As seen in Table 3.5, the estimated ages of carbonation are much younger than would be expected due to building records. It does not appear that the presence of biofilm is increasing the carbonation rate of $Ca(OH)_2$, as has been suggested by other researchers [22].

Table 3.5: Concrete carbonation and age estimation

Site	% carbonated (1 cm)	Estimated RH (%)	Estimated age by TG/DTA (yrs)	Age of structure from building records (yrs)
Atlanta	21	70	4	23
Gainesville	35	70	10	52
LaGrange	56	70	26	30
Savannah	48	75	19	33

3.4.4. Estimation of Growth Timeframe

The rate at which a biofilm covers a material surface is a factor that is rarely quantified in previous research, but one which is critical in understanding the pattern of colonization and growth and in establishing an appropriate maintenance strategy. One exception is a measure of colony forming units (CFUs) measured in samples taken from a painted façade after cleaning over a one year time period [57]. However, this

measurement was relatively short term and did not quantitatively assess a visual appearance of the structure.

The maintenance department of the GDOT provides some historical record of bridges across the state. Although the bridges are inspected typically every two years, new pictures are taken of the bridges only if conditions have "substantially changed" (personal communication, Kerry Wood, GDOT maintenance office). Digital photographs only were used for record-keeping after 1997, further limiting any analysis of growth patterns to changes occurring during last 10 years. However, suitable series of photographs were found for the Gainesville, LaGrange, and Savannah sites (Figure 3.24, Figure 3.25, and Figure 3.26, respectively). A bridge structure on the same road near the Atlanta site was found and will be used for this analysis (Figure 3.23).

Coverage was visually assessed on concrete structures present in a historic series of photographs. An example of the continuity is shown in Figure 3.25. The visually dark biofilm was manually removed from each photograph and measured using ImageJ software. An example of the measurement technique is seen in Figure 3.27, with the concrete area examined on the left and the biofilm coverage shown on the right. The ratio between the area and area covered is taken to determine coverage.

Figure 3.23 – Photos from 1999, 2005, and 2007 for Atlanta

Figure 3.24 - Photos from 1997, 2005, 2007 for Gainesville

Figure 3.25 - Photos from 1997, 2003, and 2007 for LaGrange. Consistent areas outlined in red.

Figure 3.26 - Photos from 1998, 2004, and 2007 for Savannah

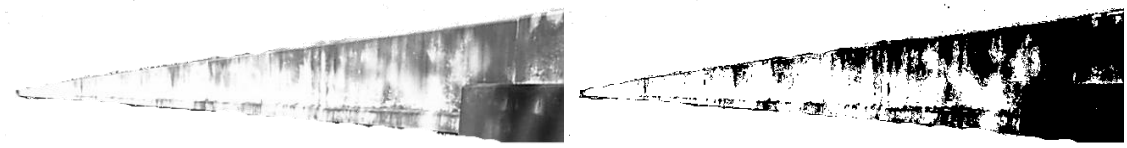

Figure 3.27 - LaGrange 1997 photo with entire area removed (52451 pixels) and biofilm area counted (29585 pixels) to determine 56% coverage

The analysis of historical coverage assumes that the concrete on the structures has not been recoated or cleaned since construction. With that assumption, the logistic model in Equation (3.4), as originally proposed by Pierre Verhulst in 1838 for human population growth rates (dN/dt) was used to estimate rates of growth.

$$\frac{dN}{dt} = r_0 N\left(1 - \frac{N}{K}\right)$$
$$N_t = \frac{N_0 K}{N_0 + (K - N_0)\exp(-r_0 t)} \qquad \textbf{(3.4)}$$

r_0: intrinsic growth rate
N: current population
N_0: starting population
K: maximum population
t: time

Logistic growth is often used for estimating the growth curve of bacteria populations [36]. The estimate of intrinsic growth rates for area fraction covered ranged from 0.19%/yr (for Gainesville) to 0.45%/yr (for Atlanta). Gainesville is the oldest structure, and because the coverage had remained relatively constant over the picture record, it was assumed the site had reached the maximum that could be sustained.

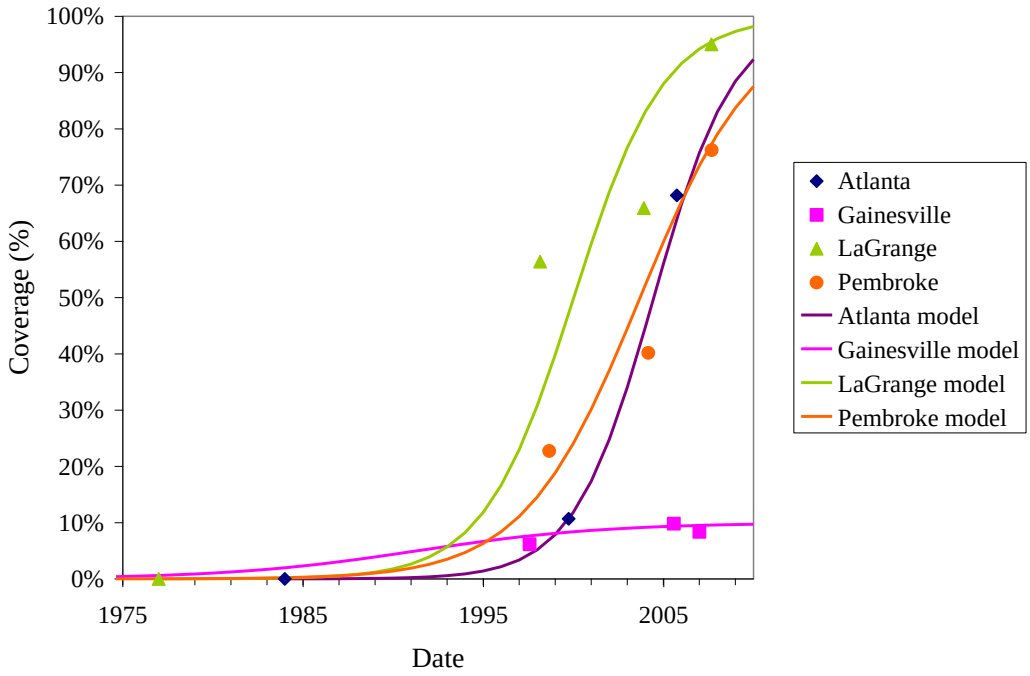

Site	Growth Rate (r_0)	Max. Area (K)
Atlanta	0.45	1.0
Gainesville	0.19	0.10
LaGrange	0.40	1.0
Savannah	0.31	1.0

Figure 3.28 - Historical Biofilm Coverage

Normalized historic precipitation, temperature, and carbon emissions were plotted against the biofilm coverage on a log scale to examine if any correlation between these parameters exists. The precipitation and temperature data show very little correlation to the growth coverage. However, carbon emissions track very well in relation to coverage, fitting with a log scale to R^2 values of 0.81 to 0.95. Assuming that carbon emissions also

indicate similar rises in other pollutants, such as VOCs and NO_x, this correlation may show that biofilm growth may increase with increased pollution. Photoautotrophic microbes may be able to take advantage of the increase in CO_2 emissions near the roadway. A chemolithotrophic, nitrifying bacteria may be able to take advantage of the increase in NO_x compounds. A chemoorganotrophic bacteria, such as a *Pseudomonas* sp., may be able to take advantage of a rise in VOCs.

However, carbon emissions also correlate strongly with time. This may indicate that the growth is merely a time-dependent growth. The logistic models indicate a lag time of 10 to 20 years before coverage has even reached 10% of the area of the surface. This is consistent with what was seen at the negative control site. Very small amounts of biofilm growth have just begun on the surface, but the amount of total coverage is still less than 1% of the surface 7 years after construction.

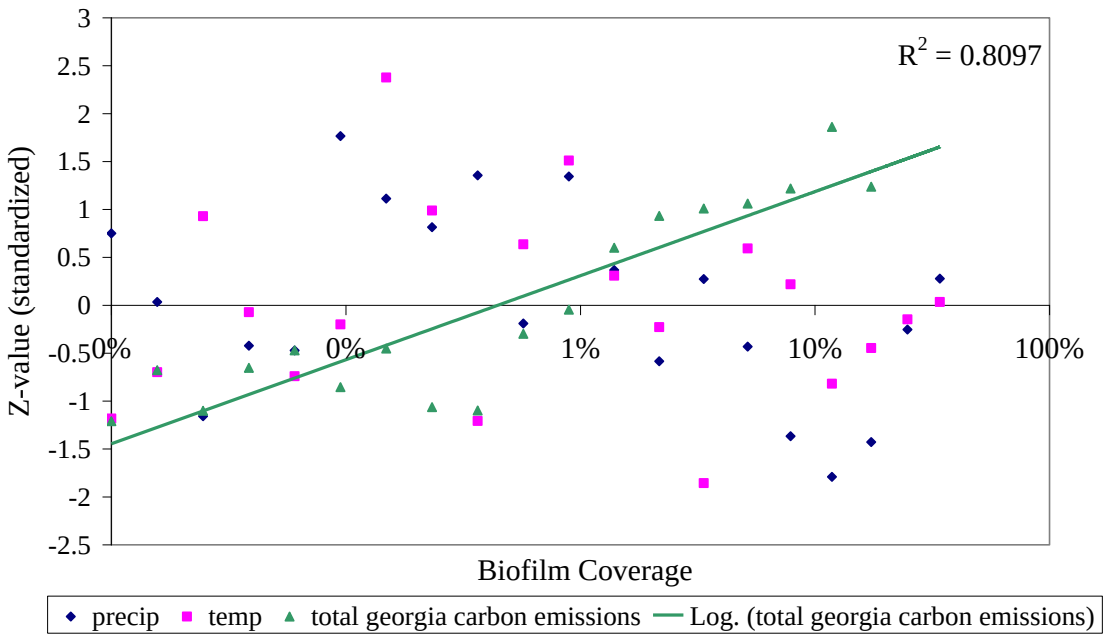

Figure 3.29 - Standardized carbon emissions versus biofilm coverage, at Atlanta site

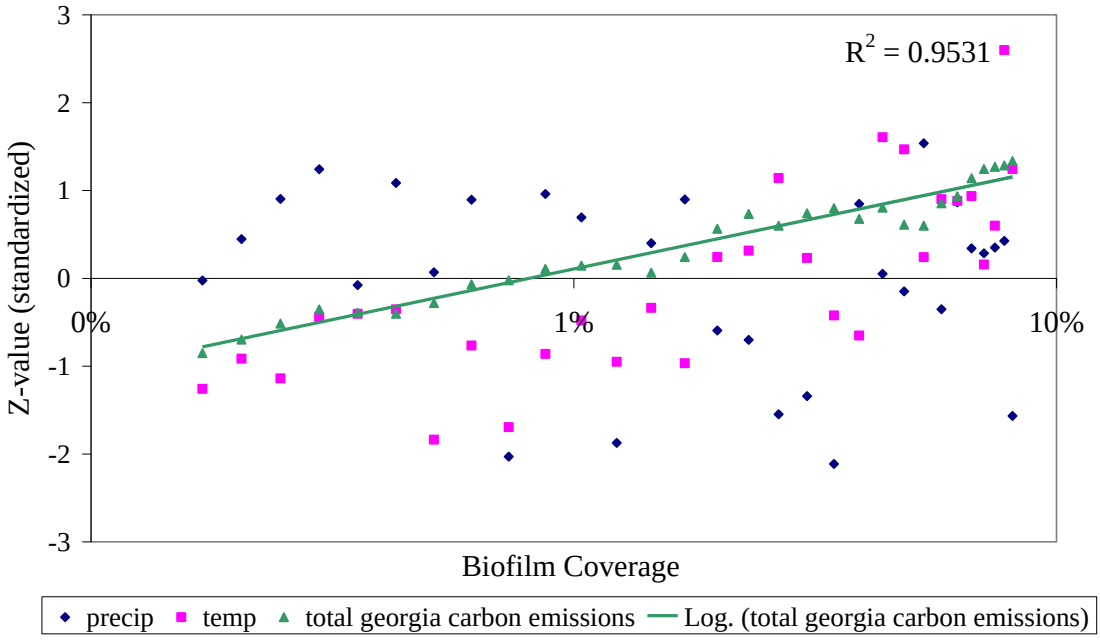

Figure 3.30 - Standardized carbon emissions versus biofilm coverage, at Gainesville

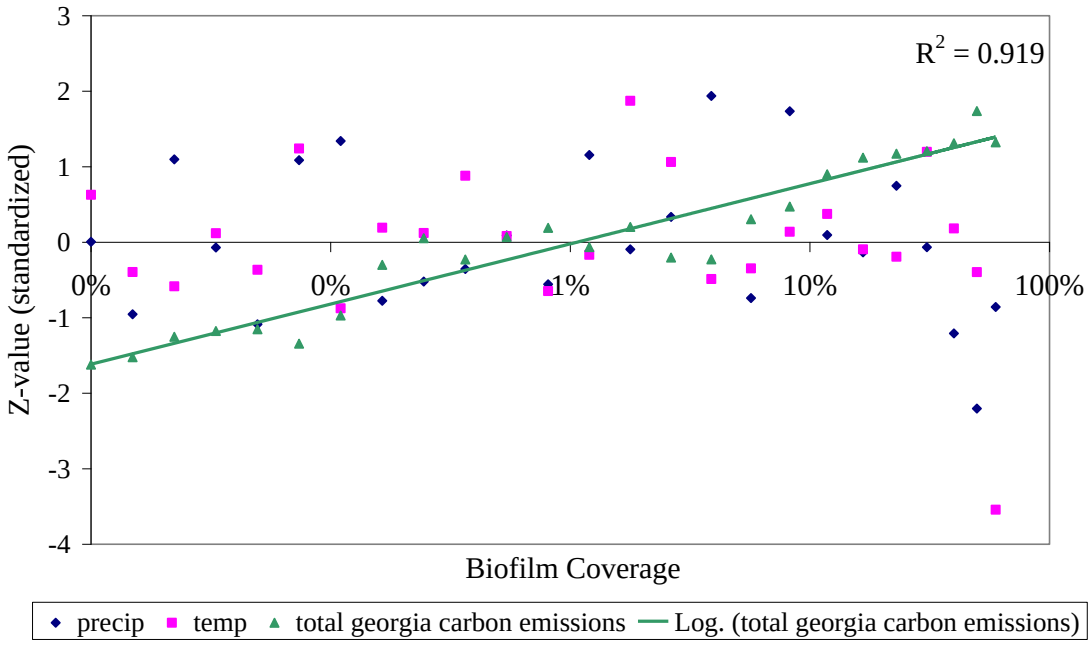

Figure 3.31 - Standardized carbon emissions versus biofilm coverage, at LaGrange

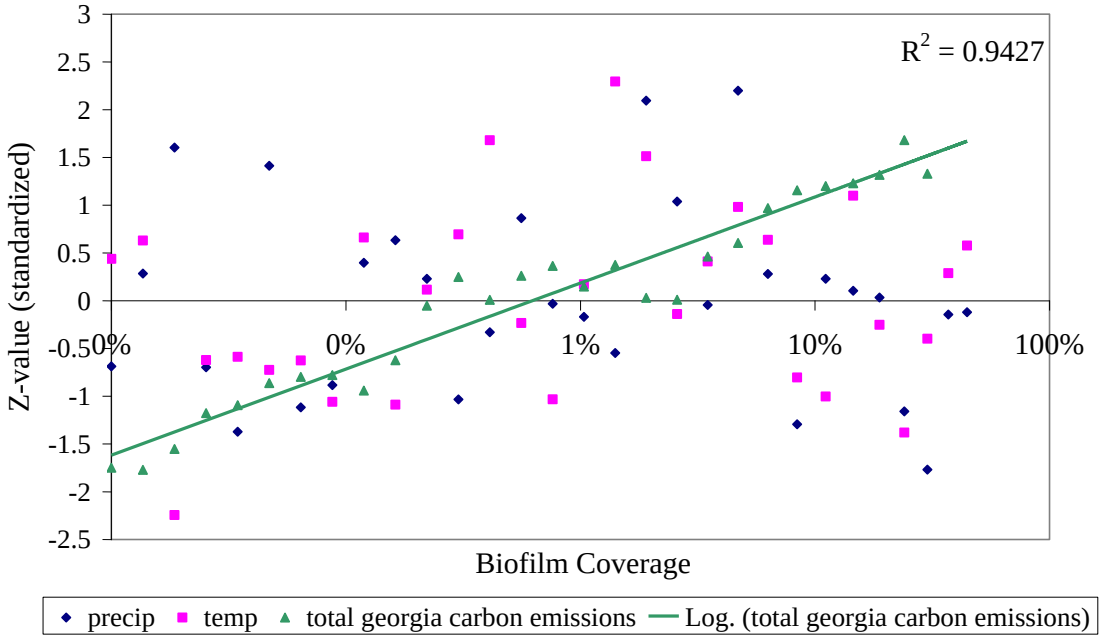

Figure 3.32 - Standardized carbon emissions versus biofilm coverage, at Savannah

3.5. Preliminary Conclusions

This research confirms that the dark films noticed on concrete structures in Georgia are due to microbial communities present on the surface. This indicates that the microbes are able to colonize and proliferate in a variety of conditions, and may acquire nutrients from various compounds present in the concrete. However, the variation in fungal and bacteria species found suggests that more than one type of organism may be responsible for dark biofilm formation, despite apparent similarities in surface appearance. Only moisture content, reflectance, and compressive strength were found to have some correlation, although data was quite scattered, due to variability in field conditions. Moisture contents and surface reflectance are likely indicators of growth already present at the site instead of indicators representing a potential for biofilm formation. The correlation of concrete strength and reduction in biofilm appearance requires further exploration to determine the fundamental relationship. XRD data were inconclusive to show evidence of compounds for biofilms to metabolize or secrete. TG/DTA data show that biofilm presence may not be actively degrading the $Ca(OH)_2$ compounds in the concrete.

The increase in growth coverage shows that, once established, the biofilm might proceed to rapidly cover the surface of the structure. The establishment point may be due to a lowering of pH due to carbonation, leaching of anti-bacterial agents in a coating, or some other initiating event. It appears that a lag period of 10-20 years often occurs for structures before the biofilm growth is noticeable (>5% coverage of a surface).

CHAPTER 4:

PATHWAYS TO MICROBIAL GROWTH AND METHODS FOR TESTING

4.1. Overview of Growth Pathway

In general, microbial growth can be idealized as a four step process, represented by the diagram shown in Figure 4.1. The first step is initial colonization by microbes. This step can include deposition onto a surface by wind, rain, or runoff, or through physical contact with soil, plants, or animals. The second step is a hospitable surface for growth. This surface must be suitable for attachment and devoid of agents or compounds that could inhibit growth, such as high saline contents or sufficient concentrations of heavy metals. The third necessity to sustain growth is the abundance of energy, water, and minerals. All microbes need suitable sources of water to carry out metabolic processes, which require energy and minerals to complete. The fourth step is growth and reproduction, which occurs if all of the previous three steps are successful.

Following this general scheme for microbial growth, this chapter considers the "pathways" to microbial growth on Portland cement concrete. First, the types of microbes identified on concrete infrastructure in Georgia are identified and their potential effect on the concrete described. Next, the characteristics of concrete which affect the hospitality of the surface to microbes are considered. Third, the potential sources of nutrients and energy to sustain growth on the concrete are described. Based upon this understanding of the necessary requirements for microbial growth, the relative advantages and disadvantages of existing accelerated methods for laboratory examination

of biofilm growth on cement-based materials are discussed. Finally, a newly developed method for accelerated biofilm growth is described.

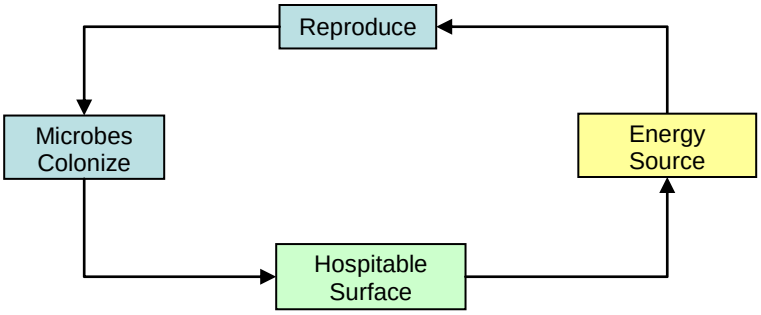

Figure 4.1 - Simplified Biological Growth Pathway

4.1.1. Microbes

4.1.1.1. Microbes identified

The microbes found on the four sites sampled in Georgia included various species of fungi and bacteria. The major groups of bacteria identified can be split into *Pseudomonas*-related and cyanobacteria-related genera. Cyanobacteria are the only microbes discovered that have been shown to fix atmospheric carbon and utilize photosynthesis for energy; thus, these microbes do not require an energy source which derives from the colonized surface material. Some species of *Pseudomonas* have been shown to consume organic carbon sources, generally in the forms of hydrocarbon from fossil fuel.

Fungal species are primarily decomposers, using dead biological matter for food sources. Many researchers, such as de Souza Saad [13], de Graef [14], and Crispim,

Gaylarde, and Gaylarde [12] assume that fungi are not primary colonizers, and that algae and cyanobacteria must first soil the surface. Due to the external requirements for carbon and energy, it can be postulated that the fungal and *Pseudomonas* spp are scavenging from any organic matter that falls on the concrete surface or is created by bacteria. Gaylarde and Morales mention that some biofilms are autotrophic based and contained substantial chlorophyll contents, but other biofilms are primarily fungal and "initiated by organic pollutant deposition" [18]. Some additional organic matter could range from paints or coatings adhered to the surface [57] to dissolved organic carbon present in rainwater [4],[68], or airborne carbon from fossil fuel emissions [8].

This uncertainty between the initial colonizers of surfaces (bacterial vs. fungal) and their energy sources (autotrophic vs. chemotrophic) indicates that multiple types of biofilms are present on inorganic mineral surfaces. Effective mitigation of growth is then dependent on the particular composition and ecology of the type of biofilm present.

Table 4.1 - Energy source and excretions of microbes found

Microbe	Energy/Carbon Source	Excretions
Major Bacterial Types		
Pseudomonas-related	Organic	
Cyanobacteria-related	Solar/Inorganic	
Fungi		
Trichoderma spp.	Organic	
Phoma-related	Organic	
Cladosporidium sp.	Organic	Organic acids
Fusarium sp.	Organic	Organic acids
Alternaria spp.	Organic	

4.1.1.2. Microbes not identified at sites

Algaes and lichens are two types of biofouling organisms, often found on stone materials [36], that were not found at any of the five Georgia sites examined in detail. Algaes are not typically resistant to long periods of desiccation and prefer places with consistent water runoff. They are phototrophic and are capable of living anywhere with a sufficient light source, adequate availability of moisture, and a suitable mix of inorganic nutrients. The frequently recurring droughts in Georgia may play a role in favoring fungal growth over algal growth on the structures examined. Since 1900, droughts in this region have occurred 1903-1905, 1924-1927, 1930-1935, 1938-1944, 1950-1957, 1980-1982, 1985-1989, 1998-2002, and 2006-present [63], and this likely accounts for their absence on the sites characterized.

Lichens are a symbiotic combination of a fungi and a phototroph (such as algae or cyanobacteria). The algae or cyanobacteria provide organic content to the fungi through photosynthesis. The fungal species provide anchorage, shelter, and inorganic compounds necessary for the photosynthesizing partner. Lichens are able to grow in many desiccation-prone and nutrient poor environments other microbes cannot, such as stone, bare soil, and rooftops [36]. Growth rates are often extremely slow, on the order of 1 to 300 mm per year, due to the difficult environment. Despite their apparent ability to exist in relatively dry conditions, no lichen were identified on the five sites characterized.

4.1.2. Suitable Growth Location

The prolificacy of biofilm growth on concrete is surprising considering the material's few advantageous characteristics for microbial growth. Of benefit to microbial colonization and growth is the relatively rough surface (on the microscopic scale) of

concrete which provides numerous attachment points for fungal spores and bacteria cells. However, because it is composed of inorganic compounds, it contains no suitable inherent energy sources for microbial metabolism. Furthermore, the surface of exterior concrete is typically exposed to high levels of UV radiation from sunlight and suffers, particularly at its surface, from long periods of desiccation between periods of rain. Additionally, "young" concrete (concrete in which the first few millimeters has not yet carbonated) has a high surface pH, typically around 12-13, which is unsuitable for the majority of microbial species.

This section reviews those characteristics of cement-based materials which influence microbial growth. The effects of surface roughness, pH, moisture availability, and toxic agents are considered below.

4.1.2.1. Important Surface Properties

4.1.2.1.1. Surface Roughness

Surface roughness can be described by various means. The most commonly used parameter for manufacturing is the average roughness, R_a, as defined in Equation (4.1), where r(x) the height of a profile over its mean and L the length of the cross-section. However, this parameter is not very suitable for precisely characterizing the roughness of concrete, because surfaces can have the same R_a but exhibit very different profiles, varying in the number and intensity of peaks.

$$R_a = \frac{1}{L}\int_0^L |r(x)|dx \qquad \textbf{(4.1)}$$

A roughness parameter more suitable to measurements of concrete is the ratio of surface area to projected area, denoted here as the roughness number (R_n). This measurement, as described by Kurtis et al [31] and used by Lange [33] and Abell [1], is sensitive to the overall variation in surface area as related to a flat surface. The technique for measuring this parameter in digital topographic images, similar to those in Figure 4.4, is described by Chinga et al [10]. The integral of 3D surface area discretized for digital use is shown in Equation (4.2).

$$SA = \int_S dA = \iint \sqrt{1 + \left(\frac{\partial z}{\partial x}\right)^2 + \left(\frac{\partial z}{\partial y}\right)^2}\, dxdy$$
$$SA = \iint \sqrt{1 + tan^2\,\theta}\, dxdy \approx \sum_{i=1}^{N_x} \sum_{j=1}^{N_y} \sqrt{1 + tan^2\,\theta_{ij}} \qquad \textbf{(4.2)}$$

In this research, the roughness number for the surface of mortar tiles were measured by a Leica SP-1 Confocal Microscope using a HC PL Fluotar 5.0x0.15 objective. Image planes of 2mm x 2mm (512x512 pixels of data) were taken every 5 μm in the z-axis. The images were aggregated into topographic maps by Leica LCS Lite version 2.6.1 (available at ftp://ftp.llt.de). The roughness number of each topographic map was measured by ImageJ software (available at http://rsb.info.nih.gov/ij/) using the SurfCharJ plugin developed by Gary Chinga (available at http://www.gcsca.net/). Roughness number was determined from the average of 8 measurement locations on a 35x35 mm surface.

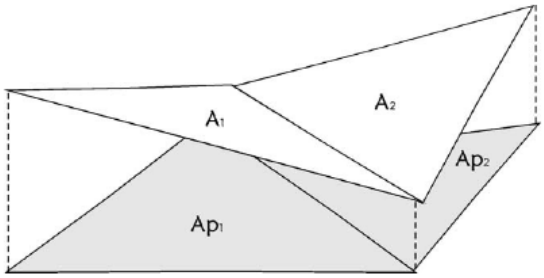

Figure 4.2 – Drawing showing relation between surface area and projected area [31]

Typical roughness numbers for the mortar tiles produced for this research range from 1.11 to 1.60, with 1.11 measured for a tile wet sanded with 600 grit sandpaper, and 1.60 measured for a tile with surface roughened by a paintbrush before curing as described in Chapter 5. The variation in surface roughness between the tiles can be seen in Figure 4.3 and Figure 4.4, which shows surfaces for mortars with measured roughness numbers of 1.11 and 1.45 respectively.

Table 4.2 shows the range of roughness values for various mortar mixes examined in this study. A smooth surface can be obtained by the surface of the tile; increasing the grit of the sandpaper resulted in only a small decrease in surface roughness, from 1.15 to 1.14. Brushed finishes for ordinary Portland cement tiles generally had a surface roughness ~1.35. On average, the addition of an SCM to the mix lowered the surface roughness to 1.30. The table shows two outliers for surface roughness: OPC with w/cm of 0.6, and silica fume at 15% replacement. The high-water OPC mix was rougher because the paste did not set up well after brushing and tended segregate from the fine aggregate. The high silica fume mix had the opposite problem; the paste was too "sticky" and remained rough after brushing.

Table 4.2 - Roughness Characteristics for Various Mortar Mixes

w/cm	SCM replacement % by wt	Binder composition	Finish	$R_n \pm \sigma$
0.3		Type I/II	brushed	1.37±0.07
0.4		Type I/II	brushed	1.34±0.08
0.5		Type I/II	brushed	1.37±0.25
0.6		Type I/II	brushed	1.60±0.45
0.5		Type I/II	120 grit sanded	1.15±0.04
0.5		Type I/II	600 grit sanded	1.14±0.04
0.5	10%	Fly Ash	brushed	1.28±0.11
0.5	18%	Fly Ash	brushed	1.41±0.16
0.5	25%	Fly Ash	brushed	1.26±0.06
0.5	10%	Slag	brushed	1.29±0.05
0.5	25%	Slag	brushed	1.32±0.10
0.5	50%	Slag	brushed	1.33±0.05
0.5	5%	Silica Fume	brushed	1.21±0.04
0.5	10%	Silica Fume	brushed	1.21±0.04
0.5	15%	Silica Fume	brushed	1.64±0.39
0.5	*8%*	*Metakaolin*	*brushed*	1.22±0.06

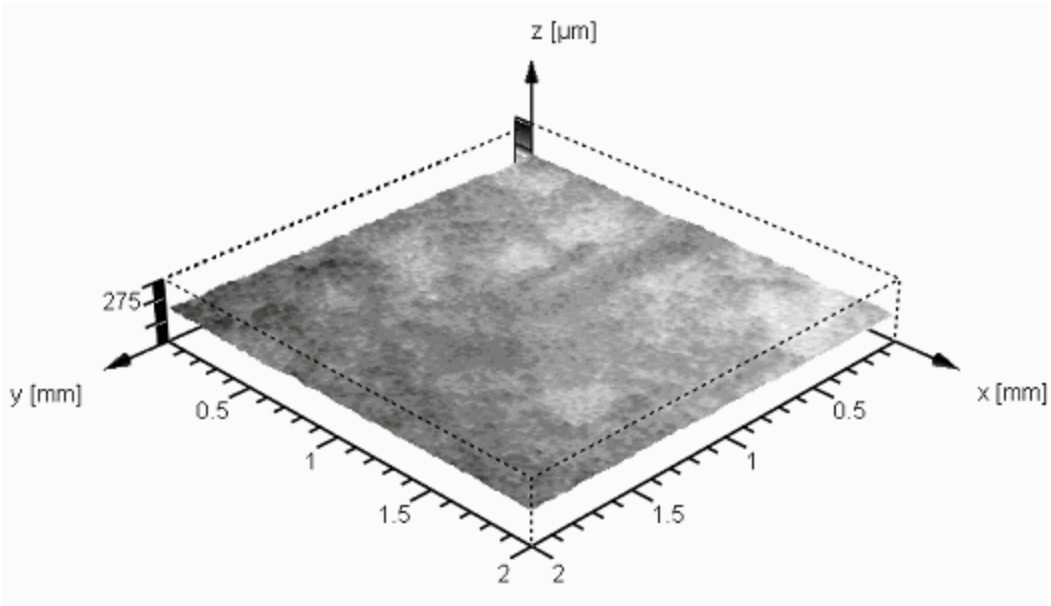

Figure 4.3 – Topographic image of 600 grit wet sanded tile with measured R_n 1.11. FOV: 2 x 2 x 0.130 mm

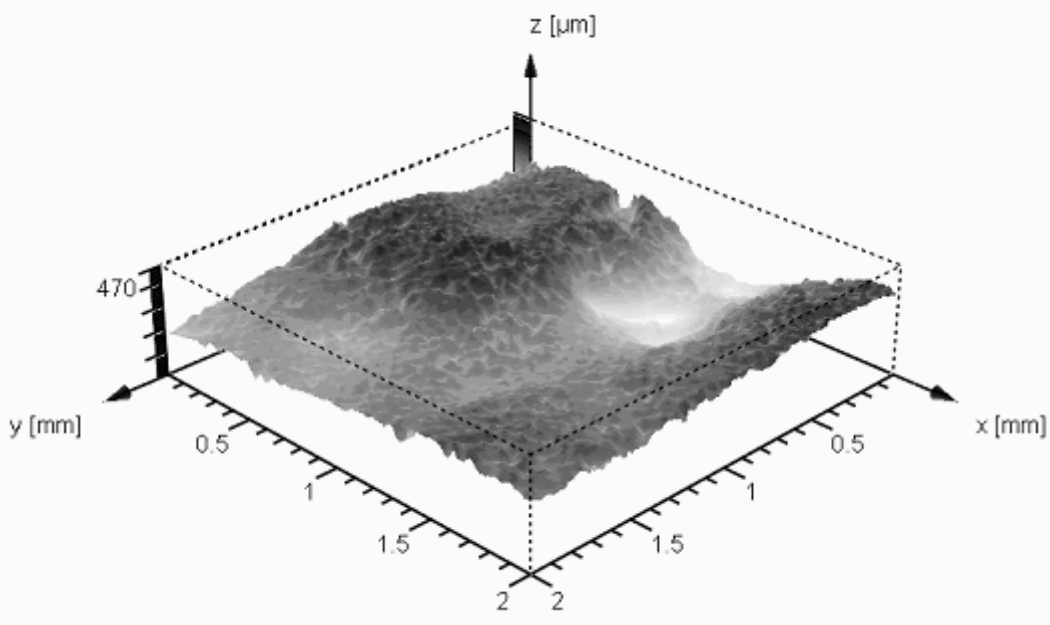

Figure 4.4 – Topographic image of brushed finish tile with measured R_n 1.45. FOV: 2 x 2 x .620 mm

4.1.2.1.2. pH (Carbonation)

The great majority of microbes grow between pH values of 2 and 9, with only a few species capable of growing outside that range. Highly alkaline environments create bioenergetic problems for microbes [36]. Previous research by Shirakawa [55], for example, identified the inability of fungi to colonize concrete with a pH greater than 10. Uncarbonated concrete typically has a pH range of 12 to 13 [59], which would be extremely unsuitable for most microbes.

Most alkaliphilic work has been done on saline-rich alkali environments, with little microbiology work done on the nonsaline alkali environments analogous to cement pore water. Bath and colleagues initially examined a nonsaline $Ca(OH)_2$ rich environment in Oman to investigate it as a model system for a cement-based radioactive waste repository [5]. Tiago et al examined a nonsaline $Ca(OH)_2$ rich environment with a pH of 11.4 in Portugal and isolated 45 different bacteria, including *Microbacterium*,

Agrococcus, *Frigoribacterium*, *Clavibacter*, and *Leifsonia* spp. However, they found that only 2 species could actively grow at a pH of 11, with most species growing at a pH of 8.0 to 9.0 [61].

In service, the pH of the concrete surface must likely be reduced by external factors, such as carbonation by CO_2 or leaching of $Ca(OH)_2$. While it is possible that initial colonizers (e.g., bacteria or cyanobacteria) may act to reduce the pH of the surface, data shown in Table 3.5 did not show any increase in carbonation depth for biofilm covered sites, suggesting that this effect is not great enough in the field to be measurable. After carbonation has proceeded a few millimeters, the surface pH of concrete will decrease to 8-9. Although still alkaline, this pH is suitable to a wider range of microbes [36]. None of the bacteria isolated at the sites are the same genera as found by Tiago. This may be due to the fact that the sites sampled were already carbonated, which allows for a much wider range of bacteria. If the highly alkaliphile organisms are initially present on a fresh concrete surface and migrate inward as the surface carbonates, the surface sampling method used would not be able to detect them.

4.1.2.1.3. Availability of Moisture

Measures of microbial growth typically include the parameter "water activity" (a_w), which is equivalent to relative humidity / 100%. Relative humidity in concrete is affected by both external conditions (temperature and external relative humidity) and internal conditions (permeability and pore solution concentrations). Internal RH in hardened concrete is typically both higher and less variable than external RH, with external RH 30% to 70% and internal RH 60% to 80% [3]. As RH changes in the external environment, the variation in RH from exterior concrete surface to the interior

occurs as a gradient. The surface of a specimen relatively quickly reaches equilibrium with the external conditions, but the interior is slower to respond. The first 5 mm from the surface are the quickest to respond to external relative humidity changes [21]. Because the near-surface concrete depends on the external humidity, its usefulness is limited as a water source for microbes over long periods of time.

However, estimates of biofilm growth rates in Georgia (see Chapter 3) do not correlate to rainfall amounts, as seen in Figure 4.5. This suggests that the amount of rainfall each site receives per year is not the limiting factor in biofilm growth. That is, ample moisture is available to support biofilm growth on Georgia infrastructure.

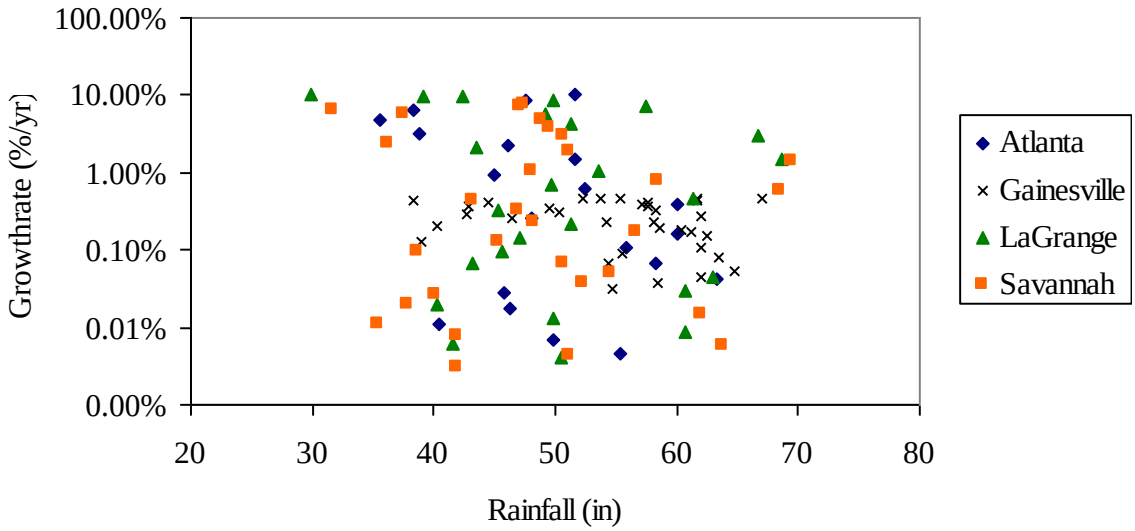

Figure 4.5 - Growth Rate vs. Rainfall

4.1.2.1.4. Naturally occurring prohibiting agents

Two types of simple compounds are prohibitive to microbial growth: heavy metals and toxic oxygen. Heavy metals (e.g., copper, zinc, lead, and silver) are lethal in high concentrations, although small amounts of these elements are necessary for their

metabolism. The microbial methods to avoid poisoning by heavy metals include enzymes that pump out the contaminants or enzymes that perform redox reactions. Tests have not yet been done on the microbes sampled to determine the presence of these enzymes. Introduction of heavy metals to the concrete itself would be environmentally undesirable due to potential contamination of groundwater and soil through rainwater leaching. However, these heavy metals may be introduced through surface coatings (e.g., lead-based paint, copper- or silver-containing paints).

Toxic oxygen is a compound that can have negative effects on a microbe by oxidizing organic compounds in a cell. The most common forms of toxic oxygen include superoxide anion (O_2^-), hydrogen peroxide (H_2O_2) and hydroxyl radicals ($OH\cdot$). Photocatalytic materials, such as anatase TiO_2, have the capability to produce these toxic oxygen species when exposed to the right wavelength of light (greater than 3.2 eV for anatase TiO_2). TiO2-contating photocatalytic cements have been recently introduced for the purpose of limiting some forms of microbial growth, among other purported effects. Microbes have various enzymes (e.g., catalase, peroxidase, superoxide dismutase, and superoxide reductase) that reduce the toxic oxygen to water and either O_2 or another less harmful oxidized compound, which limits but cannot always prevent cellular damage [36].

4.1.3. Energy, Carbon Sources, and Nutrients

Microbes must display chemoorganotrophic, chemolithotrophic, or phototrophic metabolism. A chemoorganotrophic metabolite uses an organic compound for both its energy source and carbon source. Chemolithotrophic metabolites use inorganic compounds for an energy source and CO_2 for a carbon source. Phototrophic metabolites

use light as an energy source and organic compounds (photoheterotrophy) or CO_2 (photoautotrophy) for carbon sources. The microbes found on concrete in this study are either photoautotrophic (cyanobacteria) or chemoorganotrophic (all others). Therefore, the majority of the microbes found can subsist upon locally available organics, including those sources made available by run-off, rainfall, and the presence of fossil fuels and other microbes, for example, and ambient light (in the case of chemoorganotrophs).

Other nutrient requirements for microbes to thrive include macronutrients and micronutrients. Macronutrients include nitrogen, phosphorus, sulfur, potassium, magnesium, and sometimes calcium and sodium. Nitrogen may be found in the air, while many of the other macronutrients are present in the cement and the aggregate, although prior research by Housewright, et al. [24] suggests that it is the cement, not the aggregate, where these are most available to microbes. Micronutrients are needed in much smaller quantities and include primarily iron and traces of various heavy metals. These may also be found in the cement, aggregate, and any SCMs used. The potential sources for these nutrients are considered in more detail in the following sections.

4.1.3.1. Concrete based colony

Ordinary in concrete, organic compounds are only present as contaminants, although small amounts may be present in SCMs and trace amounts can be found from admixtures. For example, Class C or F fly ash from coal combustion, often used as a SCM, may have up to 6.0% by wt. carbon (ASTM C 618).

The composition of a typical Type I/II Portland cement is shown in Table 4.3. The primary compounds are Ca and Si, two elements not essential for microbial metabolism. Ca^{2+} is normally presence in pore water from disassociated $Ca(OH)_2$ or

$CaCO_3$. Measuring either the uptake or release of Ca^{2+}, as done by Gu et al, would only indicate organic acid production and not measure direct use of calcium by microbes [22]. Many necessary micronutrients, including iron and sulfur among others, are present in cement and SCMs. In cement, iron is primarily present in ferric form (Fe^{3+}) in both unhydrated and hydrated cement compounds (C_4AF, ettringite, and monosulfate, or pore solution) [59], which is not suitable for energy extraction by chemolithotrophs. Sulfur is primarily present in hydrated cement as sulfate (SO_4^{2-}) as part of ettringite (Aft) or monosulfate (Afm), or as any residual unreacted gypsum, and is also unsuitable for chemolithotrophs.

Therefore, with the exception of acting as a potential source of micronutrients, ordinary concrete is not a likely source of nutrition to sustain biofilm growth. When SCMs are used, however, there is the *potential* that any carbon present may be metabolized by surface biofilms.

Table 4.3 - Composition of a typical unhydrated Portland cement

Compound	Abbrev	% by weight
Calcium Oxide	CaO	63.84
Silicon Dioxide	SiO_2	19.82
Aluminum Oxide	Al_2O_3	5.01
Iron Oxide	Fe_2O_3	4.06
Sulfur Trioxide	SO_3	2.87
Loss on Ignition	LOI	1.97
Magnesium Oxide	MgO	1.32
Potassium Oxide	K_2O	0.43
Titanium Dioxide	TiO_2	0.27
Phosphorus Pentoxide	P_2O_5	0.18
Sodium Oxide	Na_2O	0.14
Strontium Oxide	SrO	0.09
Manganic Oxide	Mn_2O_3	0.03
Barium Oxide	BaO	0.01

4.1.3.2. Autotroph based colony

A self-sustaining colony of microbes would not need the concrete for anything other than micronutrients. A photoautotrophic colony could be similar to a lichen, in which an algae or cyanobacteria converts CO_2 from the atmosphere to organics that can be used by fungi and other bacteria species present. A second type of autotrophic colony, chemolithotrophic, could be based on an iron or sulfur oxidizing bacteria. However, this colony is likely not possible due to the lack of suitable iron and sulfur species in concrete.

4.1.3.3. Environment Based Carbon Source

While the amount carbon available at the concrete surface is likely limited, the environment provides multiple sources for organic carbon. One particularly convenient source for concrete elements with external exposure is dissolved organic carbon (DOC) in rainwater. Research by Willey et al. [68] found that typical DOC ranged from 0.0015-0.0025 g/L. With a range of rainfall from 120-150 cm/yr, total carbon flux for the sites examined can be estimated at 1.8-3.8 $g \cdot m^{-2} \cdot yr^{-1}$. Further measurement of rainwater indicates that terrestrial environments provide more organic carbon than marine sources, even allowing for the larger quantities of water from hurricanes. Research by Avery et al. [4] determined the ratio of fossil fuel-derived organic carbon to biogenic organic carbon in rainwater by isotope analysis. Fossil fuels accounted for approximately 10-20% of the organic carbon for the rainstorms measured. Additionally, fossil fuel organic carbon content by volume was approximately doubled for a rainstorm that passed over land masses. This suggests that chemoorganotrophic microbes, which include all species found other than cyanobacteria, may be able to use organic carbon present in the rainwater for their metabolism.

Other potentially convenient sources for carbon are airborne, including soil, plant debris, and air pollution. Research by Mastalerz et al. [39] indicates that the largest organic volumes of airborne particulates are combusted and uncombusted hydrocarbons, fungal spores and bacteria. The study also implicated exhaust as a contributing factor to the spread of cytoplasmic material by acting as a carrier [39]. Air pollution may act as a doubly effective contributing factor, aiding both the growth and dispersion of biofilms. Further survey of sites, controlling for factors such as structure age, architectural design, and coatings would be necessary to implement air pollution as a significant factor in biofilm growth.

4.2. Existing Test Methods for Biofilm Growth on Concrete

Although multiple tests exist for testing biofilms on various surfaces, no universally-applied standard test exists. This study, like many, required a test that accelerated natural conditions without altering the mechanisms of reaction and which was repeatable, adaptable to various microbes, and capable of varying light sources and media. The existing test methods were evaluated and tested over the course of this project and none were found to satisfy all requirements. Therefore, in this study a new, accelerated test method was developed. It is proposed that this method is suitable for adoption as a standardized test for biofilm growth on concrete.

The existing tests were evaluated by modifying the procedures described in each for the biology and materials used in this experiment. The biologic entity used in the original procedures was modified to be an environmental species found at one of the four sites. *Trichoderma viride* was selected as the "default" singular species, due to its distinct green growth and robust growth with typical culture media. Additionally, *T.*

viride is capable of producing enzymes that inhibit other microbes, which helps control accidental contamination for inoculated samples. The material used for testing was a 6x6x0.4 cm mortar (sand and cement paste) tiles, selected to simulate typical concrete surfaces at a small, easily reproducible scale. Both visual and stereomicroscopic techniques were used to examine the presence of growth.

4.2.1. U.S. Federal Standard Test Method 141C – 6271.2

4.2.1.1. Test Description

The U.S. Federal Standard Test Method 141C-6271.2 is often used by paint and other coating manufacturers as a measure of the anti-fungal abilities of their coatings. The test method uses one of three specified fungi (*Aspergillus niger*, *Aspergillus oryzae*, *or Aureobasidium pullulans*) as a test organism, for any type of coating. Small squares of filter paper coated on both sides with the substance to be tested are placed on the agar plate. The inoculant is spread over the coating and the plate. After a specified period of time (7 days or more), the side of the coating not touching the agar is examined for evidence of microbial growth inside a boundary 2mm from each edge.

4.2.1.2. Experimental Evaluation

A mortar tile (6x6x0.4 cm) of Type I/II cement (w/cm 0.5) was placed on a potato dextrose agar (pH=7) plate. The tile and the plate were inoculated with a total of 100 μL of *Trichoderma viride* culture in a saline solution. The fungus grew on the surface of the tile in contact with the agar, as shown in Figure 4.6 and Figure 4.7.

Since growth occurred underneath the tile, the presence of the high pH mortar did not appear to inhibit growth on the agar. Although the pH of the tile was not measured

after inoculation, the presence of the neutral agar plate likely allowed the fungus to grow. The fungus did not appear to be growing on the tile itself, but rather was adhered due to the nature of the agar.

Figure 4.6 – Photo of 3x3 cm tile placed on potato dextrose agar plate

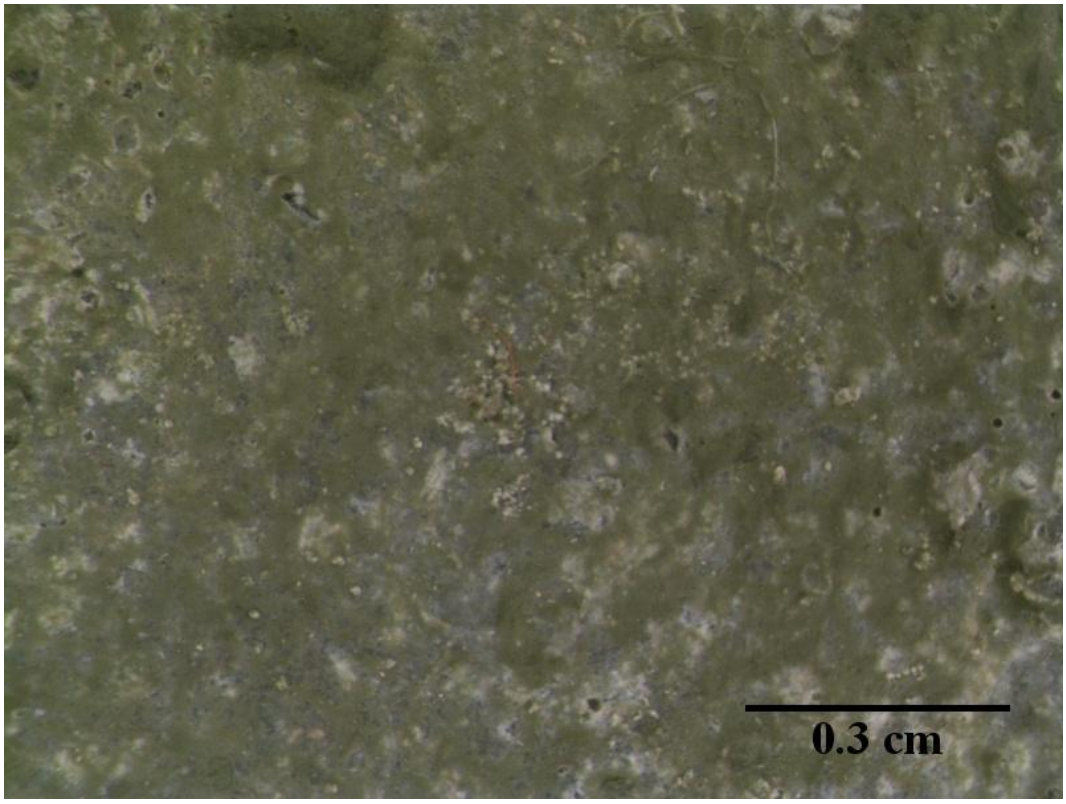

Figure 4.7 - Stereomicroscope image of tile surface

4.2.1.3. Unsuitability of Method

This method is not suitable for examining biofilm growth on concrete for several reasons. First, a thin permeable substance, such as Portland cement mortar, would allow the fungi to reach the nutrients in the agar through absorption of the nutrients. Second, this test does not simulate natural conditions. In natural conditions, biofilms must subsist on the surface and scavenge for nutrients, not merely grow on a nutrient source (i.e., the agar plate). As a result of the unlimited nutrient, supply, any differences in growth between mixes would probably be limited to permeability differences. Third, this test was withdrawn in Federal Test Methods 141D, released March 22, 2001, with no reason given or alternative test supplied.

4.2.2. ASTM D-3456

4.2.2.1. Test Description

ASTM D-3456 (2002), "Standard Practice for Determining by Exterior Exposure Tests the Susceptibility of Paint Films to Microbiological Attack", is a long term test method for paints and coatings. It tests the performance of coatings under natural exposure over periods ranging from 3 months to multiple years.

This test is not suitable for this study for several reasons. First, the species of microbes on the surface is not controlled. As a result, specific strains could not be tested as the culprits for discoloration seen at the four previously mentioned sites. Second, the test method does not accelerate biofilm growth and is too long of a timeframe for this research.

4.2.3. Non-standardized "Immersion" Method

4.2.3.1. Test Description

Testing biodeterioration of concrete samples by immersion in media is an accelerated test method used by numerous researchers [27], [55], [22], [24], [48]. A typical methodology is as follows:

1. Sterilize the specimens by immersion in 70-80% ethanol.
2. Dry the specimens in an oven. This step is omitted by some researchers [48],[27].
3. Inoculate a particular medium (Sabouraud Dextrose, potato dextrose, pond water, oil sludge). The medium is sometimes kept at a desired pH by addition of acids [24],[22].

4. Immerse the concrete specimen in the medium. The specimen is often fully immersed, but one research project only immersed half of the specimen [56].

4.2.3.2. Unsuitability of Method

This type of accelerated test is not suitable for this research. Unlike sewer pipes or underwater piles, none of the sites examined were subject to long term immersion under liquid. Additionally, artificially dehydrating the samples by submersion in ethanol and drying in an oven will alter the concrete microstructure and may accelerate drying shrinkage and increase microcracking. This could lead to an overestimation of concrete damage or skew the susceptibility of various mixes to biofilm growth.

4.2.4. Non-standardized "Dry" Inoculation Method

4.2.4.1. Test Description

Some researchers use a non-immersion inoculation technique to study microbes that do not exist in a continuously submerged environment [52], [55]. A typical methodology for this technique is as follows:

1. Accelerate carbonation of the samples with a high CO_2 (> 5%) atmosphere at 65-70% RH. This step is necessary because the surface must be at a pH lower than 9 to enable non-alkaphile microbial growth and because neutralization of media is not possible.
2. Sterilize the samples by either autoclaving or ethanol.
3. Place the samples in a saturated RH atmosphere for 5+ days.

4. Inoculate the samples with media (Sabouraud dextrose or potato dextrose) containing microbes
5. Place the samples in a high RH (> 95%) container for 60 days

4.2.4.2. Experimental Evaluation

Mortar tiles (6x6x0.4 cm) of Type I/II cement (w/cm 0.5), artificially aged through complete carbonation, were inoculated with 100 μL of *Phoma herbarum* or *Tricoderma viride* culture in an isotonic saline solution. Samples were inoculated with 20% potato dextrose broth, liquid agar medium or purified deionized water. The potato dextrose broth and liquid agar were intended as starter substances to encourage growth. Tiles inoculated with sterile water tested the ability of the fungus to grow in ambient conditions using only nutrients provided by the mortar. Samples were kept at 30° C under either 50% or 95% relative humidity. The variation in relative humidity was used to evaluate the effectiveness of concrete in providing a sustained supply of water after an initial supply. Negative control tiles, inoculated with sterile media, were used instead of sterilization of concrete by autoclaving or ethanol.

Tiles were checked regularly for growth for 6 weeks. No fungal growth was observed on any negative control tiles. No fungal growth was observed on any tiles at 50% relative humidity for the entire time frame. A typical tile with no growth is shown in Figure 4.8. In the sixth week, fungal growth appeared on a mortar tile kept at 95% relative humidity and inoculated with 20% potato dextrose broth, as shown in Figure 4.9.

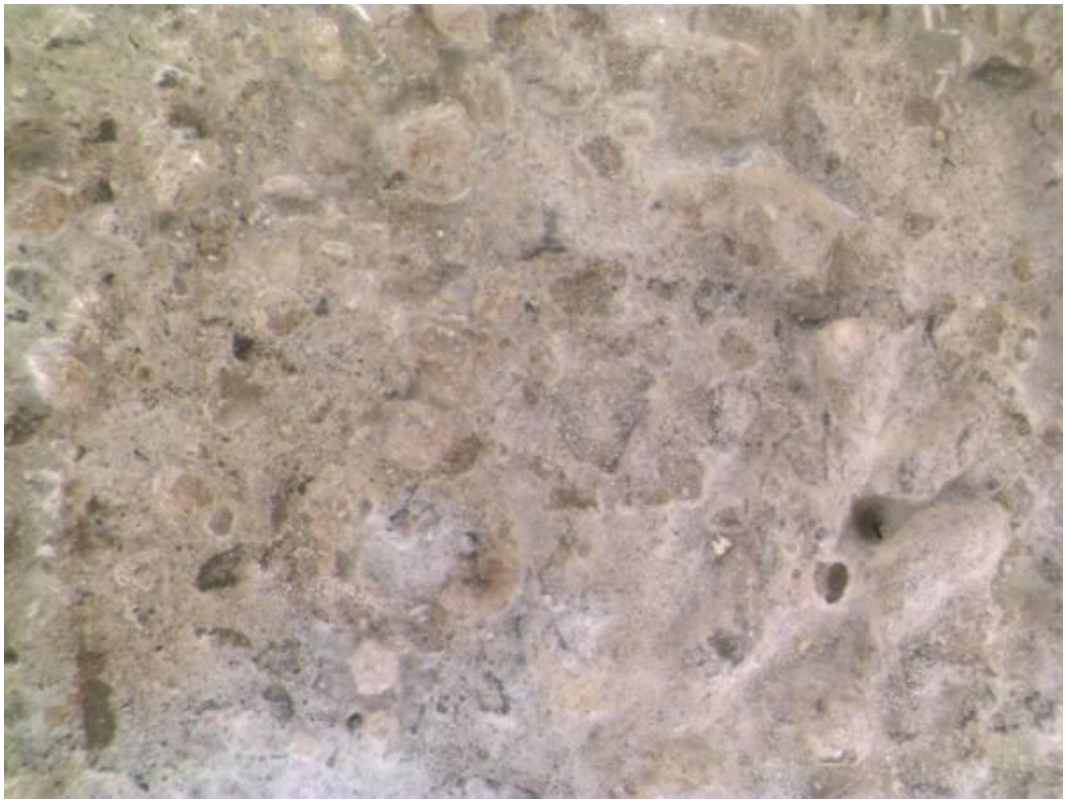

Figure 4.8 – Stereomicroscope image of soft agar and *T. viride*; no growth visible

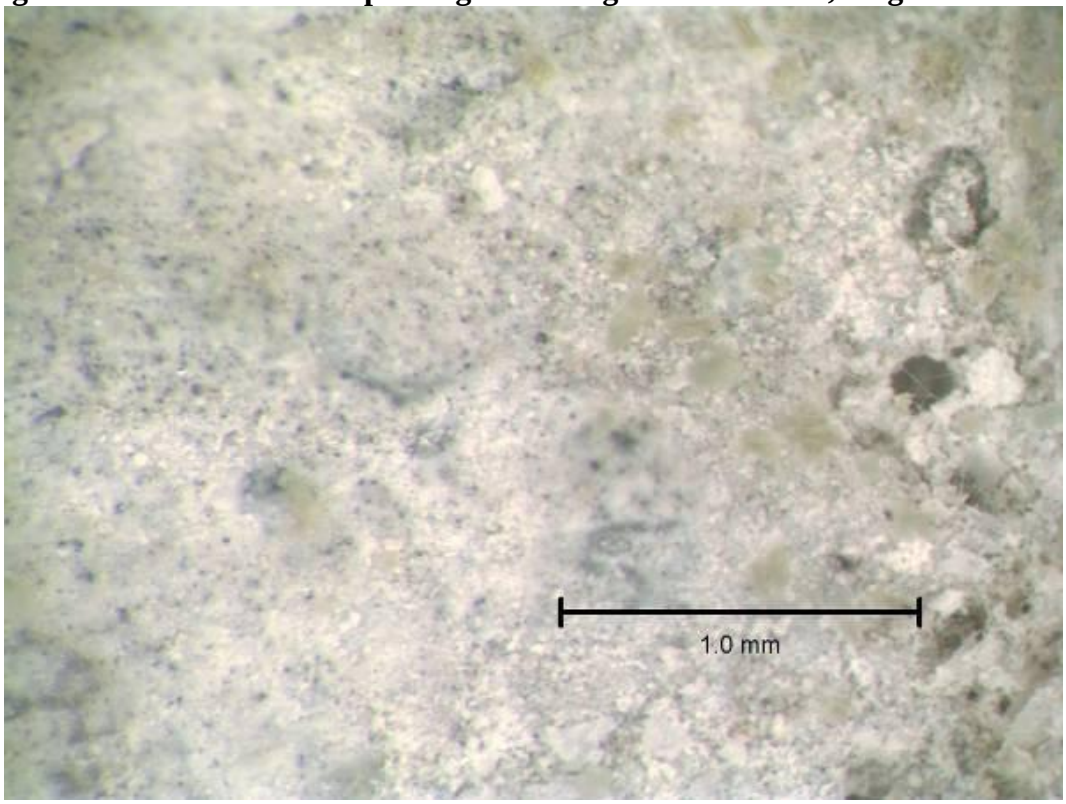

Figure 4.9 – *T. viride* visible above scale mark, 42 days after inoculation; potato dextrose broth applied as media

4.2.4.3. Unsuitability of Method

This method is unsuitable for this research for several reasons. The biofilm growth was not repeatable (growth only occurred on one tile) or very quick, requiring 42 days for visible growth. Previous research [55] performed using this method used *Cladosporidium sphaerospermum*, which may be a faster growing fungus or more suitable to this technique. This research method may have problems adapting to the wider range of microbes isolated from the four sample sites.

4.2.5. Spraying Techniques

4.2.5.1. Test Description

Some researchers have used test methods that intermittently spray concrete or mortar samples with media, in an effort to simulate and accelerate natural conditions of wetting and drying (i.e., rainfall) [22],[15]. A typical methodology is as follows:

1. Sterilize the samples by immersion in 70% ethanol
2. Inoculate a media with selected microbes (such as algae or fungal spores).
3. Sprinkle the samples with media for fungi or mineral water for algae at intermittent cycles. Cycles ranged from 3 hr on, 21 hr off to 7 days on, 7 days off. Cycles of fluorescent lighting were used for algal experiments.
4. Assess growth or deterioration for time periods ranging from 56 to 90 days.

4.2.5.2. Experimental Evaluation

This method was adapted and evaluated for this research. A system was constructed to simulate rain. A polyethylene, rectangular plastic container with lid,

approximately 24”x18”x16” (LxWxD), was the container for the system. Approximately 3 liters of media (10% potato dextrose broth or sterile water) was placed in the chamber, fully submerging an aquarium pump with an output of 320 gal/hr. Four 360° spray jets misters (Raindrip P1075U), typically used for plant irrigation, were attached to the pump by ¼” diameter tubing and used to dispense the media, as shown in Figure 4.10. The flowrate of an individual mister was measured at 150 mL/min. Tiles were placed above the level of the media but below the misters, so that media was constantly spraying over the tiles, as shown in Figure 4.11. Each of the tiles was inoculated with 100 µL of *T. viride* in an isotonic saline solution.

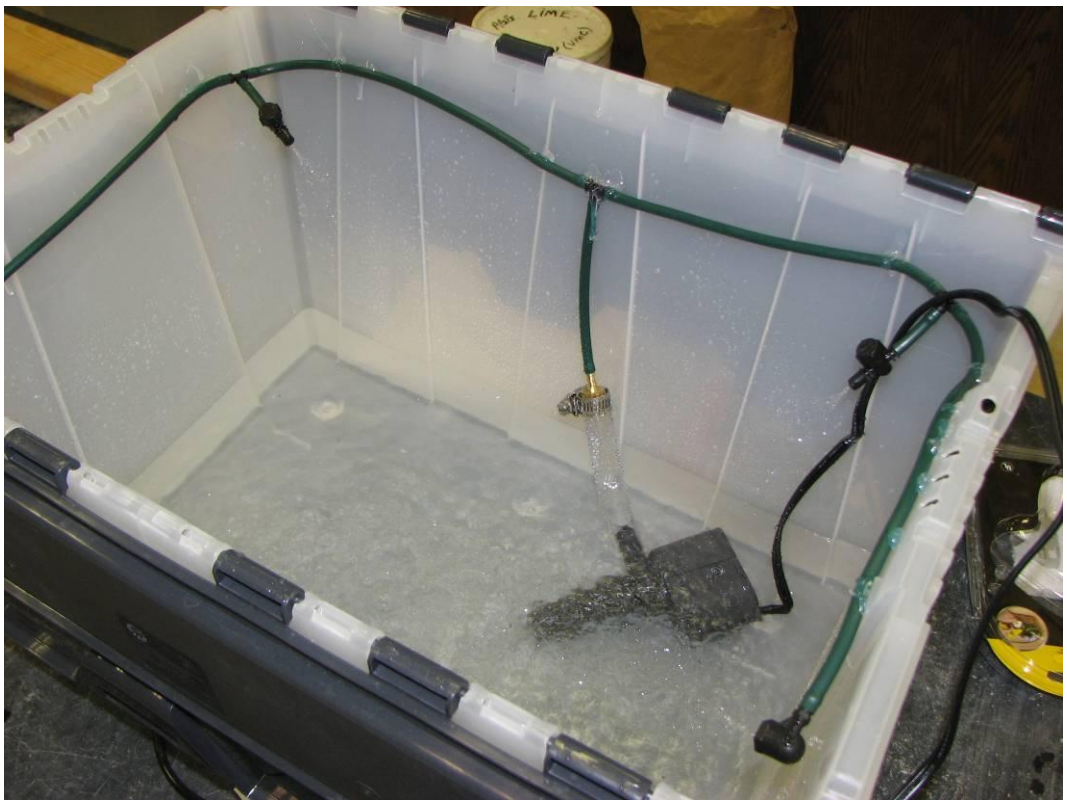

Figure 4.10 - Chamber with misters spraying

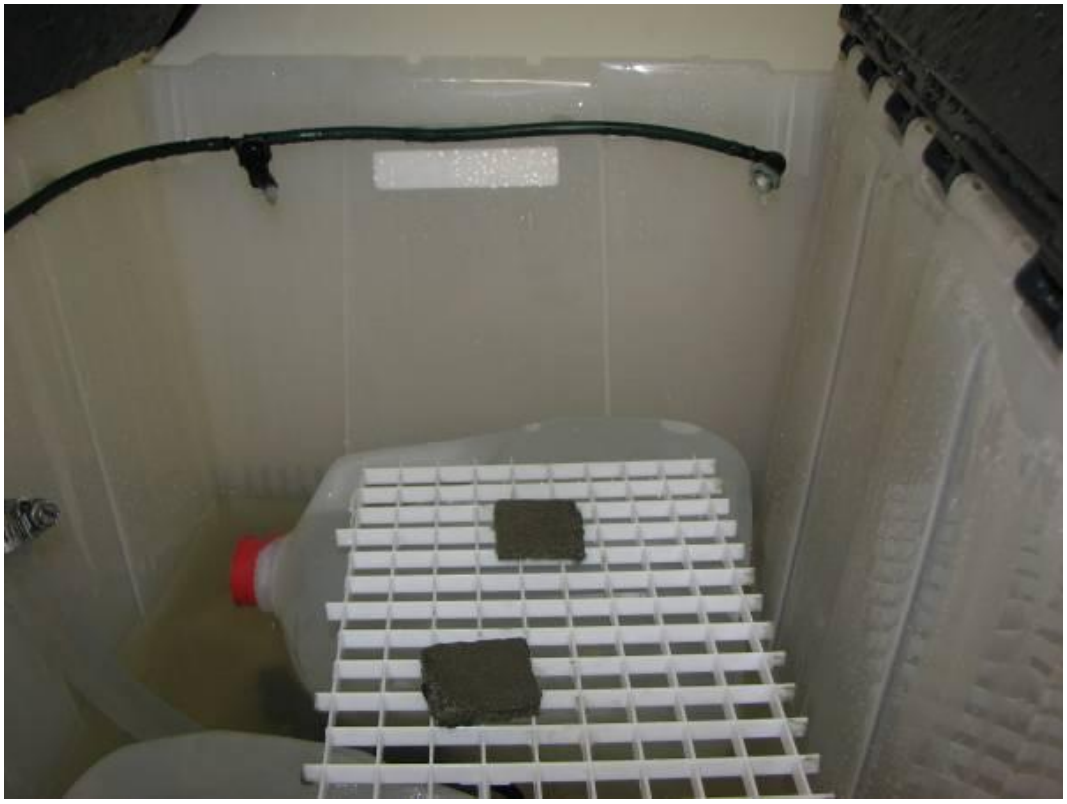

Figure 4.11 - View of Chamber

The chambers were sterilized by running a 10% bleach solution for 24 hours, emptied, and then run with sterile water for 12 hours to dilute any remaining bleach. The tiles were not sterilized by autoclaving or ethanol. Instead, a negative control chamber with 10% potato dextrose media was prepared the same way to check for contamination.

After 7 days, fungi coated the tiles and rough parts of the chamber, as seen in Figure 4.12. Chambers with deionized water as liquid showed no growth after 7 days. The negative control chamber with no fungal inoculant and potato dextrose media showed no growth.

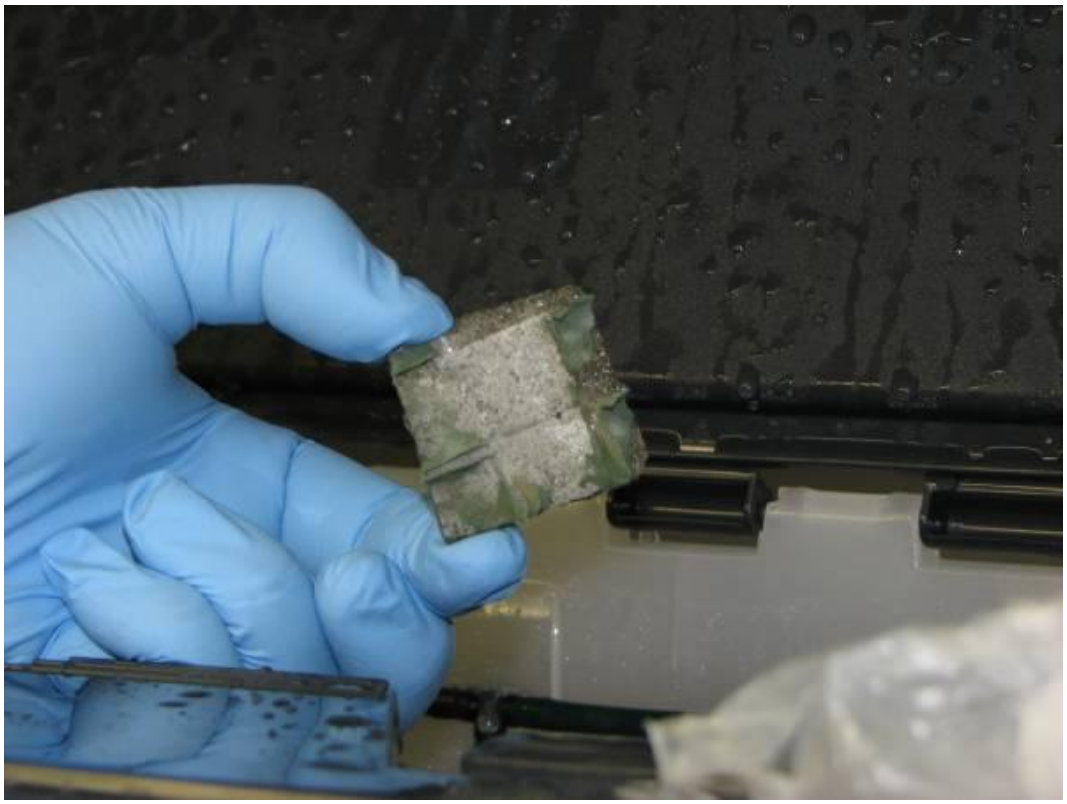

Figure 4.12 - Green *T. Viride* growth after 7 days

4.2.5.3. Suitability of Method

The technique is applicable to natural conditions for the sites examined because it can simulate natural rain and daylight cycles. Additionally the methodology also appears to be flexible, because it was shown to be suitable for growing various fungi (*Thiobacillus intermedius* and *Fusarium* sp.) and algae (cyanophyceae and chlorophyceae). Unlike the "dry" inoculation method, neither of the prior researchers carbonated their samples, and instead allowed the constant washing to leach calcium hydroxide from the surface and lower the surface pH. This may have led to the long periods necessary to identify growth in the prior research.

The test method is similar to a possible colonization method: fungi lands on a concrete surface and grows when nutrients are supplied by rain. This test allowed for

rapid growth of fungi due to a carbon loading on the tiles much higher than seen in nature. Estimating 100 μL to cover the tile, turning over once per minute leads to a loading rate of 100,000 gC/m^2yr. Typical quantities of dissolved organic carbon in rainwater range from 2-4 gC/m^2yr. However, this meets the criteria of accelerating natural processes, because the method simulates the dissolved organic carbon (DOC) present in rainwater that may act as a nutrient source. Additionally, the latent period likely due to an initially uncarbonated surface seen in nature was artificially removed.

Environmental scanning electron micrography (ESEM) was used to assess the similarity in growth between laboratory and natural conditions. A FEI Quanta 200 ESEM at Tennessee Tech University was used to image both samples taken from the Gainesville, LaGrange and Pembroke sites and from tiles tested using method 4. All samples were placed on a peltier stage capable of cooling the tiles to 5^o C and imaged in an 85% relative humidity atmosphere at 733.3 Pa.

Figure 4.13 shows the growth of *T. viride* on the surface of a mortar tiles inoculated using test method 4. Figure 4.14, Figure 4.15, and Figure 4.16 show ESEM micrographs of samples chipped from the surface of the LaGrange, Pembroke and Savannah sites, respectively.

In all the figures shown, the microbes are primarily located on the surface. The growth developed in the laboratory appears to mimic the appearance of growth in a natural environment, including filamentous hyphae, dimpled spherical spores, and multi-nucleated cells. Growth on the laboratory tile was much more dense than found on any natural environment, but this is likely due to the overabundance of food source present in the test.

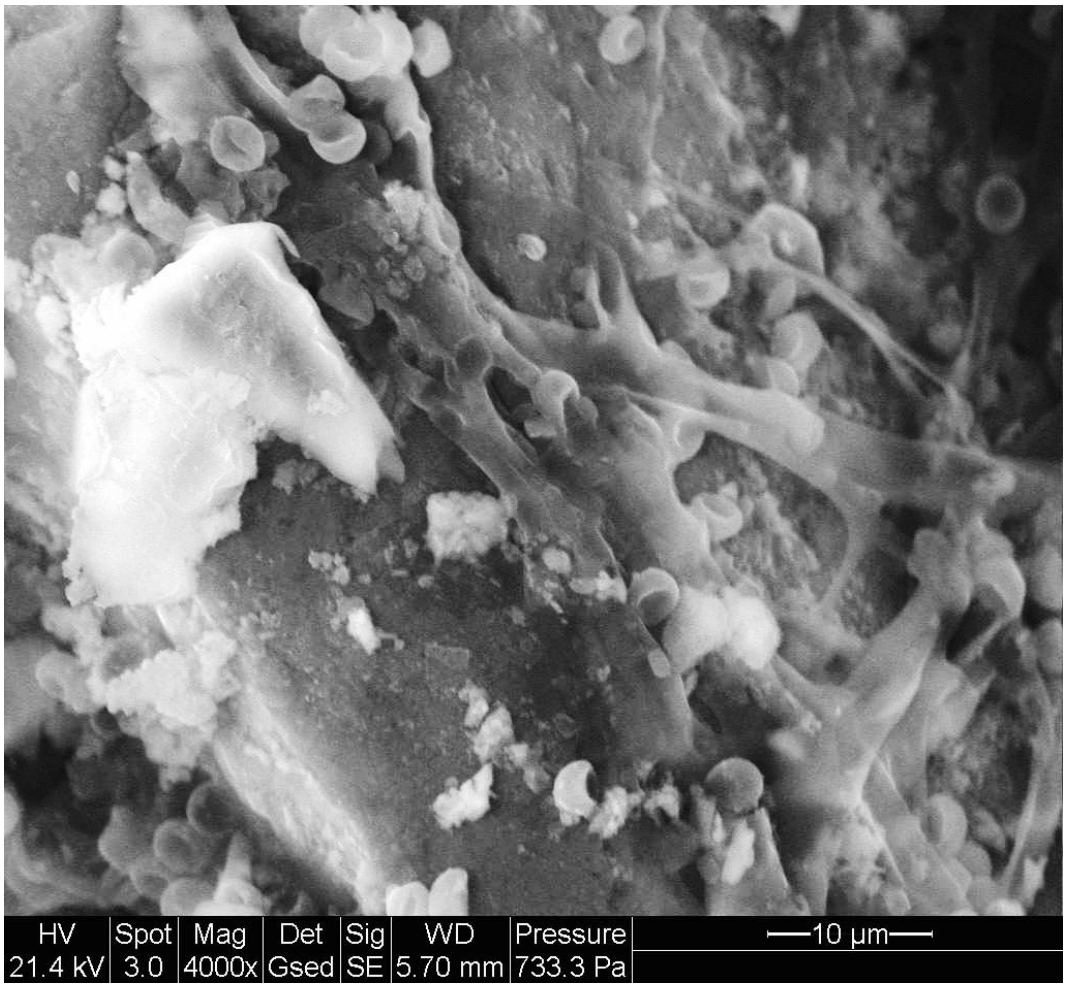

Figure 4.13 - ESEM micrograph of laboratory grown T. viride

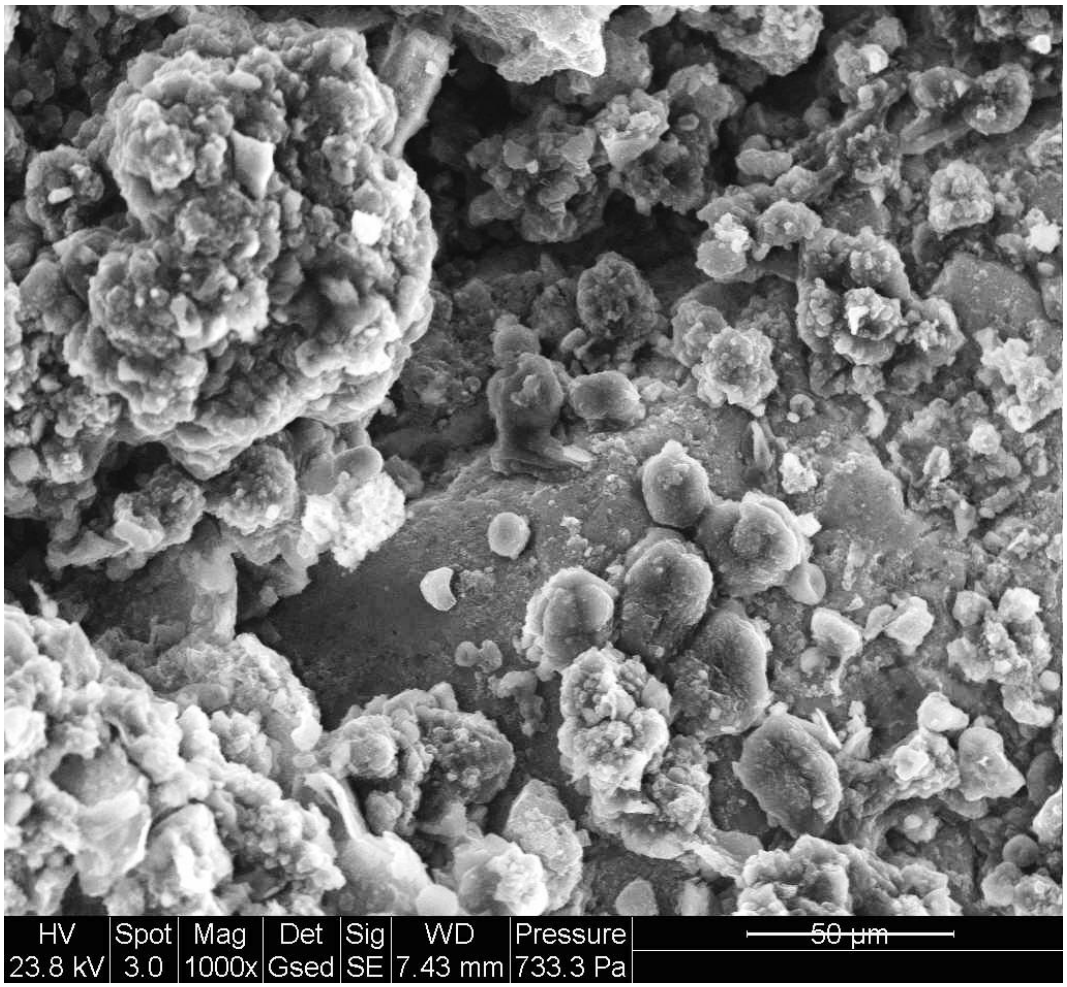

Figure 4.14 - ESEM micrograph of sample from LaGrange site

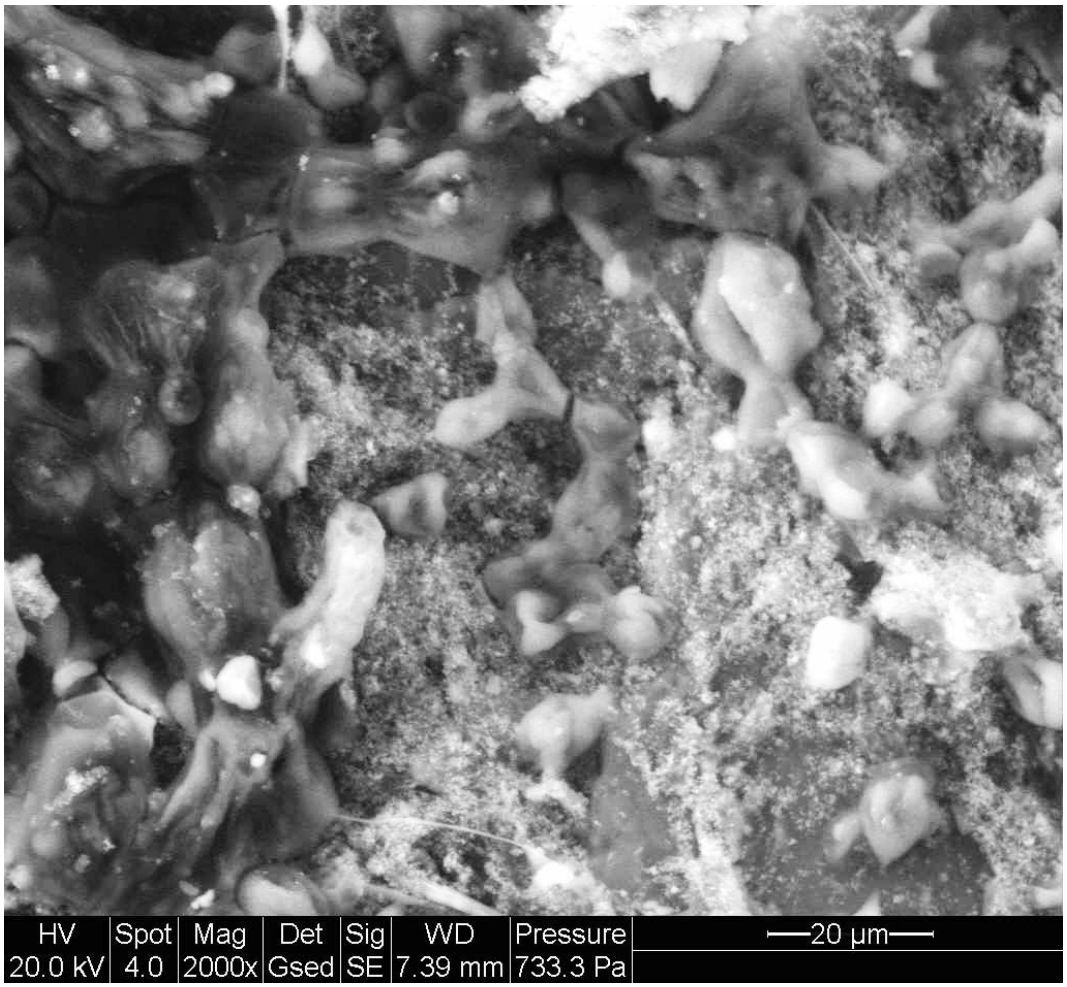

Figure 4.15 - ESEM micrograph of Pembroke site

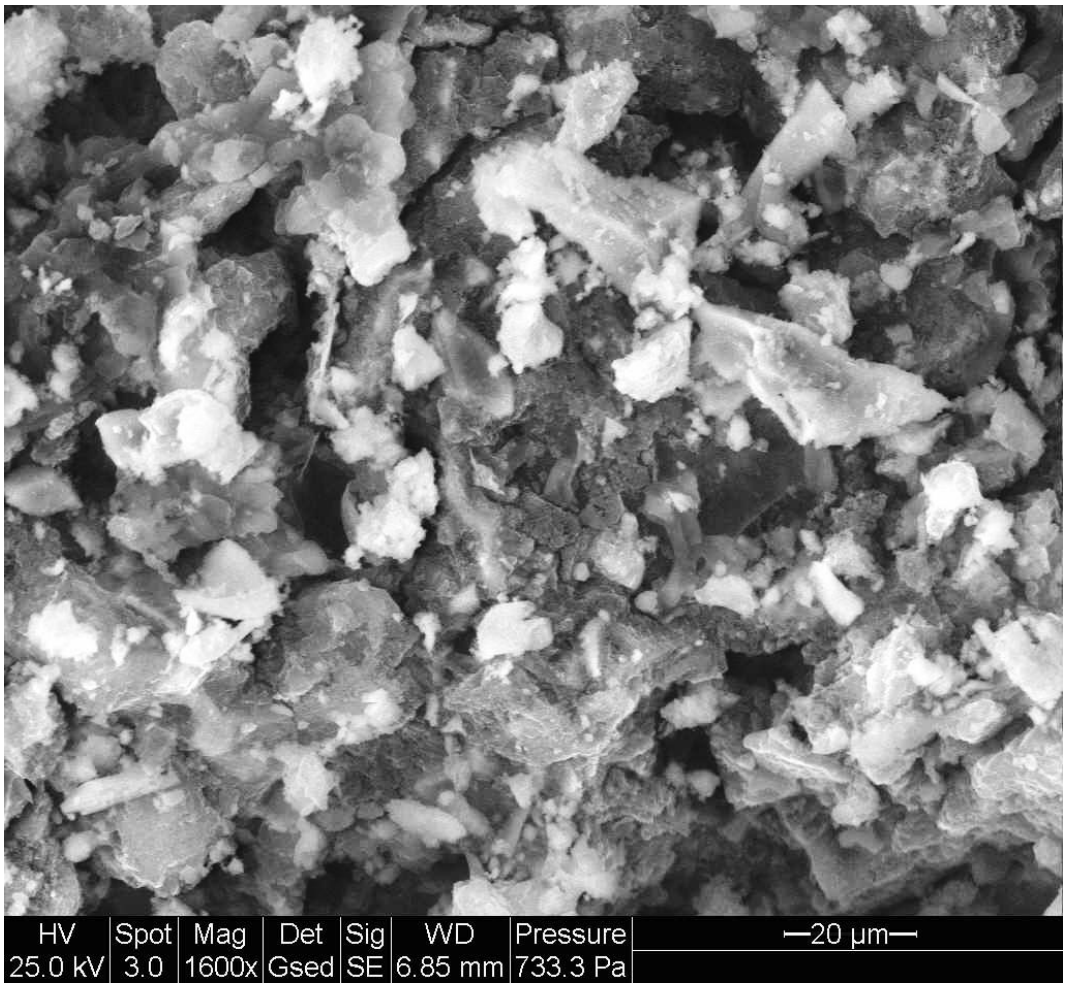

Figure 4.16 - ESEM micrograph of Gainesville site

However, it was not possible to reuse the test set up due to the difficulties in resterilization, their size, and the amount of liquid required to operate them. The large opening on the top of the chamber allows for a greater possibility of contamination when any solutions or test specimens are added. This test would be better suited for multiple experimental runs if scaled down to a smaller volume.

4.3. Development of New Test Method

The previous methods described do not meet all the criteria necessary for this research: reusability, repeatability, adaptability, and accurate, accelerated simulation of

natural conditions. Therefore, a new test method was developed that is a modification and improvement of the prior method described. This method also requires complete carbonation of the mortar tiles, to enable rapid colonization by microbes. The system used in this method will be smaller in volume, allowing for easier disposal and sterilization. Additionally, this method will allow for the use of artificial lighting to test photocatalytic effects. The accelerated experimental result will allow for the investigation of the relationship among many concrete parameters (w/cm, SCM addition, surface roughness), biological parameters (mediums, various microbes, lighting conditions), and biofilm growth rates.

4.3.1. Test Description

This method used the same principle as method 4, using a liquid media rain to wash over tiles inoculated with microbes. However, this method used the same misters and pumps as previously described in Section 4.2.5.2, but with each mister attached to a 120 mm diameter, 500 mL- capacity polypropylene autoclavable plastic canister, with a translucent container and opaque lid. The canisters were oriented with the lid on the bottom, so future tests with artificial lighting could penetrate through the translucent plastic. The pump (Maxi-Jet Powerhead/Pump Model 1200) was located in a separate container (3”x6” cylinder mold), used as the media reservoir and attached to the individual canisters by ¼” polyvinyl tubing. Drain holes were run through the lids of the plastic canisters to create a closed loop. All penetrations drilled through plastic (e.g., for sprayer and drain hole installations) were sealed with plastic hot glue, as shown in Figure 4.18. A schematic and photograph of this system is shown in Figure 4.17 and Figure 4.19, respectively.

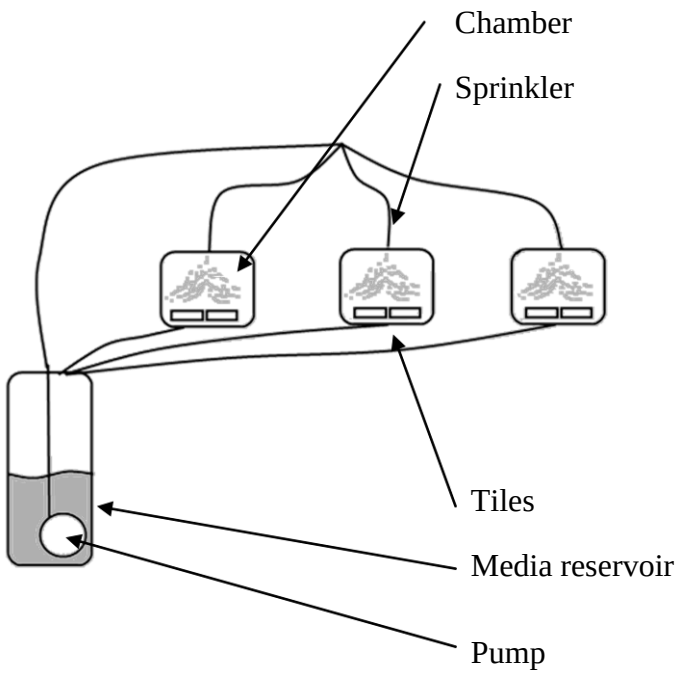

Figure 4.17 - Schematic of test setup

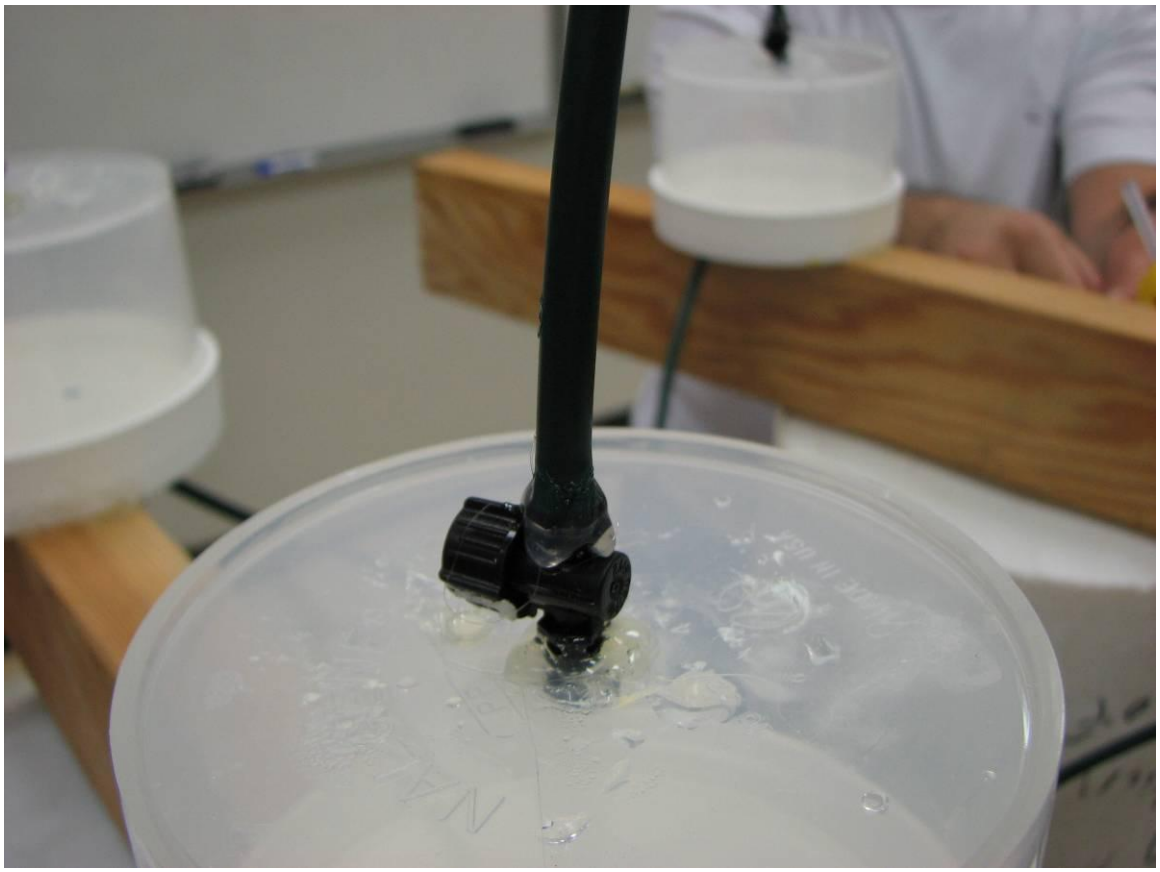

Figure 4.18 - Closeup of penetration sealed with hot glue

Figure 4.19 - Photograph of system

This system uses a smaller amount of liquid media than the larger scale chambers (~700 mL), while still allowing up to 16 3x3 cm tiles to be tested simultaneously. The individual chambers are easier to sterilize due to their smaller size. Unfortunately, the

whole system cannot be autoclaved between runs due to the incompatible nature of the sprinkler, tubing, and hot glue. However, sterilization of the system was accomplished by the following technique:

1. Run 15% bleach solution through system for 24 hours
2. Wipe the inside of the containers to remove bleach
3. Rinse with a sterile water solution for 12 hours

The most rapid and repeatable test results were obtained by running the system on 6 hour on/off cycles. Constant spray caused continuous pooling on the surface of the tiles in the chamber and may have led to reduced attachment to the surface. The "off" cycle allows the media to soak into the tile, making it easy for the microbes to attach to the concrete surface. Under these conditions, growth can be observed through the transparent plastic container between 3-6 days.

4.3.2. Laboratory Growth Compared to Site Growth Patterns

4.3.2.1. Visual Appearance

Replicating the visual appearance of the in situ biofilm growth under laboratory conditions provides further confirmation that the accelerated testing approximates field growth conditions. Thus, the visual appearance of the laboratory and in situ growth were compared. Immediately after removing the tiles from the moist environment of the test chambers, the appearance of biofilm growth is gelatinous and may be a pale green or other color, as shown in Figure 4.20. After allowing the tile to dry while covered at ambient conditions (25 C, 50% RH), the visual appearance of biofilm growth is much darker and is similar to that seen in the field. Figure 4.21 is an example of a dried tile from the test chamber and is visually similar to a typical patchy biofilm seen at the

Atlanta site, shown in Figure 4.22. The hues of the biofilms are different, which can be explained by two reasons. First, the biofilms are grown on different media: potato dextrose broth and an unknown environmental source for the site. Although the potato dextrose broth did not stain the tile, it may provide nutrients that cause the fungus to appear a different color. Second, the choice of media could be biased for certain microbes. If the proportion of one species to another is not the same as the field, the biofilm may again appear a different hue.

Figure 4.20 - T. viride on tile immediately after removal from moist chamber (3x3 cm)

Figure 4.21 - T. viride dried on surface after 4 days exposure to 50% relative humidity (3x3 cm)

Figure 4.22 - Biofilm at Atlanta site; F.O.V. 20 cm

4.3.2.2. Relating Growth Rates to Field Observations

The mean biofilm coverage was ~40% for the entire sample of tiles tested. Assuming that the test is perfectly accelerating natural processes, this would be equivalent to a site with approximately the same percent of area covered. For this study, the site in Atlanta was found at a mean of ~40% coverage. This site was constructed 23 years ago and can be estimated to receive approximately 2 $g*C^{-}1*m^{-}2*yr^{-1}$ from dissolved organic carbon in rainwater alone. As such, this site would have received a carbon flux of 46 grams/m^2 of carbon over its lifetime.

The 20% nutrient media broth contains 4.6 g/L of carbon, of which 700 mL was added to the media reservoir. Assuming that the biofilm on each tile uses 1/64 (1/4 of the 16 tiles in the tank) of the total available carbon, the carbon flux on each tile is 6.1

$g*C^{-1}*m^{-2}*day^{-1}$. This calculation can be seen in Equation (4.3), in which the carbon available is the total in the broth in the media reservoir and the utilization is the amount used by the biofilm on each tile. Over a period of 7 days, this is a total carbon flux of 42.9 g/m^2, which is remarkably close to the estimated flux for the Atlanta site.

$$flux = \frac{carbon\ available * utilization}{tile\ area * time}$$

$$6.12\ \frac{gC}{m^2 day} = \frac{\left(4.8\ g/L\right)(.7L)\left(\frac{1}{64}\right)}{(.035^2\ m^2)(7\ days)} \qquad \textbf{(4.3)}$$

4.4. Conclusions

Replicating and accelerating natural conditions in a controlled laboratory environment poses challenges. First, natural food sources vary greatly by time (variation in seasons and weather conditions), global environment (changes in local flora and fauna, temperature, and pollution), and local conditions (variations in shape and surface characteristics and lighting). Second, sampling microbes is an incomplete process. Collection by surface contact may bias the results by selecting only microbes present at that particular time. Since this is only a current state of the ecosystem, attempts to recreate the ecosystem may not be possible, since the initial colonizing organisms may no longer be present. Third, natural environmental stressors include variations in UV radiation from the sun, intermittent periods of desiccation, and variations in temperature.

Despite the difficulties of simulating a natural environment, it is believed that the newly developed method described in this chapter is a promising laboratory test. The small volume, closed loop system of containers produces repeatable results and is

reusable with simple sterilization techniques. The inoculation technique simulates the contact contamination under "Means for Colonization" in Figure 4.23. ESEM micrographs showed biofilm growth obtained under lab conditions is morphologically similar to biofilms on concrete and painted coating from the field. Photographic evidence shows that some aspects of the biofilm's macroscopic appearance can be reproduced in the laboratory. This method also allows for multiple tiles to be tested simultaneously to examine effects of "Hospitable Surfaces". Additionally, variations in "Growth Factors", such as food and water availability, can be easily implemented with varying media or cycling duration of the spray.

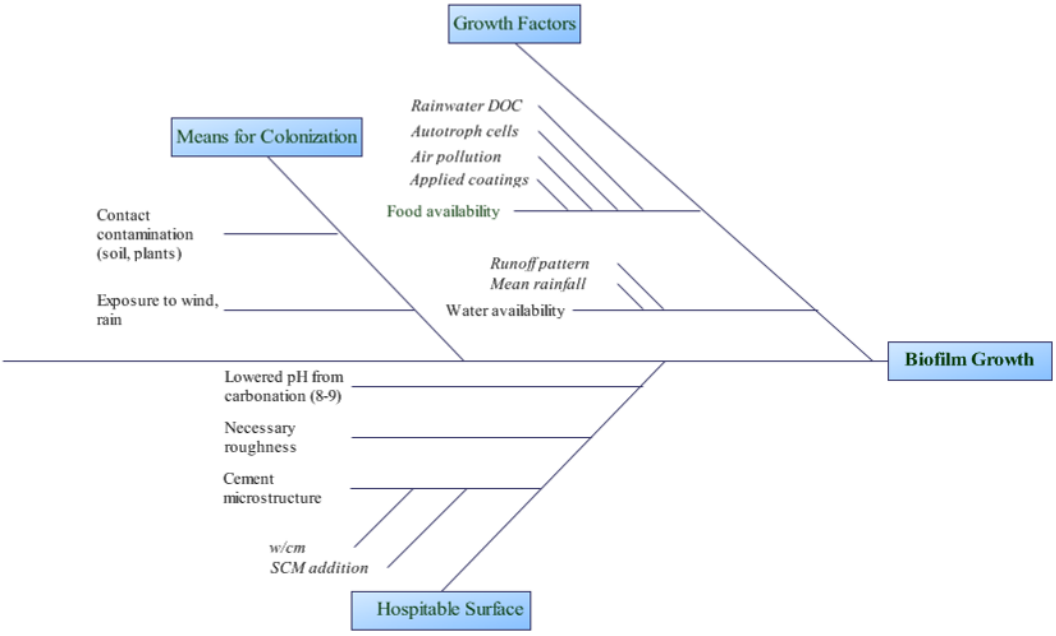

Figure 4.23 - Causes of Biofilm Growth

CHAPTER 5:

INFLUENCE OF MORTAR PROPERTIES ON BIOFILM GROWTH

5.1. Introduction

In Chapter 3, the relationships between concrete properties and biofilm coverage, both measured in the field, were described. Generally, it was observed that the influence of concrete properties, such as compressive strength and permeability, were less than other dominating site and environmental factors (e.g., rainwater runoff patterns, surface orientation, nutrient availability). Furthermore, the limited variation in concrete strength measured in the field[1] coupled with the inherent variability of field measurements of strength and permeability (as compared to laboratory methods) suggest that further investigation is necessary to understand the relationships between concrete properties and biofilm growth, as well as to assess the implications this growth on the host concrete.

Therefore, experiments were performed under controlled environmental conditions to determine the influence of concrete properties biofilm growth rates, as assessed by manual image analysis. The variables examined include: w/cm, compressive strength, SCM type and replacement level, surface roughness, and cement composition, including photocatalytic cements. In addition, biological properties including microbial community composition and nutrient source were examined. Additionally, any effects of

[1] GDOT specification 500.1.03 for the structures examined allow for only a narrow range of w/cm, 044-0.49, and minimum 28-day compressive strength, 3000-5000 psi, [20]. This consistency in desired properties provides a rather limited data range when considering concrete in the field alone.

biofilm growth on concrete performance were examined using optical microscopy and Rockwell hardness measurements.

5.2. Methodology

This study was designed to determine the differences of mortar properties on biofilm growth. The variables tested include w/cm, cement composition, use of SCMs, use of chemical admixtures, and surface finishes (i.e., roughness), as shown in Figure 5.1. Multiple cements were selected for evaluation, including two Type I/II cements, a Type I/II cement interground with 5% limestone, and a Type I/II cement produced with photocatalytic titanium dioxide. Oxide analyses for all of the cements are given in Table 5.9. The Holcim Type I/II cement used is a typical commercial cement used in Georgia. That cement, which is interground with limestone powder, conforms to ASTM C 150 and is currently under review for use in state construction projects. The Essroc cements were used to examine whether that manufacturer's photocatalytic TiO_2 (TX Aria) cement could mitigate microbial growth. That cement with and without TiO_2 (Essroc Type I/II) was examined.

Several commonly used SCMs were examined, including slag, fly ash (Class C), silica fume, and metakaolin; oxide analyses for these materials are given in Table 5.9. The cement replacement ratios for the SCMs selected range from typical minimum amounts used in practice to maximum amounts allowed by the GDOT specification 830.2.03 (fly ash) 500.3.04.D.5 (slag) [20].

The w/cm ratios were chosen to allow for variation around a typical GDOT construction w/cm of 0.44 [20], as well as higher w/cm, building upon literature which suggests that lower strength and more permeable concrete's are more susceptible to

microbial growth [55]. The w/cm's examined were 0.30, 0.40, 0.50, and 0.60, Many of the various conditions (e.g., influence of SCM type and dosage, effect of surface finish) were examined at a w/cm of 0.50, as indicated in Table 1.

The influence of various commonly used chemical admixtures was also examined. Air entraining agent (Sika AEA-14) was used with Holcim Type I/II cement at a w/cm of 0.50 for a target air content of 6%, typical for concrete exposed to freeze-thaw conditions. Water reducing agents were used to increase workability of w/cm mixes less than 0.50 and were not examined for their effect on biofilm growth, because the change in w/cm was expected to play a larger role than the presence of the chemical admixture. A mid-range lignosulfate water reducing agent (W.R. Grace WRDA 35) was used for 0.40 w/cm mixes. A high range polycarboxylate water reducer (Sika Sikament 2000 HRWR), capable of water reduction of 30%, was used for 0.30 w/cm mixes.

Roughnesses were designed to simulate various types of GDOT finishes (e.g., smoother Type III Rubbed vs. rougher Type IV Floated), as well as the application of paint to the concrete surface, as described in GDOT specification 500.3.05.AB [20]. Details about the surface preparation and alteration are provided in Section 5.2.2.

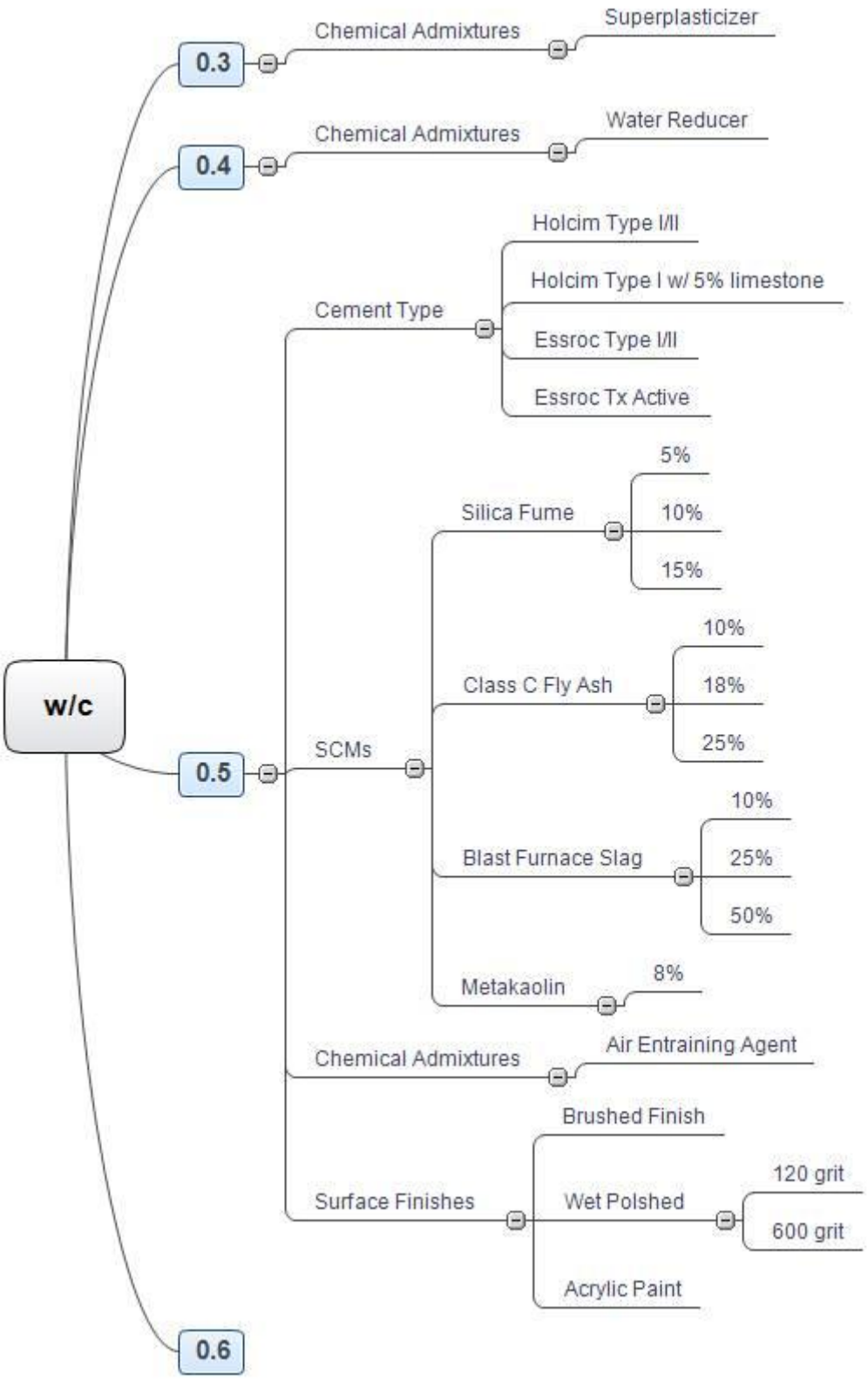

Figure 5.1 - Organization map of variables for project

Selected combinations of these concrete variables were selected for this research, with the intention of enabling comparisons from a baseline of 0.5 w/cm OPC. Table 5.1 shows the combination of mixes used in this study.

Table 5.1 - Mixes used in study

Mix ID	w/cm	SCM	Surface	Cement	Admixture
A	0.3	None	Brushed	Holcim Type I/II	superplasticizer
B	0.4	None	Brushed	Holcim Type I/II	WRDA
C	0.5	None	Brushed	Holcim Type I/II	none
D	0.6	None	Brushed	Holcim Type I/II	none
K	0.5	None	Brushed	Essroc Tx Aria	none
W	0.5	None	Brushed	Essroc Type I	none
G	0.5	None	Brushed	Holcim w/ LS	none
V	0.5	None	Brushed	Holcim Type I/II	AEA
M	0.5	FA (10%)	Brushed	Holcim w/ LS	none
N	0.5	FA (18%)	Brushed	Holcim w/ LS	none
O	0.5	FA (25%)	Brushed	Holcim w/ LS	none
P	0.5	Slag (10%)	Brushed	Holcim w/ LS	none
Q	0.5	Slag (25%)	Brushed	Holcim w/ LS	none
R	0.5	Slag (50%)	Brushed	Holcim w/ LS	none
S	0.5	SF (5%)	Brushed	Holcim w/ LS	none
T	0.5	SF (10%)	Brushed	Holcim w/ LS	none
U	0.5	SF (15%)	Brushed	Holcim w/ LS	none
MK	0.5	Metakaolin (8%)	Brushed	Holcim w/ LS	none
X	0.5	None	Painted	Holcim w/ LS	none
Y	0.5	None	polished (600 grit)	Holcim w/ LS	none
Z	0.5	None	polished (120 grit)	Holcim w/ LS	none

5.2.1. Biology Variables and Microbe Selection

Four sites (highway concrete structures in Atlanta, Gainesville, LaGrange and Savannah) were initially selected for detailed analysis from field surveys of over 20 sites, based on diversity in geographical and environmental conditions and variations in biofilm appearance. Cultures from these sites were grown on agar plates and separated by appearance to develop a supply of microbe isolates for inoculation during laboratory

studies. Additionally, a pure strain of *Trichoderma viride*, which was found to be present at the Atlanta site, was ordered from the American Type Culture Collection (Rockville, MD) and cultured. *T. viride* was selected for its morphological characteristics, (i.e., green pigmentation), and ease of cultivation which makes it ideal to use as a positive control strain. In addition to testing with pure cultures, indigenous microorganisms obtained directly from the study sites were also used in these assays.

Isotonic saline solutions for inoculation were prepared by washing the surface of the agar plate containing a single type culture. A site inoculation was created by combining equal volumes of solution (not necessarily equal concentrations of cells) from all isolates from a particular site. Tests denoted as "combined" were run with a combination of cultures from all four sites. Although the DNA analysis found both bacterial and fungal species, the cultural analysis isolates are only fungal species.

Table 5.2 - Microbial Types used in study

Fungal Population	Media
– Atlanta o *Trichoderma viride* o *Alternaria raphani* o *Fusarium oxysporum* o *Aspergillus niger* – Gainesville o *Alternaria raphani* o *Cladosporidium cladosporoides* – LaGrange o *Udeniomyces pseudopyricola* o *Phoma* sp. – Savannah o *Cladosporidium cladosporoides* o *Epicoccum* sp. – Pure culture o *Trichoderma viride*	– 20% potato dextrose broth – Sterilized rainwater – Sterilized rainwater with added diesel exhaust particulates – Sterilized rainwater with form release oil on tiles

5.2.2. Mortar Tile Preparation

Mortar tiles (sand and cement paste) were selected to best represent the growing surface in the field. Previous research by Housewright et al. [24] indicated that biofilm growth was primarily a phenomenon that occurred on the surface of the cement paste and small aggregate in concrete, not on the large aggregate. Mortar tiles (6x6x0.4 cm) for inoculation testing and mortar cubes (2x2x2 in) of various mixes were prepared in small batches. Mortar cubes were cast in general accordance with ASTM C-109, "Standard Test Method for Compressive Strength of Hydraulic Cement Mortars.", with sand/cement equal to 2.75, A local, natural sand fine aggregate was chosen with a fineness modulus of 1.7. Mortar tiles were cast against flat galvanized steel in forms made of plastic deck trellis, as shown in Figure 5.2. All surfaces were coated with a water-based form release agent (W.R. Meadows Duogard II). For the first 24 hours, samples were kept moist under plastic sheeting.

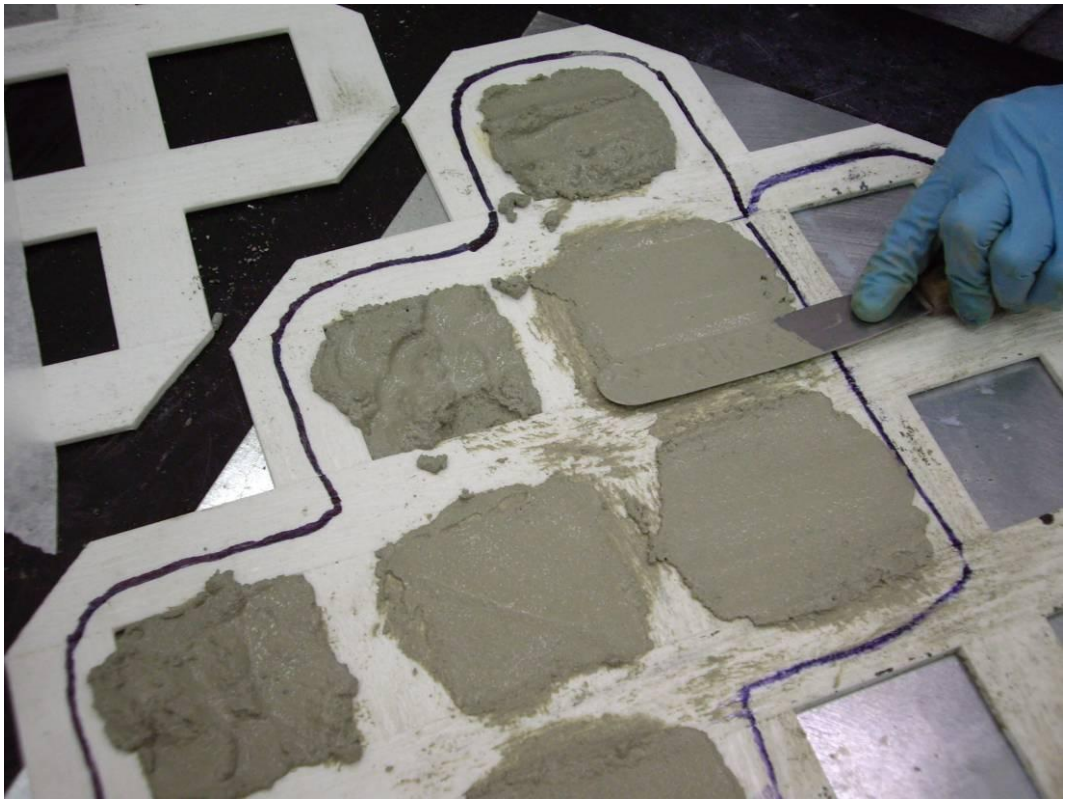

Figure 5.2 - Casting mortar tiles on metal and plastic formwork

Four surfaces finishes were tested for this study. The first and roughest type of finish was similar to a GDOT Type IV Floated Surface Finish [20]. The tile surfaces were screeded and floated with a flat stainless steel trowel and then brushed in one direction with a paintbrush. The second and third types of finishes are similar to a GDOT Type III Rubbed Finish. These finishes were performed after the tiles had cured for 24 hours. The second finish, designed to be an intermediate smoothness, was performed by wet polishing Type IV finish tiles with 120 grit Si-C polishing paper. The third finish, designed to be the smoothest, was performed by wet polishing with 120 grit Si-C polishing paper, followed by coating the surface with cement paste produced at w/cm of 0.50 (same as the tile), and wet polishing with 600 grit Si-C polishing paper 24 hours after applying the paste. All polishing was performed using a variable speed wet rotary

polisher. This third type of surface finish was designed to be similar to the field practice of "whitewashing" or "rubbing", while still controlling the surface texture. The fourth type of surface finish was similar to a GDOT Type III – Special Surface Coating Finish. After mortar tiles had been water cured for 28 days, they were dipped in water-based acrylic paint (Tamms Industries Tammscoat 2725 Fine). This is the most common paint used currently in Georgia for highway work, according to a local contractor supply store, Highway Materials, Inc. of Forest Park, GA.

After curing in limewater at 22^{o}C for 28 days, the mortar tiles were placed in a 20% CO_2, 40° C atmosphere at 55% relative humidity (Nuaire US Autoflow NU-4850 CO_2 incubator) to accelerate carbonation. The mortar tiles were exposed to accelerated carbonation to reduce the pH of the surface, thereby promoting growth of microbes and more accurately simulating field conditions. The relationship between carbonated mortar and biofilm growth was demonstrated in research by Shirakawa et al. [55]. This carbonation atmosphere was selected based on work by Papadakis [47] that indicates the rate of the carbonation reaction in concrete is near maximum at 55% relative humidity, according to Equations (5.1) and (5.2).

$$x_c = \sqrt{\frac{2D_{e,CO_2}(CO_2/100)t}{0.33CH + 0.214CSH}} \qquad \textbf{(5.1)}$$

x_c: carbonation depth(m)
CO_2: ambient atmosphere (%)
t: time (seconds)
CH and CSH: concentrations (kg/m^3)
$D_{e,CO2}$: diffusivity of CO_2 in carbonated concrete (m^2/s)

$$D_{e,CO_2} = A\left(\frac{\varepsilon_c}{\frac{C}{\rho_C}+\frac{P}{\rho_P}+\frac{W}{\rho_W}}\right)^a\left(1-\frac{RH}{100}\right)^b \quad \textbf{(5.2)}$$

A: $6.1*10^{-6}$
a: 3
b: 2.2
ε_c: total porosity
C,P,W: cement, SCM, and water (kg/m^3)
ρ_C, ρ_P, ρ_W: density of cement, SCM, and water (kg/m^3)

The CO_2 incubator is limited to operating at 20% maximum CO_2 at 5% above ambient relative humidity. Because ambient room conditions were 50-60% relative humidity at 22° C, a higher chamber temperature of 40° C was selected. This decreases the effective input relative humidity to 20%, allowing the chamber to accurately control internal relative humidity.

The carbonation depths in tiles were measured by spraying a newly fractured surface with phenolphthalein indicator solution (1% phenolphthalein, 20% water, 79% ethanol w/v). The depth to the dark pink uncarbonated region was measured with a caliper (accurate to 0.001 in) at intervals of 1, 2, 7, and 21 days, as shown in Figure 5.3. These carbonation depths are shown plotted against the depth predicted by the Papadakis model in Figure 5.4. This plot shows that the model overpredicted carbonation depth by approximately 10%. The longest period of time for complete carbonation was 35 days, for tiles with the lowest w/cm examined (0.30), as expected. Most mortar tiles were completely carbonated after 7 days of exposure.

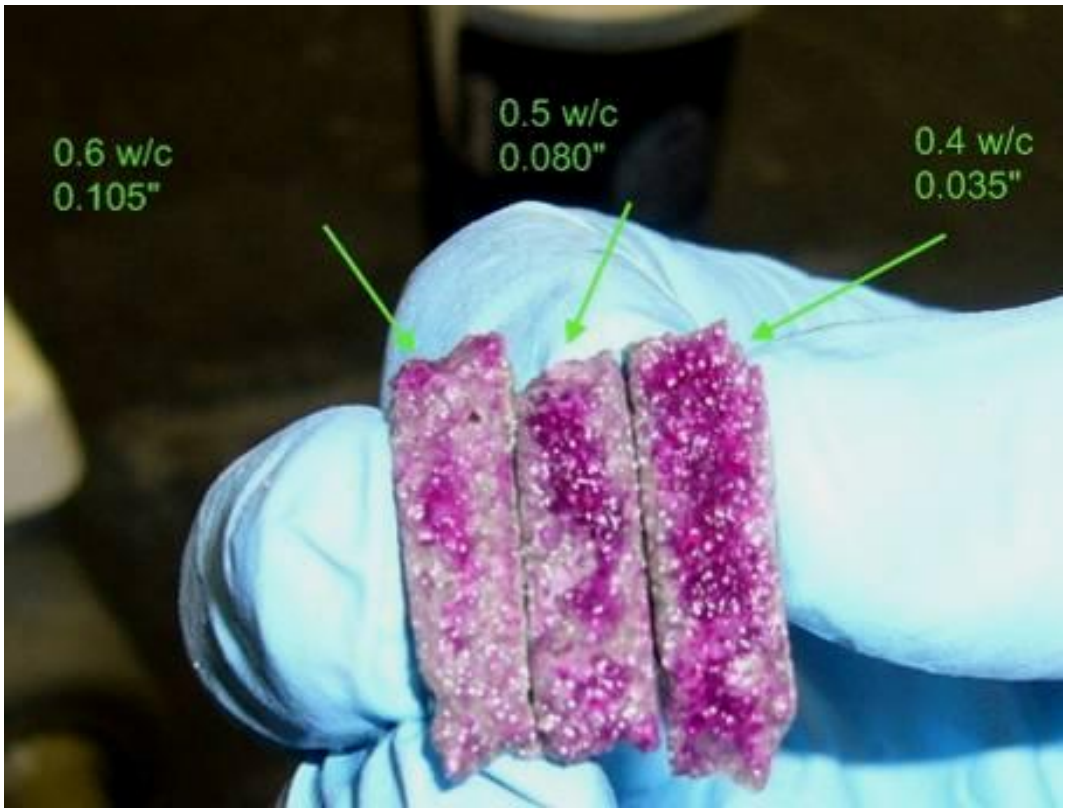

Figure 5.3 - Phenolphthalein indicator on tiles and measured carbonation depth after 1 day in incubator

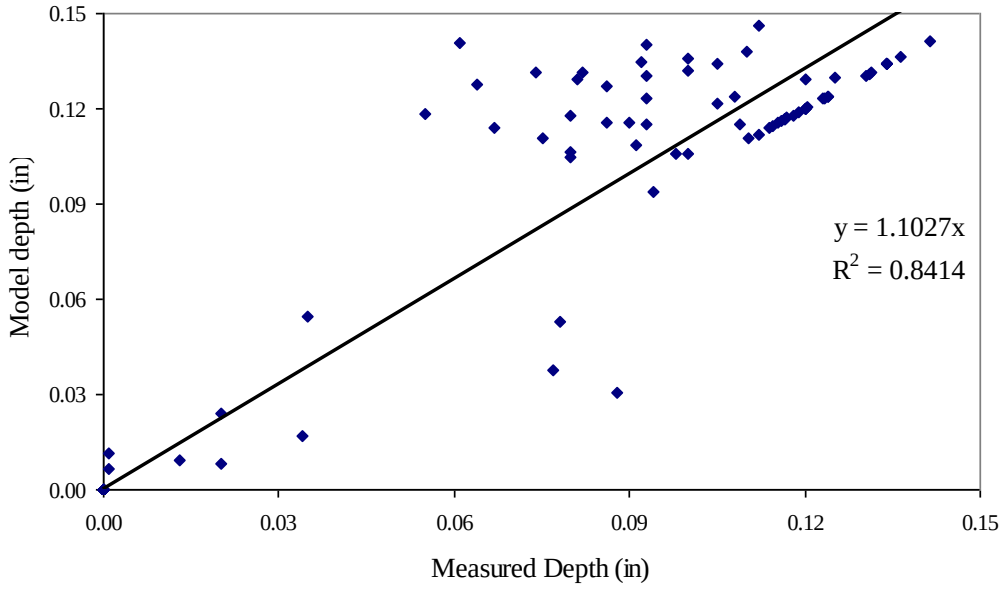

Figure 5.4 - Papadakis model vs. measured carbonation depth

5.2.3. Mortar Tile Exposure

Mortar tiles of varying compositions were exposed independently to each microbe or microbial population (e.g., *Trichoderma viride*, Atlanta, Gainesville, Lagrange, and Savannah as described in Table 5.2). That is, inoculation and exposure to each colony occurred in separate pumping systems to isolate the effects of the different microbial colonies and to prevent contamination. Mortar tiles were exposed for periods of 7 days. Further details on the exposure can be found in Section 4.3.

In addition, the effects of the photocatalytic cement were examined by comparing microbial growth under artificial lighting between Holcim Type I/II cement, Essroc Type I/II cement, and Essroc TX Active cement. Osram Ultravitalux Daylight lamps, typically used for tanning bed applications, were selected to provide a source of UV light close to a natural sunlight spectrum. The polypropylene containers described in Chapter 4 are partially transparent to UV light, absorbing approximately 50% of the UV spectrum energy. A combination UVA/UVB meter (Lutron UV-340) was used for measuring the UV irradiance under the polypropylene container. The container was moved to a distance below the lamps (approximately 14") such that the irradiance at the level of the tiles was 10 W/m^2, the recommended level for testing photocatalytic cement. The general set up with the sunlamps turned on is shown in Figure 5.5.

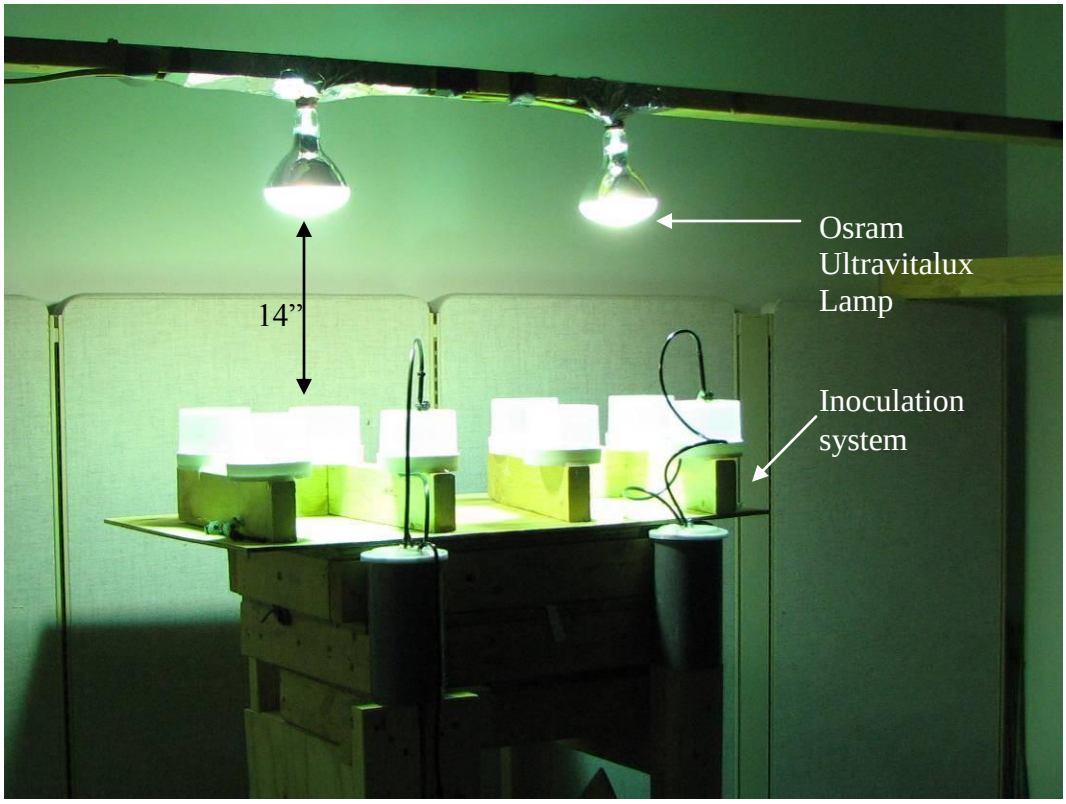

Figure 5.5 - Image of photocatalytic test

The lights were placed on a 6 hour cycle, offset by three hours from the 6 hour media cycle. As such, the tiles would experience 3 hours of media spray in the dark, 3 hours of media spray in light, 3 hours of light with no spray, followed by 3 hours of darkness also with no spray. This 12 hour cycle repeated for seven days. Photocatalytic tiles were placed in separate pumping systems from non-photocatalytic tiles, in case the photocatalytic activity affected any part of the biological system on the tile or in the media reservoir.

A second type of test was run using photocatalytic and non-photocatalytic tiles with growth from a previous run where the tiles were not exposed to UV light. In this subsequent test, these stained tiles were exposed for seven days to 6 hour cycles of artificial light at ambient conditions of 25° C and 40% RH underneath the polypropylene

containers. The containers were left with an air hole for venting, but did not have media spray.

5.3. Characterization of the Effects of Biofilm Growth

5.3.1. Rockwell Hardness Measurements

Microindentation was used to characterize any deterioration in physical surface properties due to biofilm growth. All inoculated tiles were compared to the "negative control" tiles. These tiles were run in the same media and conditions as the inoculated tiles, but were kept sterile. A Rockwell hardness tester (Wilson Instruments 103R) was used to perform superficial Rockwell 15Y hardness tests in general accordance with ASTM E 18-07 [70]. The 15Y superficial hardness test was modified to apply a 10 kgf initial load instead of 3 kgf, due to configuration of the instrument used. A 15Y superficial hardness was selected based on the paper by Winslow (1984) that presents the relation, shown in Equation (5.3), between the 15Y Hardness and compressive strength of the mortar fraction in concrete. The research by Winslow tested the mortar regions between large aggregate, and thus is applicable to the surface geometry of the mortar tiles for this study. However, the compressive strength range examined by Winslow was between 1500 and 4500 psi (10.3 – 31.0 MPa), whereas the strengths of the samples prepared are expected to be, in some cases, greater than 4500 psi (31.0 MPa). For this reason, this research will report the 15Y hardness, not the converted compressive strength.

$$15Y\ Hardness = 73.5(\log(f_c`\ in\ psi)) - 187 \qquad \textbf{(5.3)}$$

15Y Rockwell Hardness tests were performed at a minimum of 16 locations for each tile. Tiles that had non-uniform biofilm coverage were tested at a 5x5 grid of 25 locations.

5.3.2. Biofilm Coverage Measurements

A flatbed scanner, with 1200 dpi resolution, was used to capture digital images of the mortar tiles before and after exposure to the accelerated biological growth chambers. This method was selected over optical microscopy or digital photography due to its consistency in lighting and high resolution imagery of the entire surface. Because the coverage measured was macroscopic in nature, the magnification from an optical microscope was not necessary to gauge growth for most tiles.

Due to the variation in color and appearance of biofilm growth on the mortar tiles, digital image analysis performed through the commonly applied techniques of image thresholding or histogram measurement were unable to accurately describe the amounts of biofilm growth on the samples inoculated with the various combinations of microbes. Instead, a method for describing the severity of the biofilm growth, both in terms of coverage and color, was developed. Each scanned image of a mortar tile was split into a 4x4 grid of 16 squares as shown in Figure 5.6. Each square was marked with any combination of yellow, red, green, or no growth. Red and yellow growth were rarely seen in the field survey, and their increased presence in the accelerated test method may show an unintended bias in the test set up for those types of fungus. To counteract this effect, the measurements of coverage were weighted by selected amounts, as shown in Equation (5.4), to represent the field observations, which showed primarily microbial growth exhibiting dark pigmentation as is commonly seen at many of the study sites.

$$\frac{Coverage\%}{tile} = \frac{1*yellows + 1.33*reds + 1.67*greens + 2*blacks}{16\ \frac{squares}{tile} * (1 + 1.33 + 1.67 + 2)} \qquad \textbf{(5.4)}$$

The tiles were rated independently by three different observers, using digital images taken after the samples had air dried for 2 days. The ratings used for analysis were the average of these three observations. This method showed consistency between observations, with an average standard deviation between observations of 7% on a 100% scale. A standard t-test with 48 degrees of freedom (16 squares * 3 observers) quantified the differences among tiles.

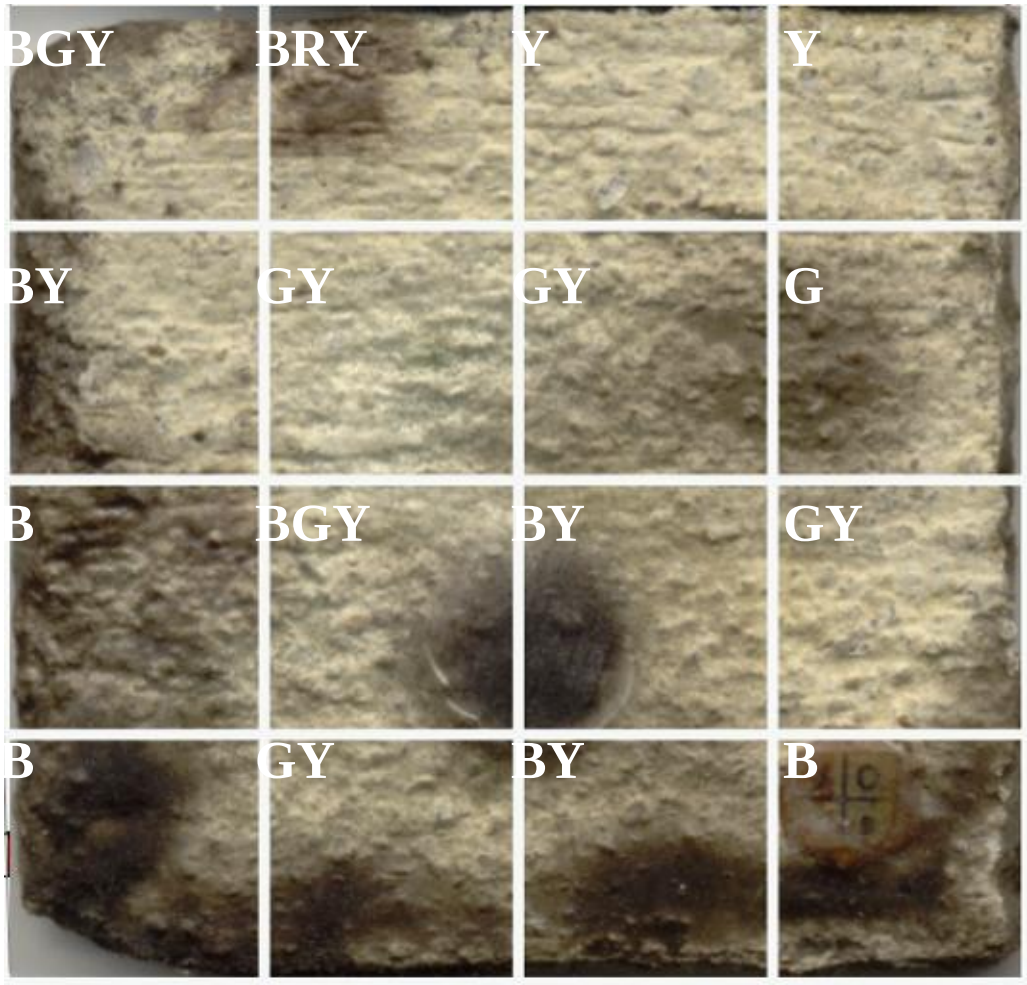

Figure 5.6 - Example of 35 by 35 mm tile split into 4x4 evaluation grid. The overall coverage rating for this tile is 43%

5.3.3. Methods of Statistical Analysis

Multiple linear regression, performed with the econometric software Limdep 7.0, was used to determine statistical significance of relation between variables and biofilm coverage. Multiple linear regression attempts to fit data into a model of the form shown in Equation (5.5). The model attempts to fit the data to a linear relation with one slope, m, accounting for differences between data sets with a constant, b_n. The models are examined for their applicability by looking at two values, R^2, a measure of how close the data lies to the model, and a p-value, a measure of statistical significance. As R^2

approaches 1, it indicates a perfect fit between the experimental data and the model. The p-value indicates the 2-tailed t-distribution probability that a coefficient is equal to zero. For this analysis, differences were considered to be statistically significant if their confidence level was greater than 90%, as determined by Equation (5.6).

$$y = mx + b_1 + b_2 ... + b_n \quad \textbf{(5.5)}$$

$$confidence\ level = 1 - P_n \quad \textbf{(5.6)}$$

28-day compressive strength (as measured on companion, unexposed mortar cubes), and surface roughness were each fit to a separate linear model. Dummy variables were used for the categorical variables, such as cement and SCM type.

5.4. Results

Table 5.3 through Table 5.5 show the roughness numbers, 28-day compressive strength, biofilm coverage, and Rockwell hardness for each tile mix, along with any measured standard deviations in those data.

Table 5.3 - 28-day mortar cube compressive strength and roughness number

Mix	f_c` (psi) ± std. dev.	Roughness Number ± std. dev.
A	10117 ± 1466	1.37 ± 0.07
B	7798 ± 1353	1.34 ± 0.08
C	6400 ± 459	1.34 ± 0.08
D	5388 ± 1007	1.60 ± 0.45
G	5232 ± 152	N/A
K	5277 ± 203	N/A
M	5400 ± 224	1.28 ± 0.11
MK	6374 ± 404	1.22 ± 0.06
N	5119 ± 303	1.41 ± 0.16
O	1925 ± 108	1.26 ± 0.06
P	5076 ± 397	1.29 ± 0.05
Q	5423 ± 362	1.32 ± 0.10

Table 5.3 (continued)

R	4578 ± 206	1.33 ± 0.05
S	4872 ± 248	1.21 ± 0.04
T	3940 ± 499	1.21 ± 0.04
U	4611 ± 183	1.64 ± 0.39
V	5277 ± 981	N/A
W	4176 ± 281	N/A
X	6400 ± 459	N/A
Y	6400 ± 459	1.14 ± 0.04
Z	6400 ± 459	1.15 ± 0.04

Table 5.4 - Biofilm coverage for each mix, separated by inoculum

Mix	Atlanta	Gainesville	LaGrange	Savannah	*T. viride*
A	34%	35%	19%	24%	24%
B	46%	41%	25%	23%	26%
C	49%	50%	21%	28%	33%
D	59%	53%	35%	37%	38%
G	41%	68%	27%	43%	25%
K	48%	56%	18%	44%	55%
M	30%	47%	43%	35%	39%
MK	45%	29%	20%	36%	40%
N	25%	50%	29%	18%	43%
O	36%	34%	40%	27%	44%
P	43%	34%	46%	38%	37%
Q	42%	28%	37%	27%	30%
R	43%	53%	43%	39%	33%
S	44%	40%	31%	27%	46%
T	42%	26%	29%	38%	36%
U	33%	29%	33%	39%	29%
V	47%	41%	28%	35%	1%
W	55%	62%	33%	32%	16%
X	37%	32%	21%	39%	6%
Y	32%	43%	28%	29%	7%

Table 5.5 - Rockwell 15Y Hardness for all measured tiles

Mix	Atlanta	Gainesville	LaGrange	Savannah	*T. viride*	neg. control
a	91 ± 4	91 ± 5	89 ± 4	90 ± 3	88 ± 4	93 ± 2
b	77 ± 10	82 ± 4	84 ± 6	84 ± 10	79 ± 14	71 ± 20
c	69 ± 16	76 ± 15	69 ± 14	80 ± 15	66 ± 11	83 ± 8
d	42 ± 15	53 ± 23	56 ± 22	48 ± 35	52 ± 23	64 ± 20
g	72 ± 12	N/A	72 ± 20	N/A	72 ± 13	66 ± 20
k	72 ± 15	74 ± 16	72 ± 11	72 ± 14	73 ± 12	75 ± 13
mk	83 ± 5	84 ± 5	83 ± 5	78 ± 7	75 ± 13	84 ± 6
m	N/A	81 ± 8	N/A	77 ± 11	N/A	78 ± 10

Table 5.5 (continued)

n	77 ± 9	82 ± 5	83 ± 7	73 ± 8	65 ± 15	77 ± 8
o	79 ± 8	83 ± 4	71 ± 11	66 ± 25	79 ± 8	81 ± 6
p	79 ± 8	79 ± 6	79 ± 11	77 ± 11	81 ± 11	86 ± 4
q	71 ± 13	72 ± 12	79 ± 6	78 ± 8	77 ± 9	65 ± 20
r	81 ± 4	78 ± 6	78 ± 10	64 ± 17	76 ± 10	80 ± 5
s	87 ± 3	85 ± 5	87 ± 4	83 ± 5	80 ± 7	81 ± 5
t	86 ± 5	80 ± 6	74 ± 13	78 ± 9	79 ± 8	83 ± 6
u	66 ± 20	74 ± 10	79 ± 8	82 ± 8	78 ± 7	80 ± 8
v	76 ± 9	80 ± 12	72 ± 18	63 ± 7	75 ± 11	69 ± 13
w	N/A	74 ± 6	84 ± 7	82 ± 15	N/A	74 ± 12
x	40 ± 11	42 ± 19	18 ± 26	20 ± 13	22 ± 14	N/A
y	85 ± 3	82 ± 30	70 ± 5	89 ± 6	92 ± 8	89 ± 9
z	82 ± 3	71 ± 7	83 ± 7	80 ± 13	87 ± 13	84 ± 7

5.5. Discussion

Generally, results with OPC tiles revealed clearer trends than mixes with SCMs. Lower w/cm and corresponding increased compressive strength generally reduced biofilm growth rates. All Type I/II OPC produced similar growth under typical test conditions, with little influence from chemical admixtures. The only cement to show significant reduction in the amount of coverage was TiO_2-modified cement under simulated sunlight. Overall, the addition of SCMs produced little change – positive or negative - in growth rates.

5.5.1. Influence of w/cm

The effect of w/cm was examined by comparing the Portland cement tiles for Mixes A, B, C, and D, with w/cm's of 0.3, 0.4, 0.5, and 0.6, respectively. All tiles were cast from the same cement and were exposed to each microbial community or microbe in a 20% potato dextrose broth.

Based upon the prior findings of Dubosc et al. [15], it was expected that the lower w/cm mixes would experience less biofilm growth due to the improved properties of the

cement microstructure, including lower permeability, smaller pores, and a stronger matrix. The results obtained verify these initial expectations, with a general trend of increasing biofilm growth from lower w/cm to higher w/cm. This relationship is similar to that found by Dubosc et al. [15], where algae growth decreased with decreasing w/cm. Unlike Dubosc's experiment, the 0.3 w/cm mix examined here did not achieve zero growth. The current research suggests that a threshold w/cm that will prevent growth may not exist for all microbial communities, although further studies at lower w/cm and with a broader range of matrix compositions should be performed.

For all w/cm examined, the Atlanta and Gainesville mixes produced greater coverage than the LaGrange, Savannah, and *T. viride* inoculums. These data do not correlate with field assessments, where the LaGrange and Savannah were determined to have the highest level of coverage. Unlike in the field where LaGrange and Savannah may have better growing conditions, each inoculation mix had the same laboratory conditions. Some possibilities for the variation between field and lab could be a higher concentration of active cells at certain sites, or a selection of media that caused more robust growth for certain species.

Table 5.6 shows the constants for multiple linear regression model shown in Figure 5.7. These numbers represent a difference in the average of biofilm growth between site inoculations. The multiple linear regression model has a higher R^2 value than most of the singular linear regression models shown in Figure 5.9 through Figure 5.13, because the multiple linear regression model can use the entire data set for estimation. Overall, these figures show a strong positive, linear relationship between w/cm and biofilm growth.

Table 5.6 - Regression model constants for w/cm

site	b_n (constant)
Atlanta	0.22
Gainesville	0.19
LaGrange	0.05
Savannah	0.03
Trichoderma	0.05

Comparing between the five different types of microbe inoculations shows a linear offset. This linearity is best seen by comparing Figure 5.7 and Figure 5.8. Figure 5.7 shows biofilm coverage plotted against w/cm. Figure 5.8 contains the same data, but with each inoculation adjusted by the constant shown in Table 5.6. This figure shows, independent of the microbe source used, the strong linear relationship between w/cm and biofilm coverage.

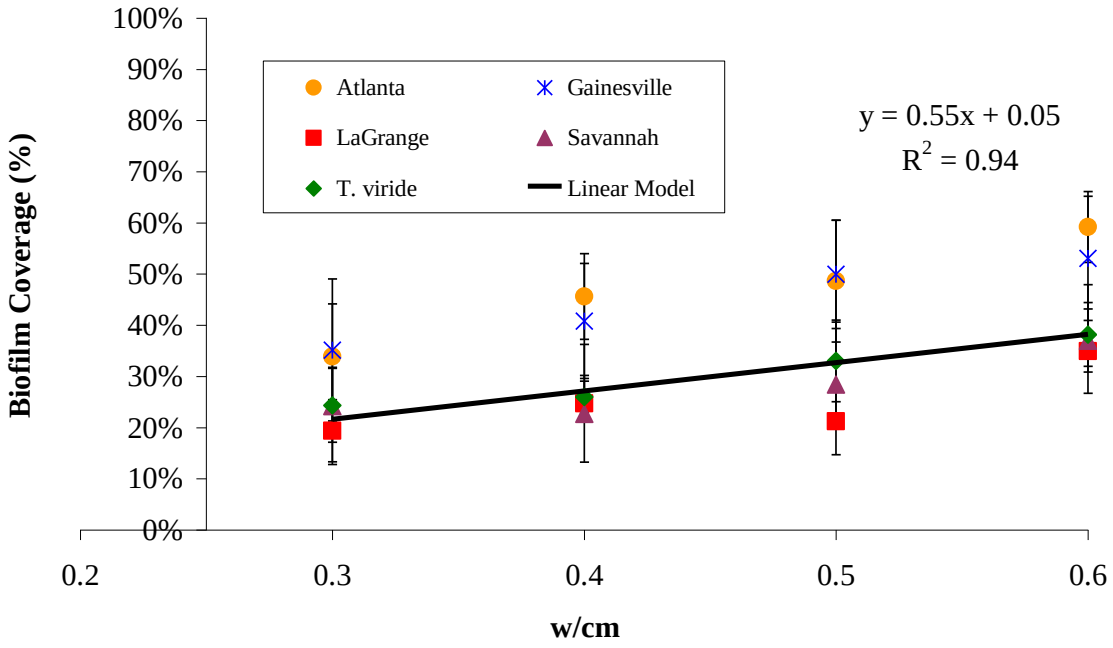

Figure 5.7 - Biofilm coverage vs. w/cm, for multiple linear regression model

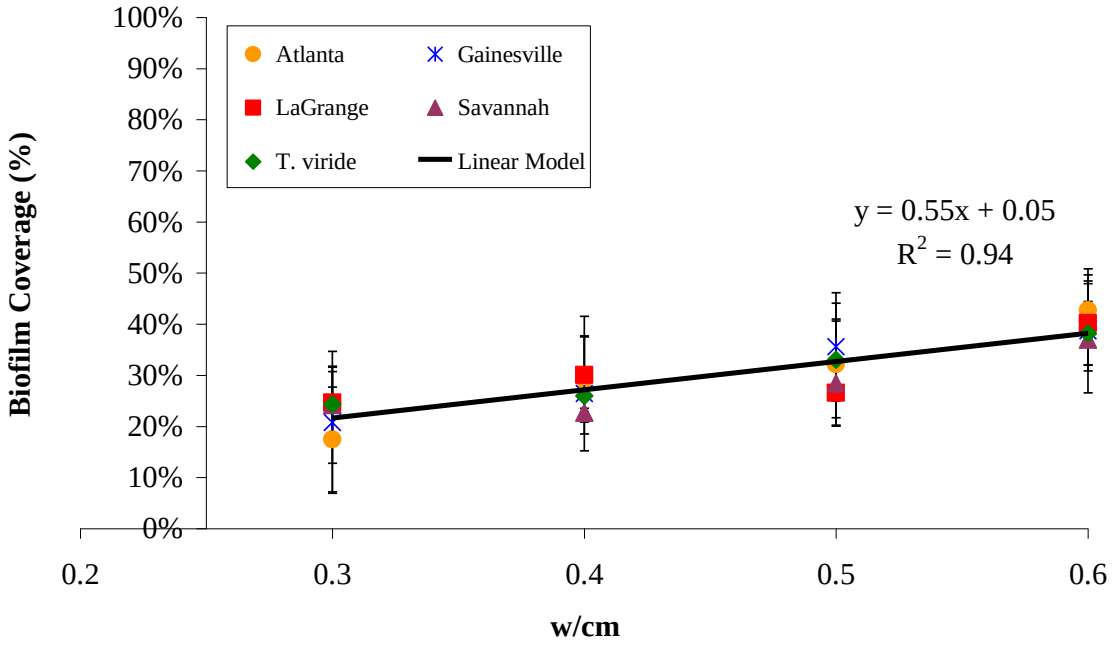

Figure 5.8 - Biofilm coverage vs. w/cm, linearly adjusted for differences in growth among site microbial communities

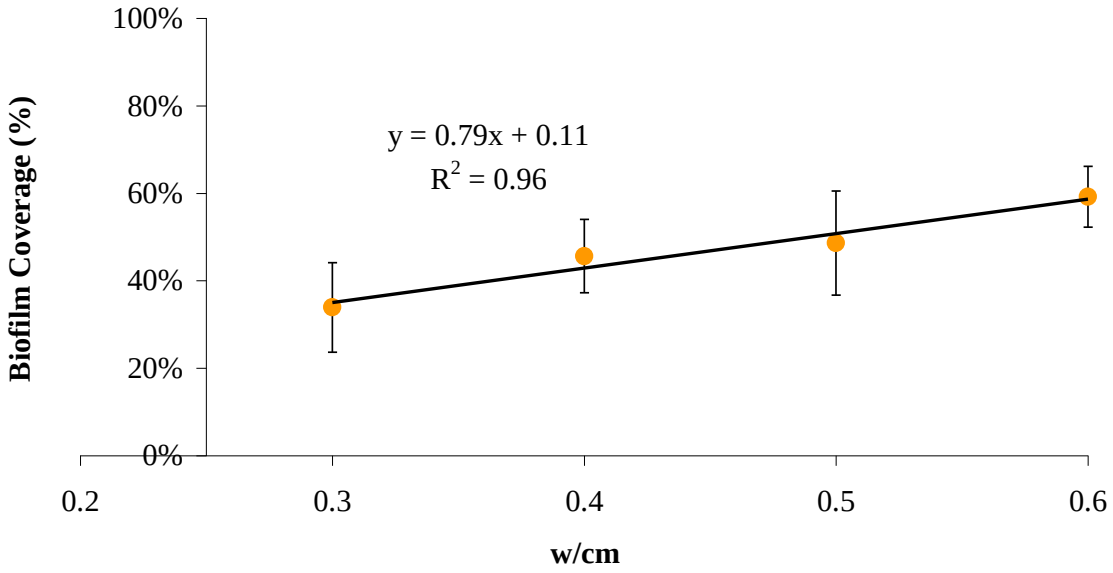

Figure 5.9 - Atlanta Biofilm Coverage vs. w/cm

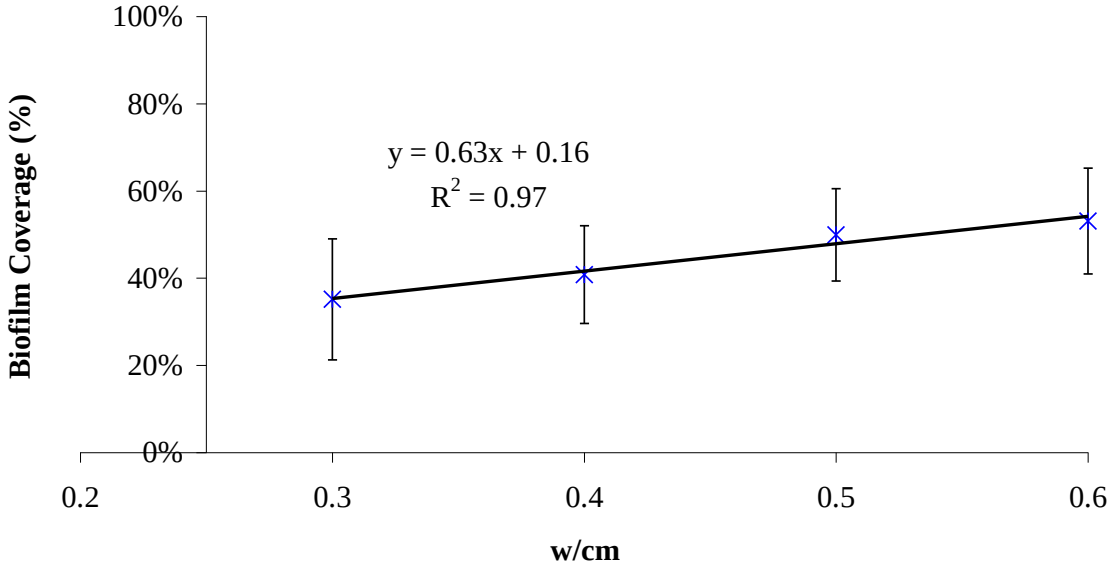

Figure 5.10 - Gainesville Biofilm Coverage vs. w/cm

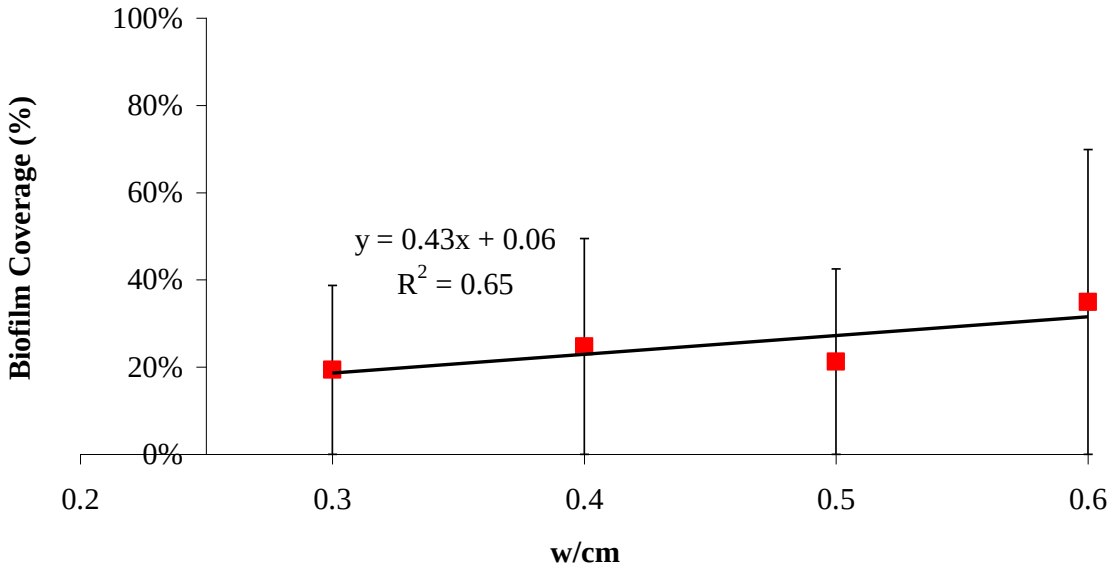

Figure 5.11 - LaGrange Biofilm Coverage vs. w/cm

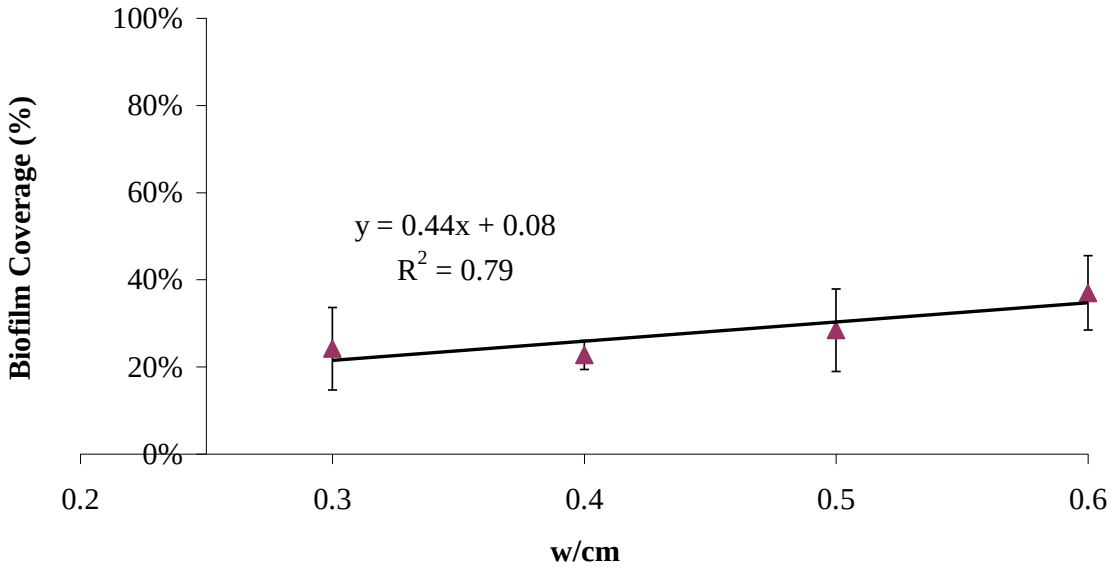

Figure 5.12 - Savannah Biofilm Coverage vs. w/cm

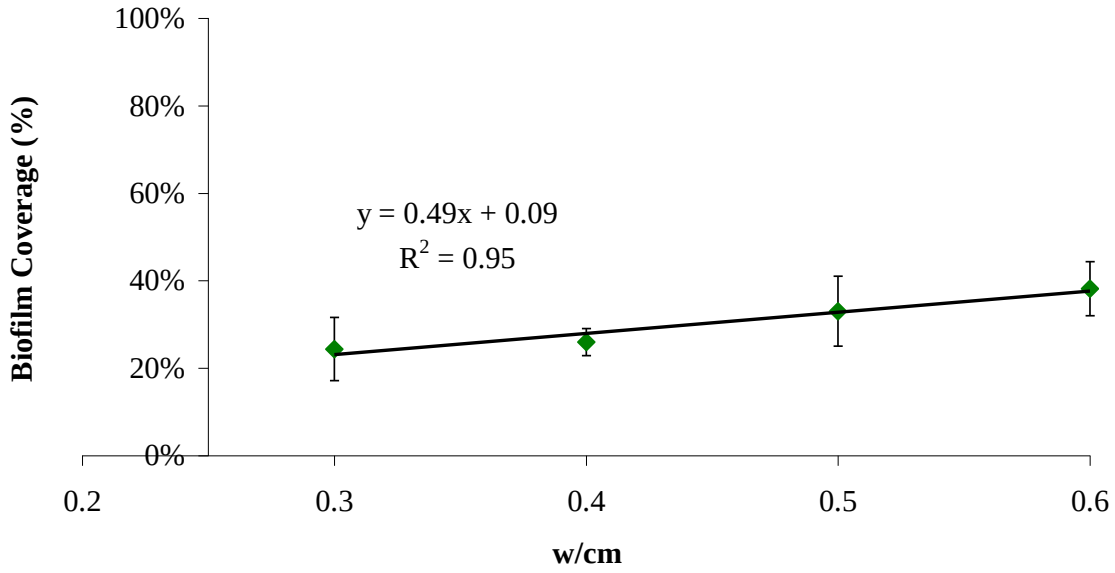

Figure 5.13 - *T. viride* Biofilm Coverage vs. w/cm

5.5.2. Influence of Compressive Strength

Compressive strength was measured for the purpose of creating a robust estimator for biofilm susceptibility that would apply across a variety of concrete mixtures, accounting for variations in w/cm, cement content, and the use of SCMs. Compressive strength is a key factor in design and can be measured in cored samples or non-destructively on site, making this a potentially convenient measure for predicting potential for biofilm growth.

Increased compressive strength generally indicates a denser cement paste matrix. A dense cement paste is expected to reduce biofilm growth, possibly through decreased permeability and decreased absorption of water and nutrients.

Biofilm coverage was first compared with compressive strength for a limited sample set that included only one type of Portland cement, as shown in Figure 5.14. The data in Table 5.7 show the constants in the multiple linear regression model shown in

Figure 5.14. For this small sample, the R^2 value of 0.89 in Figure 5.14 is less than the R^2 value of 0.94 for w/cm. The higher R^2 value for w/cm indicates that w/cm is a better estimator for biofilm coverage than compressive strength. This may be because compressive strength is a macroscopic quantity, and is dependent on both the cement paste and aggregate arrangement. Biofilm growth occurs on the microscopic level, and thus will be more directly influenced by the paste alone, which is measured directly by w/cm.

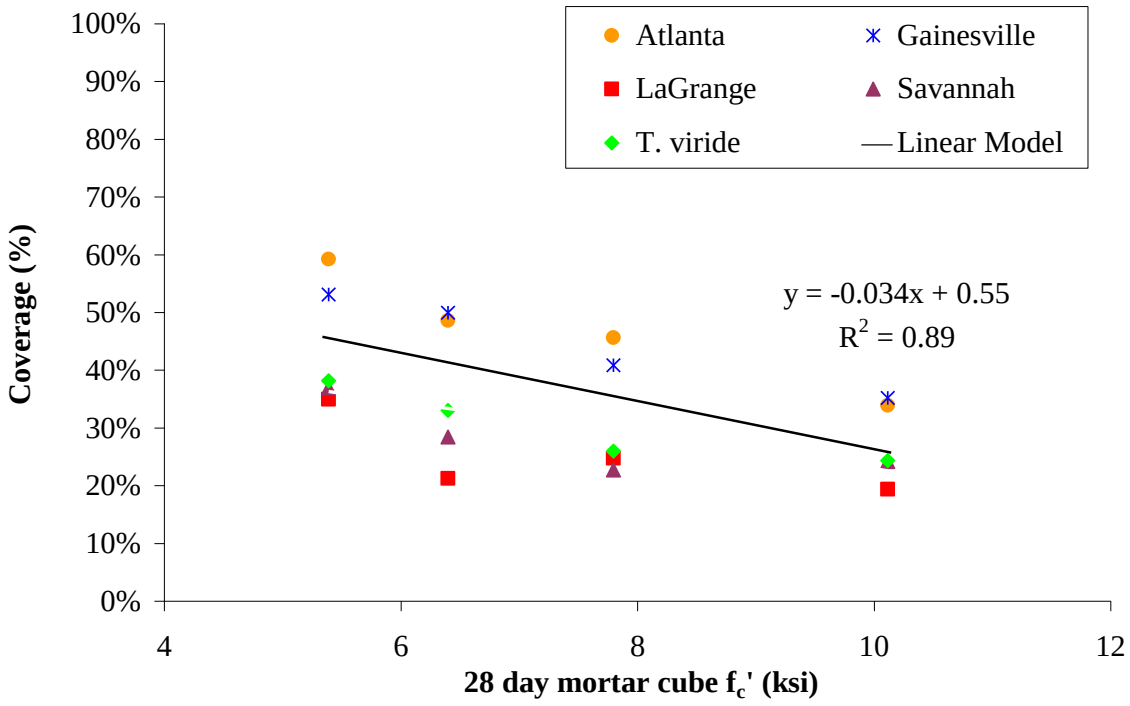

Figure 5.14 - Biofilm coverage vs. compressive strength for selected OPC tiles

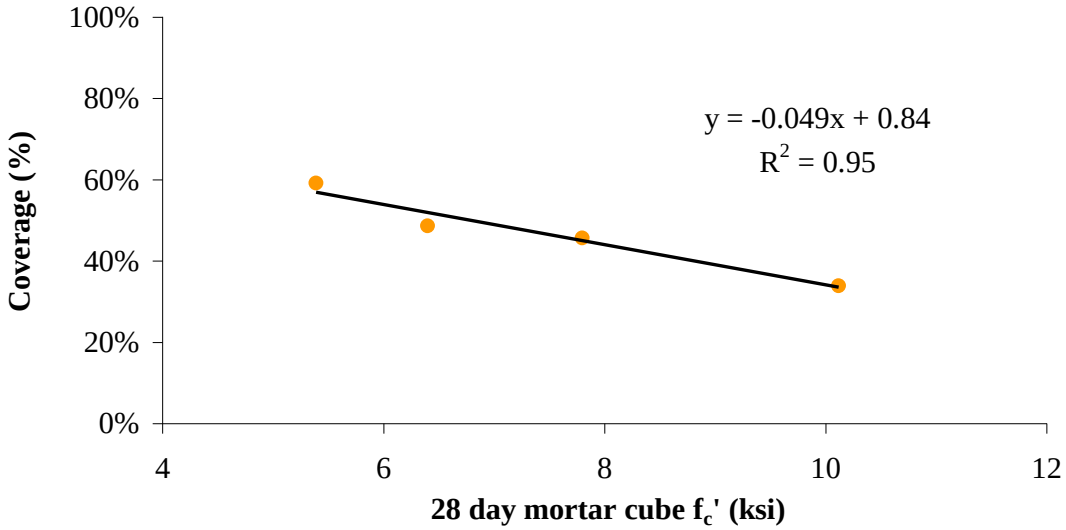

Figure 5.15 - Biofilm coverage vs. compressive strength for selected OPC tiles, Atlanta microbes

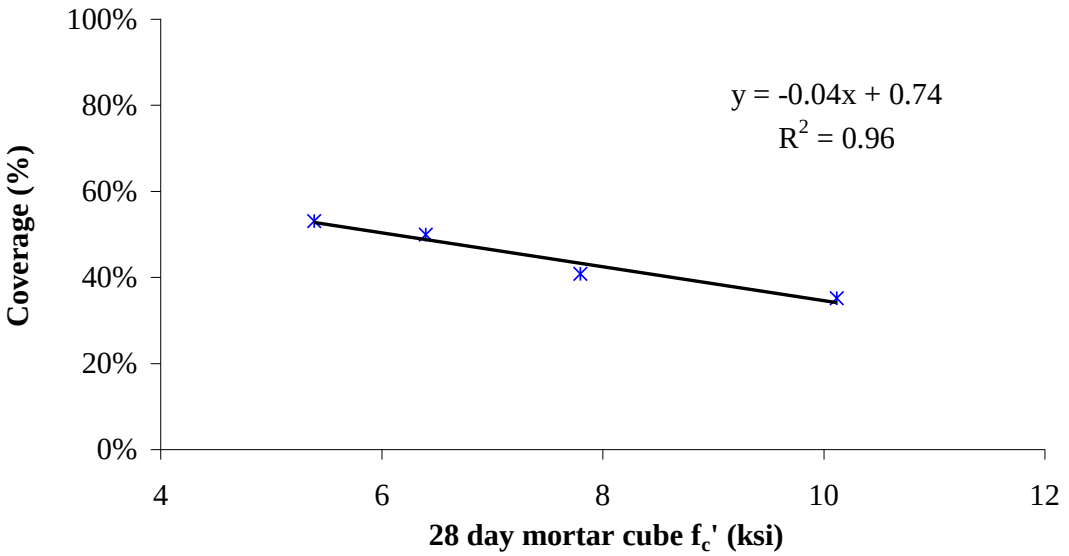

Figure 5.16 - Biofilm coverage vs. compressive strength for selected OPC tiles, Gainesville microbes

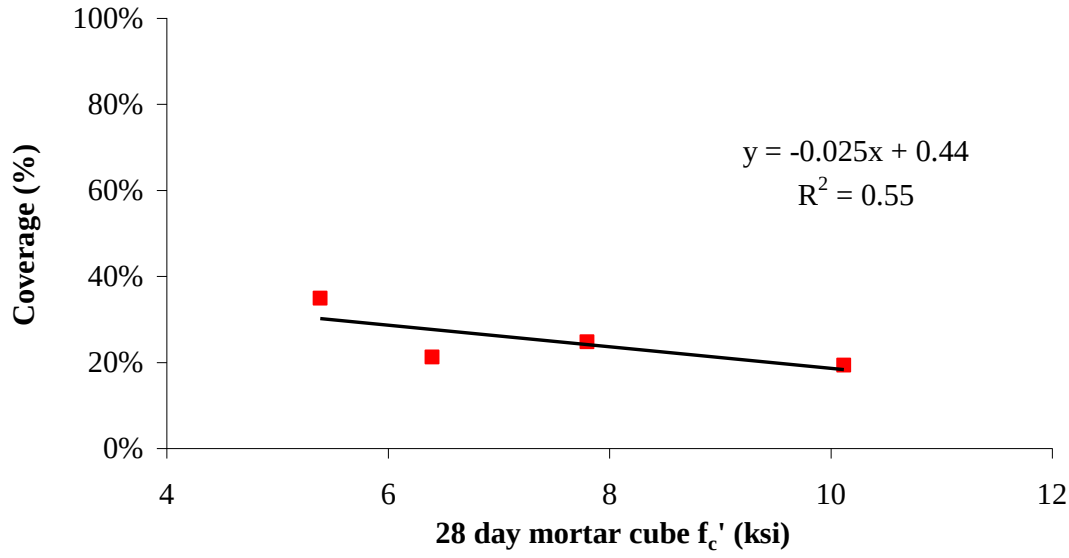

Figure 5.17 - Biofilm coverage vs. compressive strength for selected OPC tiles, LaGrange microbes

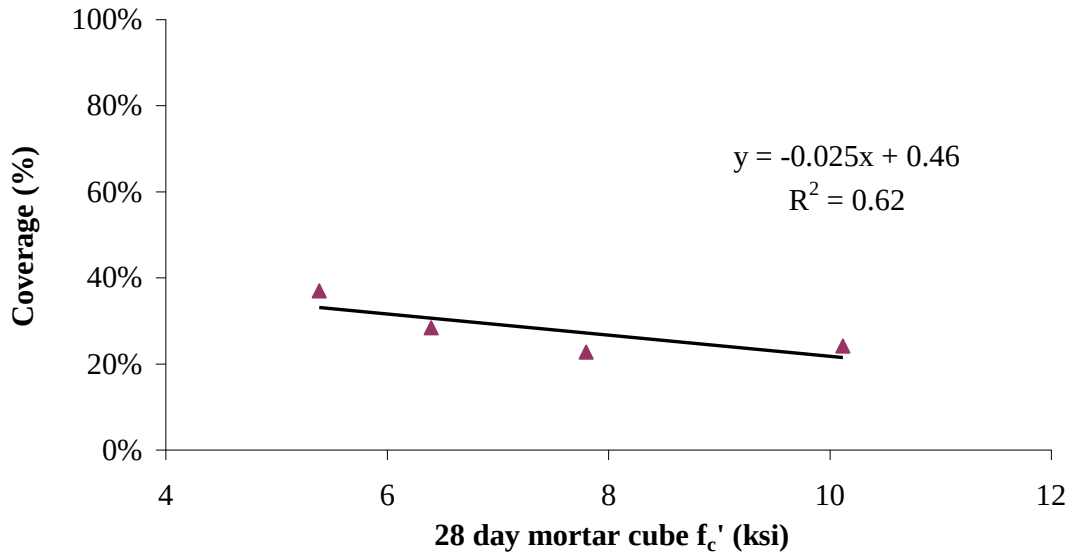

Figure 5.18 - Biofilm coverage vs. compressive strength for selected OPC tiles, Savannah microbes

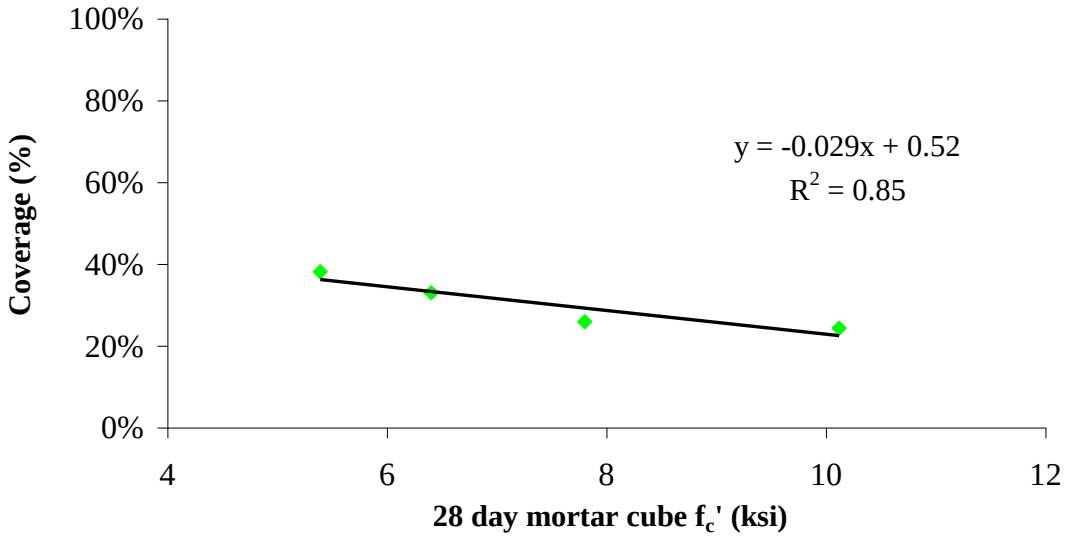

Figure 5.19 - Biofilm coverage vs. compressive strength for selected OPC tiles, *T. viride*

Table 5.7 - Regression model constants for compressive strength

site	b_n (constant)
Atlanta	0.73
Gainesville	0.69
LaGrange	0.50
Savannah	0.53
Trichoderma viride	0.55

Extending the sample set to include all tiles of brushed surfaces inoculated in the same trial run (Mixes A, B, C, D, G, K, O, R, U, V, and W) likewise reveals a somewhat negative relationship, similar to that found with the smaller sample set, as shown in Figure 5.20. Trend lines have been shown for illustration, and these values have been adjusted for variation between biological sites using the coefficients found in Table 5.7. Adjusting the values using these coefficients is successful in keeping the same slope in the linear trend while increasing the R^2 value, from 0.11 to 0.14. However, this R^2 value is much lower than for the previous, limited set, indicating that the relationship between compressive strength and biofilm growth cannot be generalized to all the mortar mixes examined.

The far outliers, labeled #1 and #2 in Figure 5.14 do not appear to be related to other trends. For example, #1 is a tile containing 50% slag and inoculated with *T. viride.* The following section, 5.5.8, further examines SCMs and did not find any strong increase due to replacement. Another example, #2, is an Essroc Type I tile also inoculated with *T. viride*. In a following section, 5.5.4, the Essroc Type I cements are shown to not have any general trend different than other Type I cements. This figure shows the variability in results inherent in performing a biological test.

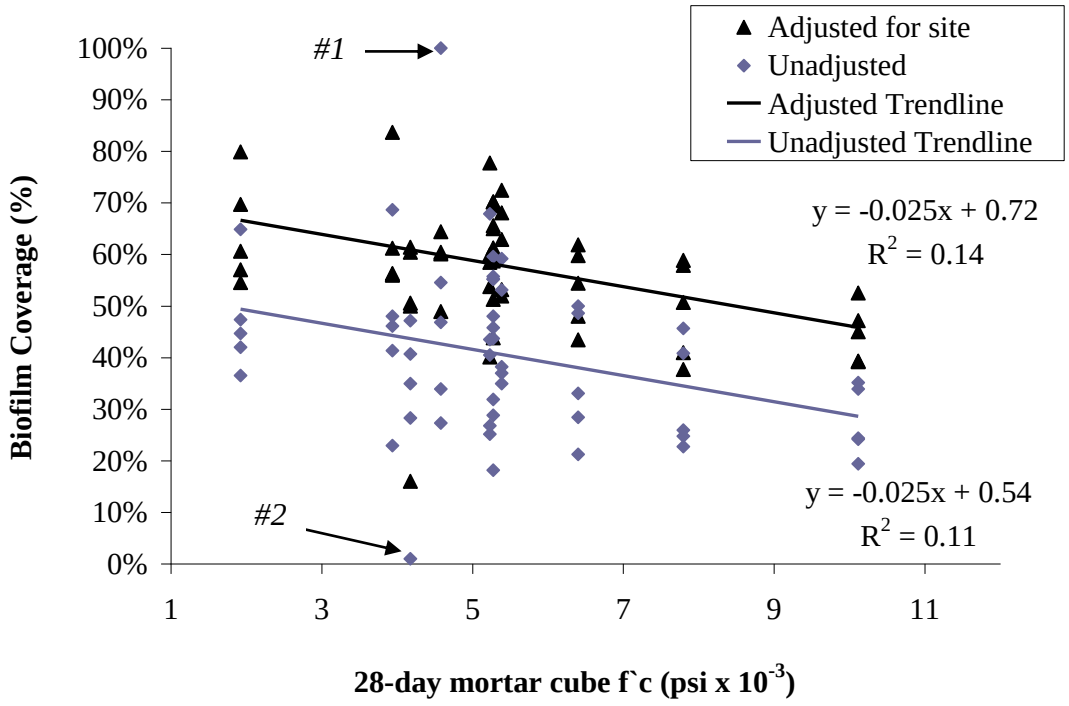

Figure 5.20 - Biofilm Coverage vs. 28-day mortar cube compressive strength

5.5.3. Influence of Surface Roughness

Surface roughness has been previously indicated to influence biofilm growth rates, with smoother surfaces generally decreasing growth. The research by Pinheiro and Silva [53] performed qualitative assessments of the fungi *Cladosporium sphaerospermum* growth on two surfaces. However, this variation in surface roughness was not quantified in a repeatable way. Measuring the surfaces of the mortar tiles with a laser scanning confocal microscope, as described in the previous chapter, provides a quantitative and objective measure of surface roughness.

The surface roughness was measured for a selected set of mortar tiles (Mixes C,Y,Z) produced with the same type of cement and w/cm. The surface roughnesses were relatively close to 1 (a completely flat surface), because the physical size measured by the

confocal was only 2mm x 2mm, with typically less than 0.5mm in peak to trough height. Based on qualitative observation, the samples most similar to field conditions would have a roughness number of ~1.2. To compare between biological sets, the biofilm coverages were adjusted for each site by linear constants for w/cm in Table 5.6.

Roughness number and biofilm coverage show a positive relationship, which agrees with the relationship previously described qualitatively by Pinheiro and Silva [53]. This trend is shown in Figure 5.21, with error bars representing standard deviations in both biofilm coverage and surface roughness measurements. The relationship is not as clear for the overall group as w/cm or f_c'. However, both the Atlanta and *T. viride* groups showed a very strong linear trend, as shown in Figure 5.22 and Figure 5.23, respectively. This difference could suggest that *T. viride* and the Atlanta microbial community, which contained *T. viride*, were more sensitive to surface roughness, while LaGrange, Gainesville, and Savannah communities (where *T. viride* was absent), were not. For example, one way a fungi may be sensitive to surface roughness is the ability of its hyphae to extend over peaks and valleys. A less filamentous fungal species may not be able to cross a rougher surface. In addition, the sample tiles for *T. viride* and Atlanta groups happened to have a larger spread in roughness number, which would exaggerate the relationship.

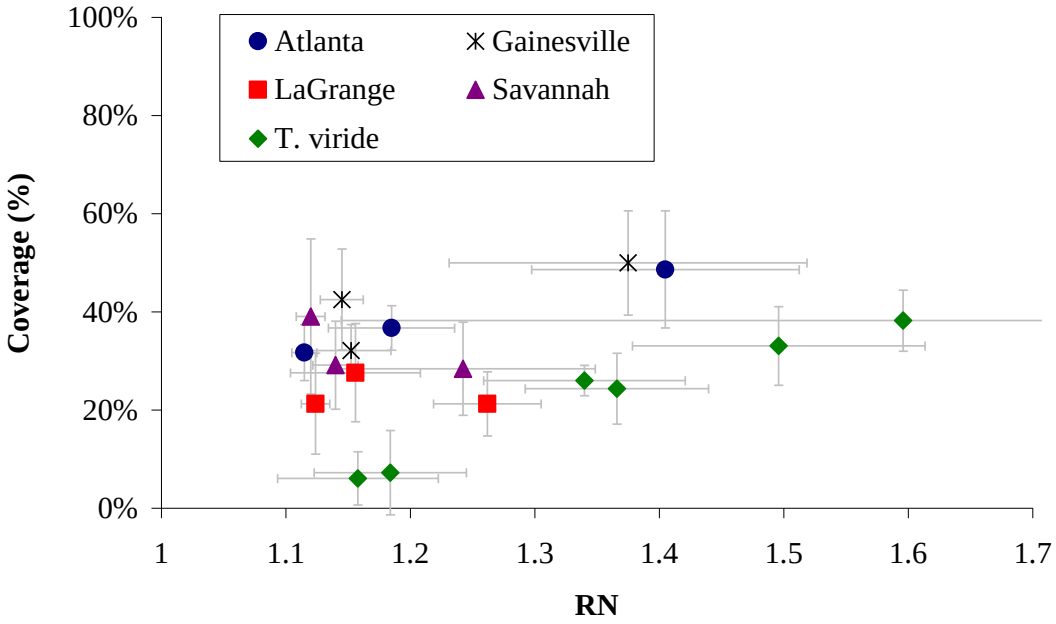

Figure 5.21 - Surface Roughness vs. Biofilm Growth

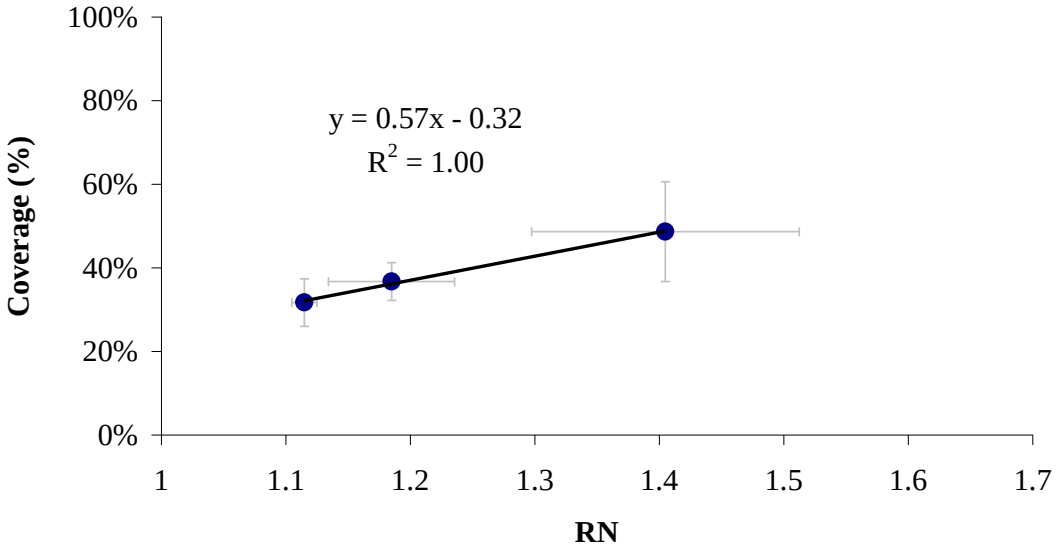

Figure 5.22 - Surface Roughness vs. Biofilm Growth, Atlanta Microbes

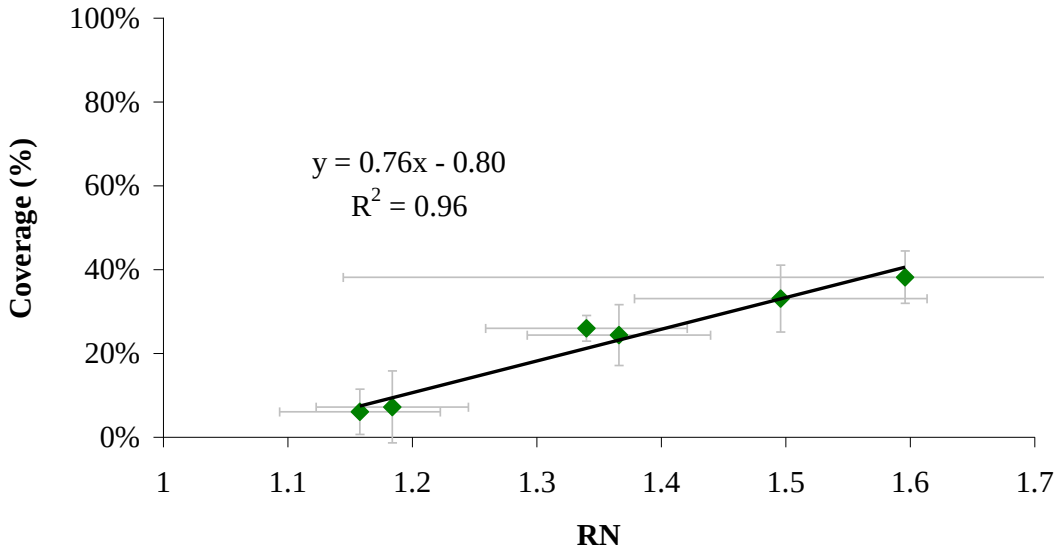

Figure 5.23 - Surface Roughness vs. Biofilm Growth, *T. viride* Microbes

5.5.4. Influence of Cement Source

The influence of cement Type was examined by comparing biofilm coverage on tiles prepared at constant w/cm of 0.5 to determine if the variation in chemical composition affected biofilm growth. The biofilm coverage was averaged for results from all five microbial exposures. Table 5.8 shows both the actual measured biofilm coverage and adjusted biofilm coverage, created by controlling for the 28-day compressive strength, which varied from 4200 to 6400 psi, using Equation (5.7). The coefficient of 0.034 in the equation comes from the slope of the linear regression line in Figure 5.14. A 2-tailed t-test was used to examine variation between the population means.

$$biofilm = -0.034 * \left(6400\,psi - f_{c\,sample}^{`}\right) \qquad \textbf{(5.7)}$$

Table 5.8 - Biofilm coverage compared for multiple cements

	Unadjusted coverage	P-value for difference from Type I/II (Holcim)	Adjusted biofilm coverage	P-value for difference from Type I/II (Holcim)
Type I/II (Holcim)	37%	1.00	37%	1.00
Type I/II (Essroc)	38%	0.86	30%	0.10
Type I/II (Tx Active)	41%	0.38	38%	0.92
Type GU-LS (5% LS)	45%	0.15	41%	0.48

No statistically significant variation was found between any of the three Portland cements (Holcim Type I/II, TX Active Type I, and Essroc Type I), when comparing the value at their unadjusted levels. These cements had variation between LOI, iron contents, and alkali content, but contained roughly the same trace heavy metals, as seen in Table 5.9.

When comparing the biofilm coverages adjusted for the compressive strength, Essroc Type I/II appeared to be significantly different than Holcim Type I/II cement. The largest difference between the two appears to be in their potential Bogue compositions, such that the Holcim cement has more C_3S and less C_2S than the Essroc cement. One possibility is that the slower reacting C_2S allowed for a denser paste to develop over time, even though the 28-day compressive strength was lower. The tiles were inoculated approximately 150 days after casting, so this reaction could have developed.

For the Holcim cement with 5% limestone, there was an increase in biofilm growth relative to Holcim Type I cement, before adjusting for differences between compressive strength. After adjusting for the difference in compressive strength, the

cement with added limestone was no longer significantly different than the Holcim Type I/II cement. This result matches with the oxide analysis data, because both these cements are very similar in chemical composition.

Table 5.9 - Oxide Analyses and Potential Bogue Compositions for cements and SCMs

	Holcim Type I	Holcim 1157	Tx Active	Essroc Type I	Fly Ash	Blast Furnace Slag	Silica Fume	Metakaolin
SiO_2	19.82	18.69	19.18	20.09	35.47	38.21	97.12	52.10
Al_2O_3	5.01	4.76	4.71	5.65	18.38	8.47	0.01	44.03
Fe_2O_3	4.06	3.39	2.07	2.95	6.92	0.35	0.05	0.92
CaO	63.84	64.29	60.1	61.67	25.01	36.39	0.37	0.47
MgO	1.32	1.13	2.84	3.2	5.71	13.16	0.28	0.13
SO_3	2.87	3.09	2.82	3.4	1.89	1.70	0.04	0.00
Na_2O	0.14	0.18	0.27	0.32	1.95	0.27	0.04	0.02
K_2O	0.43	0.32	0.5	0.73	0.50	0.35	0.58	0.14
TiO_2	0.27	0.21	4.19	0.25	1.41	0.35	0.02	1.42
P_2O_5	0.18	0.14	0.13	0.1	1.27	0.00	0.08	0.17
Mn_2O_3	0.03	0.00	0.05	0.04	0.03	0.63	0.04	0.01
SrO	0.09	0.08	0.12	0.14	0.39	0.05	0.01	0.01
BaO	0.01	0.05	0.00	0.05	0.71	0.05	0.00	0.02
LOI	1.97	3.62	3.04	1.4	0.36	0.03	1.36	0.56
Bogue Potential Compositiion								
C_3S	61.54	73.97	56.19	46.44	--	--	--	--
C_2S	10.73	-1.84	12.90	22.83				
C_3A	6.42	6.88	8.98	9.99				
C_4AF	12.34	10.31	6.29	8.97				

These results may indicate that the amount of micronutrients provided by the cement for the microbes were available for all the Type I or Type I/II cements examined. The increase in growth on the cement with limestone may be due to the lower actual w/cm ratio. That is, although w/cm remained the same as the other tiles, the actual amount of cement in the powder was reduced by 5% by mass. This would follow the results presented in the prior section where w/cm was shown to correlate strongly to

growth. It is also possible that the addition of limestone changes the cement paste in another way that is more favorable to growth.

5.5.5. Photocatalytic Cement

The potential effectiveness of photocatalytic cement can be examined by comparing the performance of three types of tiles (Mixes K, W, and C), containing Tx Active, Essroc Type I, and Holcim Type I/II respectively. All were produced at w/cm of 0.50. The tiles were inoculated with an equal volume combination of microbes from all sites and were subjected to 6 hour cycles of media rain, followed by 6 hour without media rain. This biological combination was intended to give the opportunity for any UV-resistant fungi to grow, in case some sites did not contain any cultural isolates that were UV-resistant. The tiles were exposed to UV light (λ = 290-390 nm) for 6 hour intervals, offset by 3 hours from the wetting and drying cycles. After seven days of incubation, the tiles were removed, kept in plastic agar plates, and allowed to dry for 48 hours at 23^{o} C and 50% RH.

As seen in Figure 5.24 and Figure 5.25, OPC and photocatalytic cement tiles, respectively, the exposure of microbes to UV light partially inhibited growth in all samples. However, red, black, and green colonies were all able to form on the surface of the non-photocatalytic tiles, covering 30% and 20% of the two tiles. The photocatalytic tiles did not have any red, green or black colonies, and only one tile had spots of yellow discolorations, as seen in Figure 5.25. These biofilm coverages were rated at 8% and 0%. Cultures taken from both photocatalytic and non-photocatalytic sets of tiles grew a wide variety of fungal species, even though growth was not apparent on the photocatalytic tiles.

Photocatalytic degradation of bacterial cells is well known. Research by Kikuchi et al. showed that photocatalytic TiO_2 inhibits bacterial growth on thin films, and Maness et. al demonstrated that TiO_2 is able to cause cell death when in liquid suspension [30], [37]. Photocatalytic TiO_2 inhibition of fungal cells is less researched but has still been demonstrated. For example, Sichel et al. measured almost complete cell mortality after 1-6 hours for *Fusarium* spp. in suspended TiO_2 solution, and Lonnen et al. showed a 4 log unit reduction in *Candida albicans,* and *Fusarium solani* after 8 hours of exposure [58], [35]. However, this research is the first to demonstrate fungal inhibition on photocatalytic cement tiles.

The biofilm growth on these tiles did not depend on the bacteria species, as evidenced by the previous growth of *T. viride*, a single strain of fungus without added bacterial species. The photocatalysis reaction was therefore inhibiting fungal growth, through one of two ways. The potato dextrose broth contained a variety of carbon based compounds for fungal "food", which could be mostly oxidized to CO_2 and water. Eliminating this would prevent fungal growth, because the cement tiles contained no substantial amount food source.

Alternatively, the photocatalytic reaction may be interacting directly with the fungal cells. Although these eukaryotic cells will have mechanisms to repair oxidation damage, the oxidation levels from the photocatalytic cement may be too high for the cells to overcome. This would leave very few active cells on the surface, yet probably not be able to damage the well-protected fungal spores. It is most likely the photocatalysis affected both the nutrients and the fungal cells. This is because small amounts of growth did occur, but with a different visual appearance than the non-photocatalytic tiles.

Ultimately, the photocatalytic cement reduced growth by 30%, which is greater than the 20% difference in growth between w/cm 0.6 and w/cm 0.3.

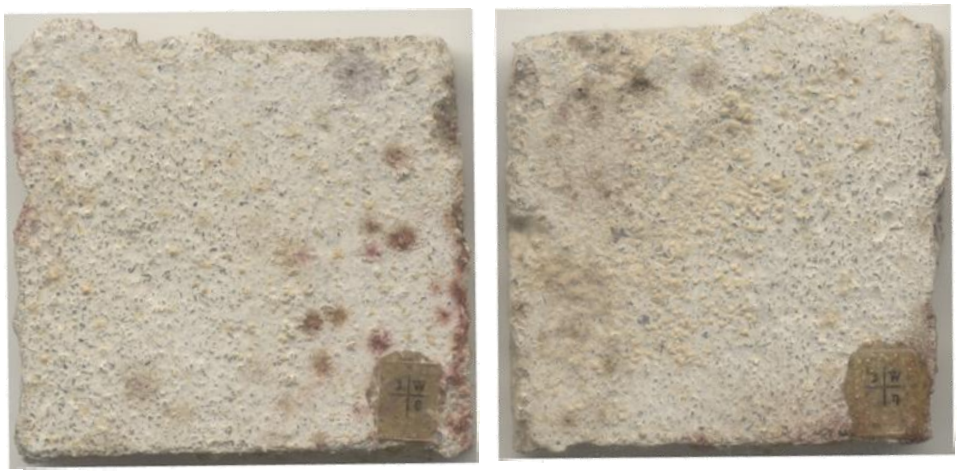

Figure 5.24 - Essroc OPC tiles inoculated with combination mix, after 7 days exposure to artificial light. Biofilm Coverage = 30% and 20%, respectively

Figure 5.25 - Essroc TX Active tiles inoculated with combination mix, after 7 days exposure to artificial light. Coverage = 8% and 0%, respectively

5.5.6. Influence of Chemical Admixtures

Samples were prepared at a w/cm of 0.5 with Holcim Type I cement and WR Grace Darex AEA (ASTM C260). The target air content for the mix was 6%, but the

volume of cement paste made was too small to be tested. Sample roughness was not measured, but appeared to be similar between air entrained and non-air entrained tiles.

Cement tiles with air entraining agent showed no statistical significant difference from non air-entrained tiles. When using a t-test to examine variation between means of biofilm coverage, the difference between air entrained and non-air entrained cement ties was below a 90% confidence level (P=0.19). This may be due to the fact that the addition of micropores did not modify the surface in a way to make it more hospitable. Average micropores are on the scale of 75 to 500 μm, which is much larger than the average fungal (~10 μm) or bacteria (~1 μm) cell.

5.5.7. Influence of Painted Coating

The population means of biofilm growth for acrylic paint coating, shown in Figure 5.26, (41% ± 15%) were compared to an uncoated mortar tile of the same composition, shown in Figure 5.27, (37% ± 15%). The acrylic paint coating did not significantly increase growth when compared using a two-tailed t-test (P-value: 0.37). These mortar tiles had a w/cm of 0.5, which is higher than the typical w/cm of 0.45 used in construction. The growth patterns on both tiles were substantially similar in color, with the acrylic coating tiles forming more defined, "rounder" colonies. These differences appear to be within typical variation of growth patterns for a single site. Although the examination of a single type of acrylic paint is not an exhaustive study on paints, this suggests that coated concrete is not more resistant to biofilm growth than concrete alone. Future research should examine multiple painted coatings and compare their biofilm growth rates to uncoated concrete. The influence of environmental

interactions on coating performance should also be investigated to determine which coatings are most suitable for long-term mitigation of microbial growth.

Figure 5.26 - Tile with acrylic coating, inoculated with Atlanta microbes

Figure 5.27 - Tile without acrylic coating (w/cm = 0.5), inoculated with Atlanta microbes

5.5.8. Influence of SCMs

Class C fly ash (Holcim), ground blast furnace slag (Holcim), silica fume (W.R. Grace Force 10000D), and metakaolin (MK 349) were examined for their influence on biofilm growth. SCMs have significant potential to affect biofilm growth rates. Silica fume and metakaolin increase early strength, which may reduce early colonization in the natural environment. However, fly ash and slag reduce early strength, which may increase early colonization. Some SCMs, such as fly ash, slag, or metakaolin may

contain carbon impurities, which are a potential nutrient source for microbes. For example, fly ash may contain up to 6% as carbon impurities by weight (ASTM C618-05), which could be up to 1.5% of the cement paste by weight. Additionally, the secondary cementitious reactions consume calcium hydroxide, which leads to a lower buffer for carbonation, as shown in research by Papdakis [47]. A lower carbonation buffer would then lead to a shorter "lag time" before biofilm growth. The cement tiles were all completely carbonated before exposure, eliminating this potential variation. However, Papadakis' research also showed that the SCM replacement at any level decreased the chloride permeability. This decreased permeability could indicate a lower affinity for cement paste to absorb the nutrients required by the biofilm, leading to slower growth.

Table 5.10 - Loss on ignition for cement and SCMs

Cement	***LOI***
Fly Ash	0.36%
Slag	0.03%
Metakaolin	0.56%
Silica Fume	1.36%
Type I/II Cement	1.97%

The influence of these SCM type at varying dosage rates was examined for five different microbe communities (Mixes M,N,O,P,Q,R,S,T,U,MK, and C for control, Table 5.1) at w/cm of 0.50. All the microbes were exposed to microbial communities in 20% potato dextrose broth, on 6-hour on/off cycles for 7 days. Figure 5.28, Figure 5.29, Figure 5.30, and Figure 5.31 show the observed biofilm coverage for various cement replacement percentages by fly ash, slag, silica fume, and metakaolin, respectively. The mean for all 5 microbe types is also shown to indicate the general trend. Figure 5.32 plots all the mean values of biofilm coverage vs. SCM replacement percentage to show

that the same general trend is observed for all SCMs. Generally, moderate replacement levels for each type of SCM tend to decrease the biofilm coverage, while larger replacement levels increase biofilm coverage relative to a comparable OPC mix. However, variations in biofilm coverage with SCM replacement were generally very moderate.

Figure 5.33 shows the mean biofilm coverage vs. 28-day mortar cube compressive strength for each type of SCM and OPC controls produced at the same w/cm. No trend is discernible between 28-day compressive strength and biofilm coverage. Additionally, the means for biofilm coverage among all mixes are not statistically different at a 90% confidence interval.

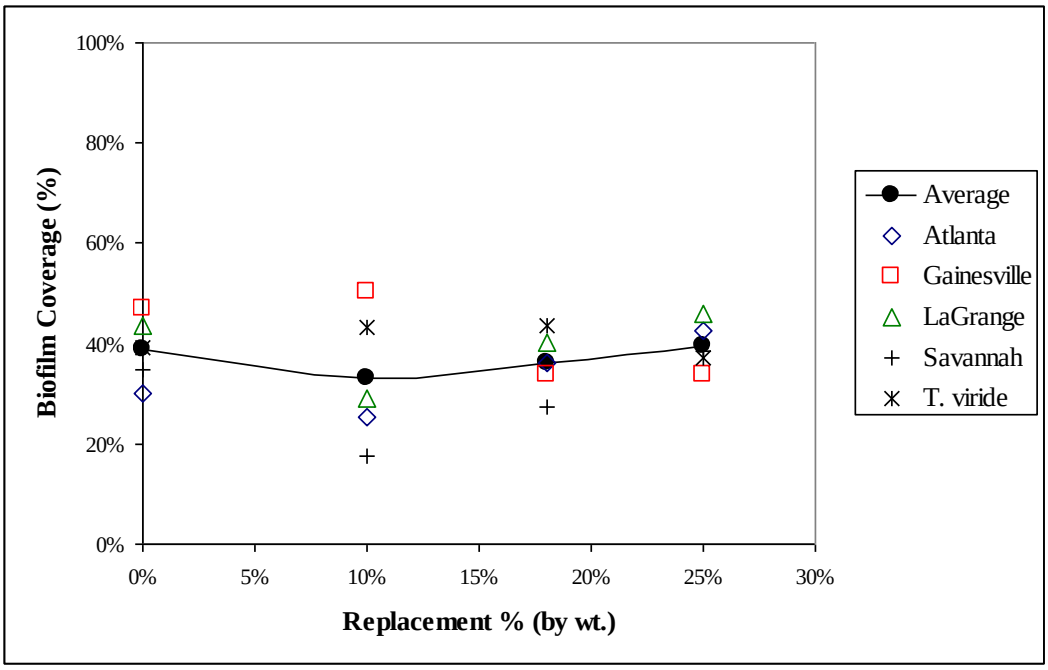

Figure 5.28 - Biofilm coverage vs. fly ash replacement

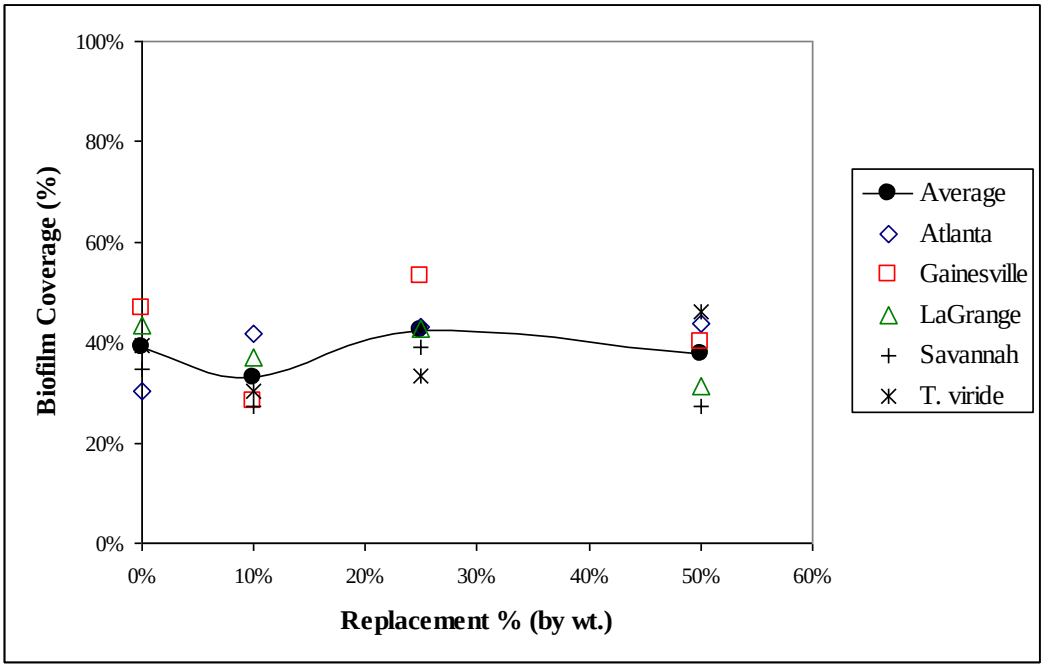

Figure 5.29 - Biofilm coverage vs. slag replacement

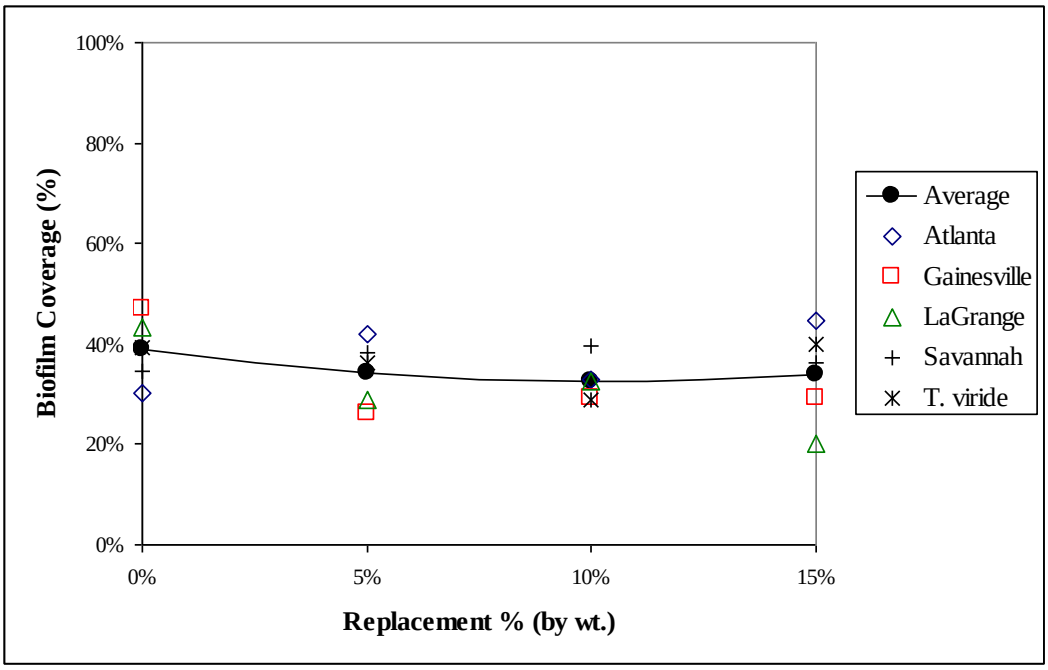

Figure 5.30 - Biofilm coverage vs. silica fume replacement

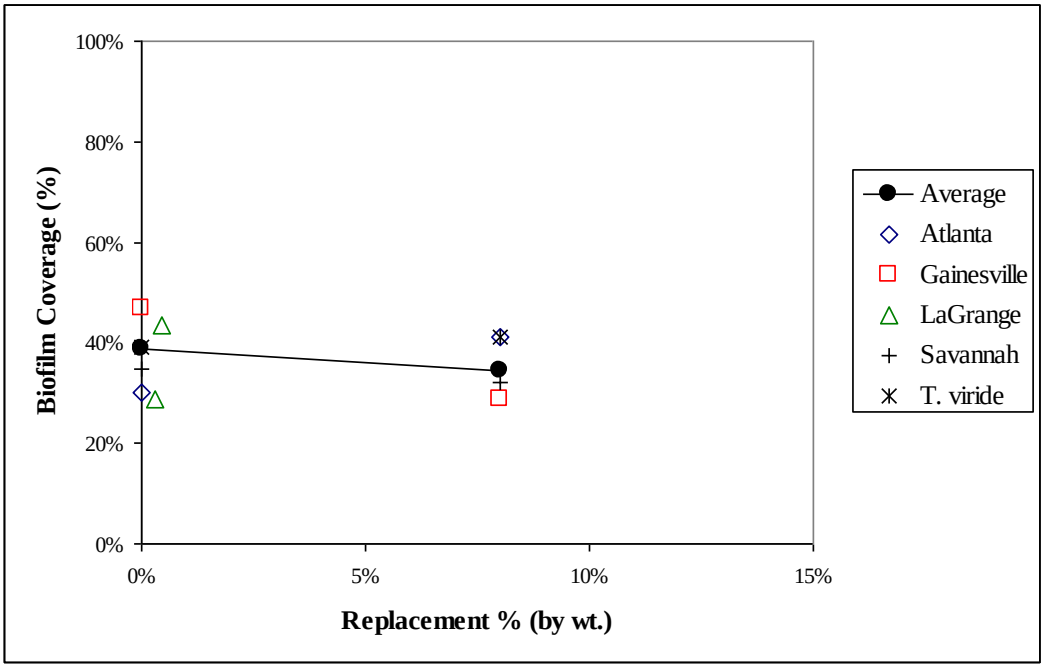

Figure 5.31 - Biofilm coverage vs. metakaolin replacement

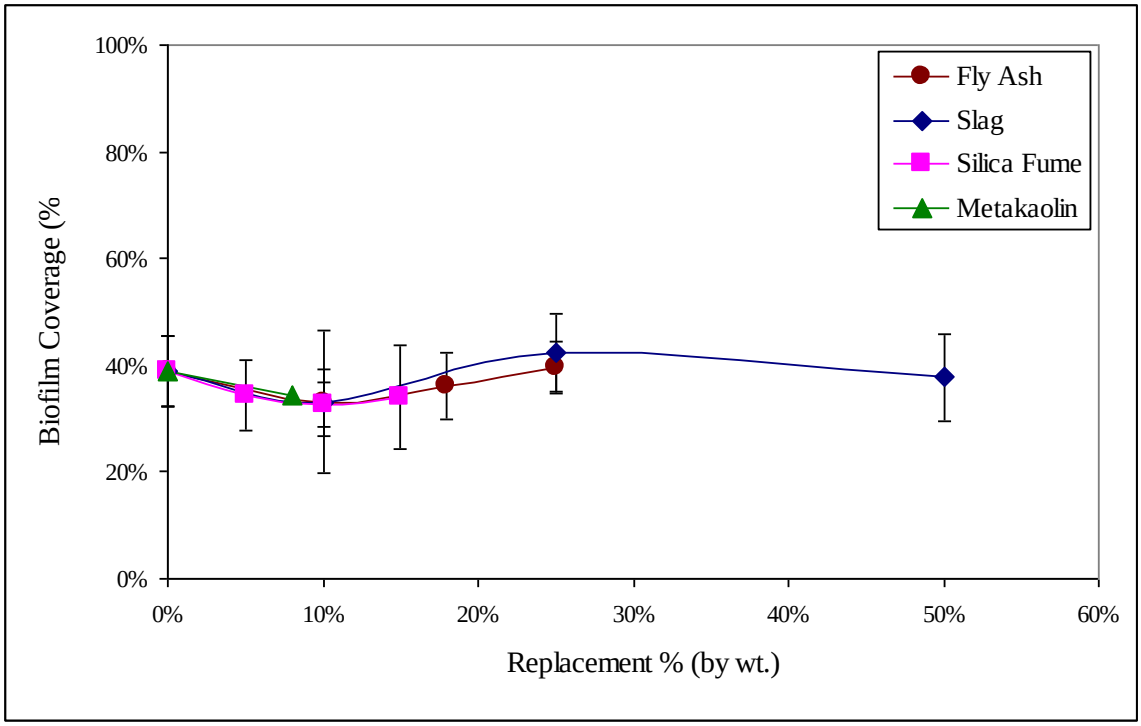

Figure 5.32 – Mean biofilm coverage vs. SCM replacement

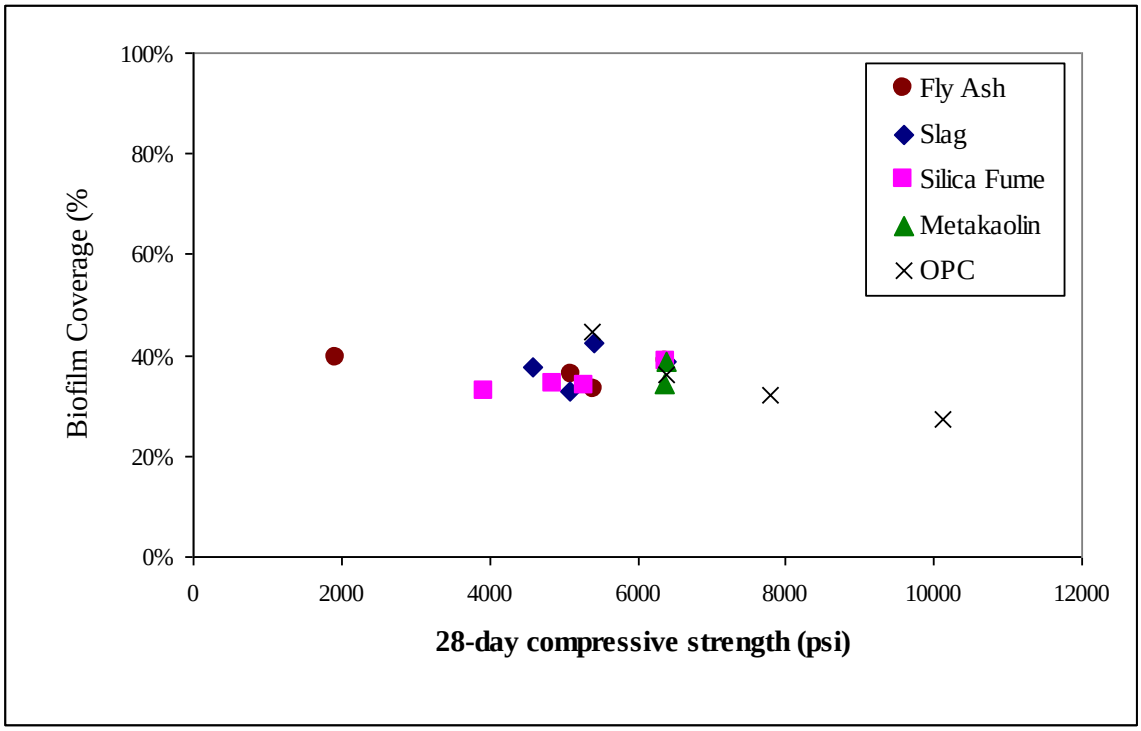

Figure 5.33 - Biofilm Coverage vs. 28-day compressive strength

However, unlike the similarities in 28-day compressive strength, measurements of Rockwell hardness after exposure did indicate differences between OPC and SCM mixes. Figure 5.34 and Figure 5.35 show the relations between biofilm coverage and hardness for OPC mixes and SCM mixes, respectively. OPC mixes showed increased coverage for lower Rockwell hardness, which could either be a cause or an effect of the biofilm growth. However, Rockwell hardness measurements were more uniform, generally centered on a value of 80, for SCM mixes, which may indicate the improved resistance of SCM mortar to biofilm coverage and any subsequent deterioration. The SCM addition may make the cement paste more dense and uniform, allowing for similar results, even for increasing replacement levels. However, the R^2 values for the relation between Rockwell hardness and growth are very low, indicating little confidence in this relationship.

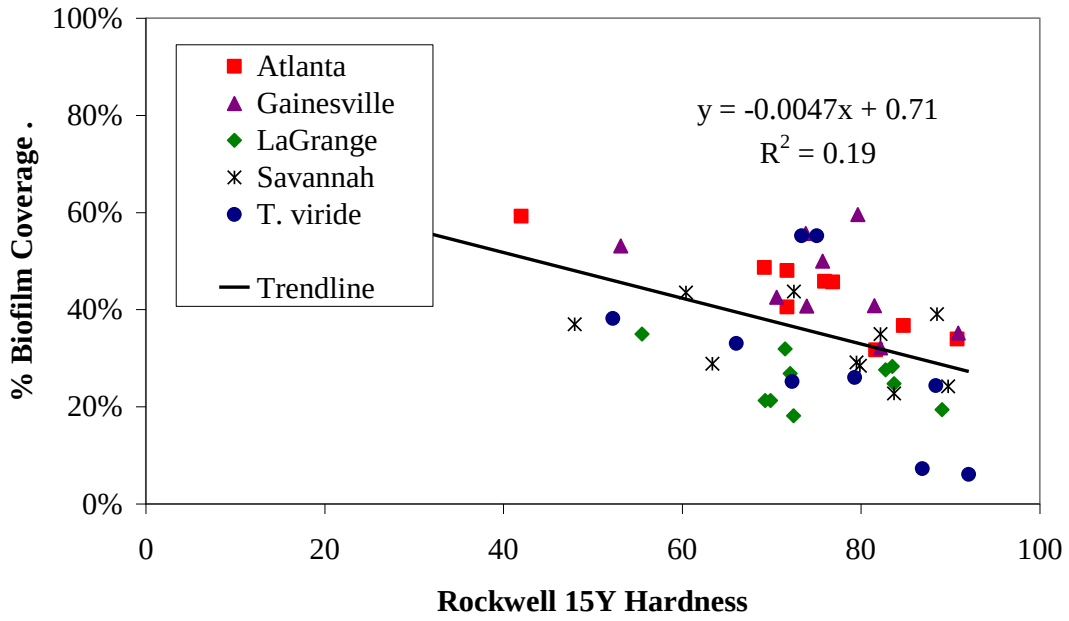

Figure 5.34 - Biofilm Coverage vs. Rockwell 15Y for OPC mixes

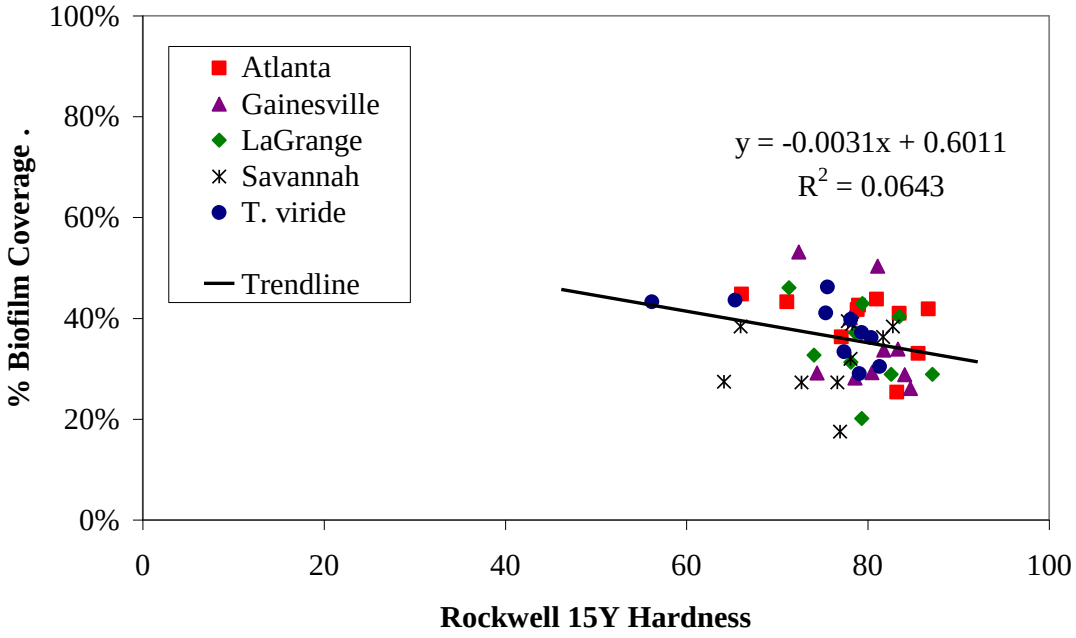

Figure 5.35 - Biofilm Coverage vs. Rockwell 15Y for SCM mixes

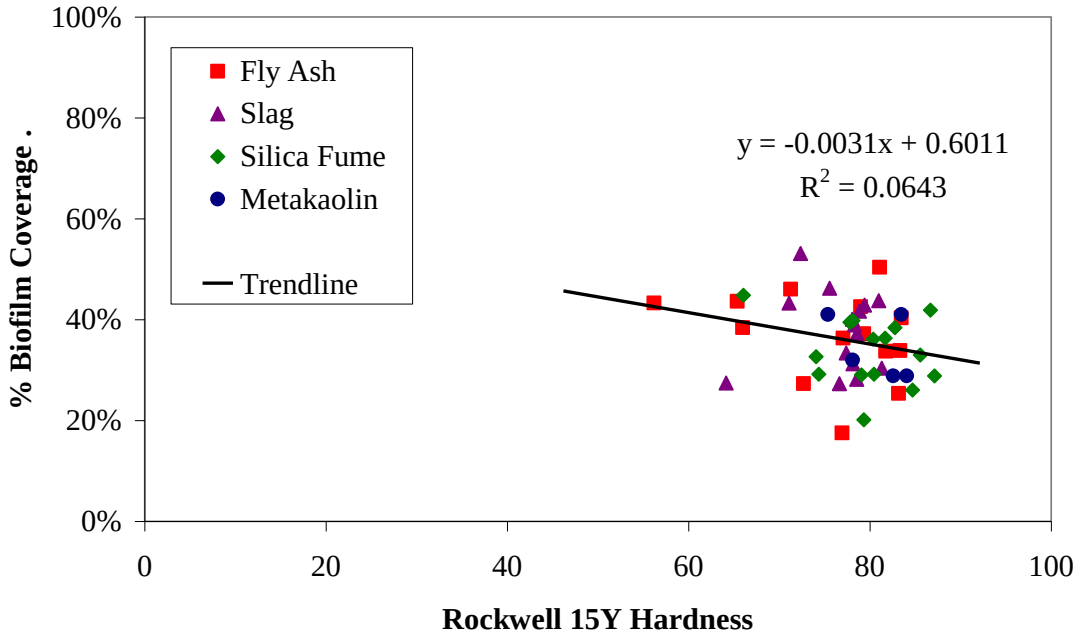

Figure 5.36 - Biofilm Coverage vs. Rockwell 15Y for SCM mixes, organized by SCM

Overall, the addition of SCMs seemed to "level" the amount of biofilm growth. using only the OPC results would predict increased biofilm coverage for lower compressive strength resulting from higher SCM replacements. However, the relationship between compressive strength and biofilm coverage was found to be minimal for SCMs. The general uniformity of biofilm coverage is due to the complicated interaction between the cement paste changes due to the secondary reactions. It appears that the factors encouraging growth (additional carbon impurities, greater variation in micronutrients, lower early strength, smaller pH buffering) were balanced by the factors discouraging growth (lower permeability, lower porosity, any additional heavy metals). The relative importance of some factors was changed by the experimental method. The smaller pH buffer was not a factor, because all samples were aggressively carbonated before inoculation. The nutrients provided by additional carbon impurities would be

small in comparison to the nutrient rain. However, the lower early strengths influence may have been greater, because the samples were tested approximately 6 months after casting. Cements with SCMs in the natural environment would have, at minimum, a few years of "lag time" to hydrate before biofilm growth initiation.

This research only examined one SCM of each type. SCMs, particularly fly ash and slag, are quite variable in composition. For example, class F fly ash has much more silicon and less calcium than class C fly ash, leading to lower early strength. Variations in the raw material source lead to differences in trace impurities, which may play a role on the microbial scale. Although the Rockwell hardness relations were low in confidence, the level of biofilm growth, when compared between multiple SCMs, was quite consistent. Further research is needed to verify this relationship for biofilm growth on multiple SCMs to make a definitive conclusion.

5.6. Summary of Findings

Many of the concrete properties tested, including w/cm, compressive strength, and surface roughness, were found to have significant influence on the rate of biofilm growth in a controlled experiment. This supports the previous research indicating concrete properties play a role in the growth rate of biofilm, as proposed by Dubosc et al [15], Shirakawa et al [55], and Pinheiro and Silva [53], even if those differences are masked by unmeasured environmental properties such as water runoff patterns and surface orientation.

Biologically, both pure culture strains and mixed microbial communities were shown to create similar trends in relation to concrete properties. However, the pure culture of *Trichoderma viride* generally had less variation from the estimated

relationships between coverage area and w/cm, compressive strength, and roughness number. This is likely due to the fact that it is not competing with other species for nutrients and space, and more uniformly covers over the mortar tile surface. The mixed cultures contained equal volumes of culture-separated strains, which may not have produced the same proportion of species as found in the field. As a result, a minor player in nature would have the potential to be the fastest growing species in the lab. However, aggregating the results between all sites allows these differences to be smoothed out.

Photocatalytic cement was the only material found that showed substantial reduction in biofilm growth. The TiO_2 only reduced growth after exposure to simulated sunlight, confirming the reduction was due to a photocatalytic effect. In comparison, this was twice the level of reduction gained by using a 0.3 w/cm mix instead of a 0.6 w/cm mix. Additionally, typical admixtures (air entrainer, water reducing agents) appeared to have no effect on growth.

The addition of SCMs (fly ash, slag, silica fume, and metakaolin) did not appear to have any appreciable effect on biofilm coverage, even though 28-day compressive strengths were not the same as the equivalent OPC w/cm, showing that compressive strength alone may be an incomplete estimator for biofilm growth. The changed development of cement microstructure through SCM replacement may play a role through decreased porosity and permeability of the mortar.

Some cement variables were found to affect biofilm growth. A Type I based cement with interground limestone showed increased growth, although this difference disappeared when the lower compressive strength of the mix was accounted for. Also, differences between two Type I/II cements from different manufacturers did appear after

accounting for differences in compressive strength. Oxide analysis of both cements did not reveal a definitive explanation for this difference.

Various mortar properties can be adjusted to influence biofilm growth rates. The addition of photocatalytic cement was the most effective way to reduce biofilm growth. Lowered w/cm and subsequent increased compressive strength, were the most effective way to decrease biofilm growth for OPC. Smoothed surfaces were a less effective way of reducing biofilm growth, possibly due to the similarity in surface roughnesses tested. Typical construction practices, such as adding air entrainer and SCM replacement, were found to have negligible effect on biofilm growth. This allows for SCM replacement to reduce the amount of cement used, while retaining adequate biofilm resistance.

CHAPTER 6:

CONCLUSIONS, RECOMMENDATIONS FOR PRACTICE, AND RESEARCH NEEDS

6.1. Summary of Conclusions

Based upon field and laboratory assessments of concrete discoloration at five field sites across the state and accelerated testing in the laboratory, the following conclusions regarding biofilm growth on GDOT concrete structures can be made:

- The investigated concrete discoloration in the field was found to be due to biofilms composed of various bacteria and fungal genera, including *Pseudomonas*, *Pantoea*, *Alternaria*, *Udeniomyces*, and *Cladosporidium* spp, among others.
- After an initial lag period of a number of years (where the duration depends upon the rate of carbonation), biofilm growth occurs on concrete surfaces and proceeds to cover the surface if nutrients are available. These nutrients may be present in rainwater, paints or form oils left on the surface, or compounds in the atmosphere.
- A rapid laboratory test was developed that can recreate the appearance of biofilms using microbial communities cultured from actual sites. Biofilm coverage after 7 days of the developed accelerated test was determined to be approximately equivalent to 10 to 20 years of field exposure.
- Decreasing w/cm (and subsequently, increasing compressive strength) is the most effective way to reduce biofilm growth on OPC.

- Anatase-TiO_2 cement greatly reduces biofilm growth, due to a photocatalytic effect when exposed to ultraviolet light.
- Smoothing the concrete surface reduces biofilm growth.
- While the addition of a limited number of SCMs at moderate cement replacement levels was not found to increase biofilm growth, further research which considers a wider range of materials compositions and addition rates is necessary to validate this preliminary observation.
- Use of an acrylic paint coating was found to have little effect on biofilm growth. Further research with a wider range of materials is necessary to determine if painted coatings increase or decrease biofilm growth.

6.2. Recommendations for Practice

6.2.1. Concrete Property Modification

6.2.1.1. Lower w/cm and increase strength

Water-to-cementitious materials ratio (w/cm) is related to compressive strength in concrete, and both were found to influence biofilm growth in ordinary Portland cement concrete. This research showed that increasing OPC compressive strength by 1000 psi decreased growth by 3.4%, for normal strength (3000 psi to 6000 psi) concrete. Similarly, decreasing w/cm by 0.10 for OPC decreased growth by 5.5%, for w/cm in the range 0.3 to 0.6. This is the same relationship, because the compressive strength of the mortars tested was relatively unaffected by the aggregate. Because the compressive strength of concrete is more affected by the aggregate, a decrease in the w/cm would be a better metric to gain improvement in the cement microstructure and subsequent decrease

in biofilm growth rates. Improving either of these properties typically increases the cost of concrete in construction but should be included as a requirement for increased durability.

6.2.1.2. Photocatalytic cement

Photocatalytic cement was found to significantly decrease biofilm growth under simulated sunlight conditions. While these types of cements can be used to produce entire concrete elements, it may be more cost-effective to apply them during whitewashing to produce a Type III – Rubbed Finish. Considering that most of the growth observed is exposed to sunlight, this could be an effective deterrent to biofilm growth, although this form of application was not examined in this (or other) research, to the authors' knowledge. Further research could establish the necessary thickness and quantity of TiO2 necessary to effectively mitigate biofilm growth.

6.2.1.3. Use of different cements

SCMs were observed to either slightly decrease or have negligible effect on growth rates at the replacement levels currently specified by GDOT (less than 15% for fly ash and less than 50% for slag). More importantly, mortar tiles with SCMs did not show a decrease in surface compressive strength, unlike many OPC tiles. Using SCMs may be a cost-effective way to reduce biofilm growth rates and any deterioration, without necessarily reducing the w/cm. However, further research, examining a broader range of SCM composition and dosage rates, is necessary before recommendations for practice may be made.

Type I/II cement with 5% crushed limestone added during the manufacturing process was found to increase biofilm growth when compared to OPC. However, the 5%

LS cement also reduced 28-day mortar prism compressive strength. Considering SCMs at least as environmentally beneficial as the 5% LS cement, the use of SCMs appears to be a better way to decrease the environmental "footprint" of concrete while retaining equal biofilm growth resistance. Therefore, the use of Portland cements containing limestone is not recommended where biofilm resistance is required.

6.2.1.4. Surface Finishes

Current practice for the GDOT calls for various types of surfaces, shown in Table 6.1. The results of the variation in surface roughness showed that smoother surfaces tended to reduce growth rates, possibly due to decreased ability of fungal species and/or nutrients to adhere to the surface. The Type III – Rubbed finish creates a dense surface that should be similar to the wet-sanded tiles that decreased growth rates. Thus, the Type III – Rubbed finish is recommended to reduce biofilm growth.

However, this type of surface finish is typically expensive and/or time consuming for contractors to produce, and the Type III – Special Surface Coating is often used instead (personal communication, Myron Banks, GDOT). The type of coating material typically used for this finish (Tamms Industries Tammscoat 2725 Fine) was found to have significantly higher growth than a basic OPC mortar tile with a brushed finish (similar to a Type IV – Floated Surface Finish). An alternative to the Type III – Rubbed Finish that would create a smooth surface is a Type I or Type II formed surface finish against steel forms. Alternatively, the effect of other surface coating materials on biofilm growth could be quantified through further research, to provide additional options for resistant surface finishes.

Table 6.1 - GDOT Concrete Finishes

Surface	Finish Type
Formed	Type I—Ordinary Formed Surface Finish
	Type II—Special Formed Surface Finish
	Type III—Rubbed Finish
	Type III—Special Surface Coating Finish
Unformed	Type IV–Floated Surface Finish
	Type V–Sidewalk Finish
	Type VI–Stair Tread Finish

6.3. Research Needs

While this study discovered the microbial communities in concrete biofilms and their relation to certain concrete properties, further research is necessary to better understand the following items.

6.3.1.1. Field Verification of Results

This study examined the relationship between accelerated biofilm growth and various concrete properties. Artificial media (potato dextrose broth) and controlled climatic conditions were used to greatly increase growth rates and likely altered the composition of the biofilm colony from its natural balance. This changed some of the visual qualities of the biology growth (e.g., color and uniformity on the tile surface).

The experimental study aimed to test biofilm growth rates for accelerated aged mortars. As such, it did not examine any interaction between biofilm growth and carbonation. For example, photographic evidence from GDOT maintenance records shown in Chapter 3 indicates that there is a "lag time" between initial construction and the onset of growth. This lag time is likely due to the higher pH of an uncarbonated, freshly constructed surface.

To verify the relationship between an accelerated test and natural conditions, a long term test on concrete specimens should be performed. This could be accomplished by comparing photographs of a new structure on an annual or semi-annual basis, over a period of approximately 10 years. Alternatively, large test blocks could be produced at the Georgia Tech structures lab and monitored over a number of years.

6.3.1.2. Extended Condition Survey

The influence of environmental factors, such as precipitation amounts, average temperatures, elevation, or pollution, on biofilm growth could not be satisfactorily determined in this study. This was likely due to the limited number of sites which could be examined in depth in this preliminary study. A wider survey should be undertaken that examines a greater number of concrete structures. By observing a greater number of structures in Georgia, localized climate factors, such as influences due to air pollution, could be determined.

This wider range study should also include bridges in other states, because Georgia's climate tends to be relatively uniform in comparison to the entire range of possibilities in the country. Climatic extremes, such as hot deserts in Arizona and long winters in Minnesota, would be more likely to show an effect on biofilm growth rates.

6.3.1.3. Longer Term Biofilm Effects Test

Although the rapid biological growth did show some deterioration in compressive strength for the mortar tiles, it is unknown how this effect scales to concrete over long time periods. The rapid test may allow for the higher concentrations of organic acids or enzymes on the mortar tile than would occur in a natural environment. In a natural environment, any deleterious byproducts of microbial metabolism may be washed away

by rain before they have any adverse effects. Alternatively, periods of drought may allow for greater deterioration by allowing any slow acting enzymes and organic acids a longer time to react and deteriorate concrete. The best way to account for these unknown time factors is a long term examination of biofilm growth on concrete strength, modulus, and permeability.

6.3.1.4. Influence of SCMs

This limited study examined only one fly ash (Class C) and one slag. Both materials examined had relatively low LOI values, which may favor resistance to biofilm growth. Since these SCMs, in particular, are known to vary in their composition, further study is necessary on a broader range of fly ash and slag samples to better understand their influence of biofilm growth rates and the effect of biofilm growth on SCM-containing concrete.

Further more, the Class C fly ash was used at moderate replacement rates in which the entire portion could be hydrated by available lime. High volume fly ash replacements, as well as the use of Class F fly ash, may affect growth rates differently. High volume fly ash may not be able to hydrate completely and act more like very fine aggregate in the mix. Class F fly ash will react slower than Class C fly ash and will use more free $Ca(OH)_2$, reducing the ability of the concrete to act as a buffer to reducing pH through carbonation.

Some metakaolins naturally contain anatase TiO_2, which is currently removed from during processing. This material has the potential to produce a similar photocatalytic effect to the cement containing anatase TiO_2. Samples of naturally TiO_2

rich metakaolin should be obtained and tested at typical replacement rates to see if it has a photocatalytic effect capable of reducing biofilm growth.

6.3.1.5. Influence of Coatings

The painted coating examined in this study, and widely used in Georgia, was found to significantly increase the biofilm growth rate, when compared to an OPC of the same mix as the tile coated with paint. However, only one of the multiple products approved by GDOT was tested. A wider range study should test the effectiveness of other paints and coatings by the same accelerated test method used in this study for mortar tiles. Current test methods for these outdoor concrete paints are inadequate due to their inaccurate simulation of nutrient, water, and microbe availability.

The photocatalytic effect in TiO_2 relies on the surface properties of the material. As such, using TiO_2 cement to cast an entire structure may not be cost effective. One potential way to achieve the photocatalytic effect at a lower cost is applying the material as a "whitewash", to finish the surface of cast concrete. This should be tested to determine the minimum thickness and application necessary to reduce biofilm growth.

REFERENCES

[1] Abell, A. B., & Lange, D. A. (1998). Fracture mechanics modeling using images of fracture surfaces. *International Journal of Solids Structures, 35*, 4025-4033.

[2] Anderson IC, Campbell CD, Prosser JI. 2003. Potential bias of fungal 18s rDNA and internal transcribed spacer polymerase chain reaction primers for estimating fungal biodiversity in soil. Environmental Microbiology, 5: 36-47.

[3] Andrade, C., Sarría, J., & Alonso, C. (1999). Relative humidity in the interior of concrete exposed to natural and artificial weathering. Cement and Concrete Research, 29, 1249-1259.

[4] Avery Jr., G. B., Willey, J. D., & Kieber, R. J. (2006). Carbon isotopic characterization of dissolved organic carbon in rainwater: Terrestrial and marine influences. *Atmospheric Environment, 40*, 7539-7545.

[5] Bath, A. H., Christofi, N., Neal, C., Philip, J. C., Cave, M. R., McKinley, I. G., et al. (1987). *Trace element and microbiological studies of alkaline groundwaters in Oman, Arabian Gulf: a natural analogue for cement pore-waters*. Keyworth, United Kingdom: British Geological Survey.

[6] Bhatty, J. I., Reid, K. J., Dollimore, et al. (1988). The Derivation of Kinetic Parameters in Analysis of Portland Cement for Portlandite and Carbonate by Thermogravimetry. In *Compositional Analysis by Thermogravimetry, ASTM STP 997* (pp. 204-215).

[7] Boon, A. G. (1995). Septicity in Sewers - Causes, Consequences, and Containment. Water Science and Technology, 31(7), 237-253.

[8] Brook, J. R., Graham, L., Charland, J. P., Cheng, Y., Fan, X., Lu, G., et al. (2007). Investigation of the motor vehicle exhaust contribution to primary fine particle organic carbon in urban air. *Atmospheric Environment, 41*, 119-135.

[9] Case RJ, Boucher Y, Dahllof I, Holmstrom C, Doolittle WF, Kjelleberg S. 2007. Use of 16s rRNA and rpoB genes as molecular markers for microbial ecology studies. Applied and Environmental Microbiology, 73: 278-288.

[10] Chinga, G., Johnsen, P. O., Dougherty, R., Berli, E. L., and Walter, J. (2007). "Quantification of the 3D microstructure of SC surfaces." Journal of Microscopy, 227, 254-265.

[11] Crispim, C. A., & Gaylarde, C. C. (2005). Cyanobacteria and Biodeterioration of Cultural Heritage: A Review. Microbial Ecology, 49, 1-9.

[12]Crispim, C. A., Gaylarde, P.M., & Gaylarde, C.C. (2003). "Algal and Cyanobacterial Biofilms on Calcaeous Historic Buildings." *Current Microbiology* 46: 79-82.

[13]De Souza Saad, D., & Gaylarde, C. C. (2004). *Biodeterioration of Concrete – A Brief Review*. Paper presented at the Second International RILEM Workshop on Microbial Impact on Building Materials.

[14]DeGraef, B. e. a. (2005). A sensitive study for the visualization of bacterial weathering of concrete and stone with computerized X-ray microtomography. Science of the Total Environment, 341, 173-183.

[15]Dubosc, A., Escadeilas, G., & Blanc, P. J. (2001). Characterization of biological stains on external concrete walls and influence of concrete as underlying material. Cement and Concrete Research, 31, 1613-1617.

[16]Field, J. S., & Swain, M. V. (1993). A Simple Predictive Model for Spherical Indentation. Journal of Materials Research, 8(2), 297-306.

[17]Gaylarde, C. C., & Glyn Morton, L. H. (1999). Deteriogenic Biofilms on Buildings and their Control: a Review. Biofouling, 14(1), 59-74.

[18]Gaylarde, C. C., Ortega-Morales, B. O., & Bartolo-Perez, P. (2007). Biogenic Black Crusts on Buildings in Unpolluted Environments. . *Current Microbiology, 54*, 162-166.

[19]Gaylarde, C. C., Ribas Silva, M., & Warscheid, T. (2003). Microbial impact on building materials: an overview. Materials and Structures, 36(June 2003), 342-352.

[20]GDOT. Section 500 - Concrete Structures. The Source - Standard Specifications Retrieved 12/08/07, from http://tomcat2.dot.state.ga.us/thesource/specs/index.html

[21]Grasley, Z. C., Lange, D. A., & D'Ambrosia, M. D. (2006). Internal relative humidity and drying stress gradients in concrete. Materials and Structures, 39, 901-909.

[22]Gu, J. D., Ford, T. E., Berke, N. S., & Mitchell, R. (1998). Biodeterioration of concrete by the fungus Fusarium. *International Biodeterioration & Biodegredation, 41*, 101-109.

[23]Horvath, A., & Hendrickson, C. (1998). Steel vs. Steel-reinforced Concrete Bridges: Environmental Assessment. Journal of Infrastructure Systems, 4(3), 111-117.

[24]Housewright, M., Van Dam, T., Sutter, L., & Peterson, K. (2004). Preliminary Investigation of the Role of Bacteria in Concrete Degradation (No. RC-1444): Michigan Technological University.

[25]http://climate.engr.uga.edu/savannah/daily_2000s.html

[26]Katyal, N. K., Ahluwalia, S. C., & Parkash, R. (1999). Effect of TiO2 on the hydration of tricalcium silicate. Cement and Concrete Research, 29, 1851-1855.

[27]Kawai, K., Morinaga, T., & Tasawa, E.-I. (2000). The mechanism of concrete deterioration caused by aerobic microorganisms. Paper presented at the First International RILEM Workshop on Microbial Impact on Building Materials.

[28]Kiel, G. G., C.C. (2006). Bacterial diversity in biofilms on external surfaces of historic buildings in Porto Alegre. World Journal of Microbiology & Biotechnology, 22, 293-297.

[29]Kiel, G. G., C.C. (2007). Diversity of salt-tolerant culturable aerobic microorganisms on historic buildings in Southern Brazil. World Journal of Microbiology & Biotechnology, 23, 363-366.

[30]Kikuchi, Y., Sunada, K., Iyoda, T., Hashimoto, K., & Fujishima, A. (1997). Photocatalytic bactericidal effeect of TiO2 thin films: dynamic view of the active oxygen species responsible for the effect. Journal of Photochemistry and Photobiology A: Chemistry, 106, 51-56.

[31]Kurtis, K. E., El-Ashkar, N. H., Collins, C. L., and Naik, N. N. (2003). "Examining cement-based materials by laser scanning confocal microscopy." Cement and Concrete Composites, 25, 695-701.

[32]Lackhoff, M., Prieto, X., Nestle, N., Dehn, F., & Niessner, R. (2003). Photocatalytic activity of semiconductor-modified cement—influence of semiconductor type and cement ageing. Applied Catalysis B: Environmental, 43, 205-216.

[33]Lange, D. A., Jennings, H. M., & Shah, S. P. (1993). Analysis of surface roughness using confocal microscopy. *Journal of Materials Science, 28*, 3879-3884.

[34]Linsebigler, A. L., Guangquan, L., & Yates, J. T. (1995). Photocatalysis on TiOn Surfaces: Principles, Mechanisms, and Selected Results. Chemical Review, 95, 735-758.

[35]Lonnen, J., Kilvington, S., Kehoe, S. C., Al-Touati, F., & McGuigan, K. G. (2005). Solar and photocatalytic disinfection of protozoan, fungal, and bacterial microbes in drinking water. Water Research, 39, 877-883.

[36]Madigan, M. T., & Martinko, J. M. (2006). *Brock Biology of Microorganisms* (11th ed.). Upper Saddle River, NJ: Pearson Prentice Hall.

[37]Maness, P.-c., Smolinski, S., Blake, D. M., Huang, Z., Wolfrum, E. J., & Jacoby, W. A. (1999). Bactericidal Activity of Photocatalytic TiO2 Reaction: toward an Understanding of Its Killing Mechanism. Applied and Environmental Microbiology, 65(9), 4094-4098.

[38]Martinez, R. J., Mills, H. J., Story, S., & Sobecky, P. A. (2006). Prokaryotic diversity and metabolically active microbial populations in sediments from an active mud volcano in the Gulf of Mexico. *Environmental Microbiology, 8,* 1783-1796.

[39]Mastalerz, M., Glikson, M., & Simpson, R. (1998). Analysis of atmospheric particulate matter; application of optical and selected geochemical techniques. *International Journal of Coal Geology, 37*(1-2), 143-153.

[40]May, E. L., Pereira, F. J., Tayler, S., Sweaward, S., & Allsopp, M. R. D. Microbial Deterioration of Building Stone - a Review. *Biodeterioration Abstract, 7*(2), 109-123.

[41]Midgley, D. J., Saleeba, J. A., Stewart, M. I., Simpson, A. E., & McGee, P. A. (2007). Molecular diversity of soil basidiomycete communities in northern-central New South Wales, Australia. *Mycological Research, 111*, 370-378.

[42]Milde, K., Sand, W., Wolff, W., & Bock, E. (1983). Thiobacilli of the Corroded Concrete Walls of the Hamburg Sewer System. Journal of General Microbiology, 129, 1327-1333.

[43]Mills, H.J., Hodges, C., Wilson, K., MacDonald, I.R., and P.A. Sobecky. 2003. Microbial Diversity in Sediments Associated with Surface Breaching Gas Hydrate Mounds in the Gulf of Mexico. *FEMS Microbiology Ecology* 52:39-52.

[44]Mills, H.J., Martinez, R.J., Story, S., and P.A. Sobecky**.** 2005. Characterization of microbial community structure in Gulf of Mexico gas hydrates: a comparative analysis of DNA- and RNA-derived clone libraries. *Applied and Environmental Microbiology* 71:3235-3247.

[45]Neubert K, Mendgen K, Brinkmann H, Wirsel SGR. 2006. Only a few fungal species dominate highly diverse mycofloras associated with the common reed. Applied and Environmental Microbiology, 72: 1118-1128.

[46]Oliver, W. C., & Pharr, G. M. (2004). Measurement of hardness and elastic modulus by instrumented indentation: Advances in understanding and refinements to methodology. Journal of Materials Research, 19(1), 3-20.

[47]Papadakis, V. D. (2000). Effect of Supplementary Cementing Materials on Concrete Resistance against Carbonation and Chloride Ingress. *Cement and Concrete Research, 30*, 291-299.

[48]Parande, A. K., Muralidharan, S., & Saraswathy, V. (2005). Influence of microbiologically induced corrosion of steel embedded in ordinary Portland cement and Portland pozzolona cement. Anti-Corrosion Methods and Materials, 52(3), 148-153.

[49]Parker, C. D. (1945). The Corrosion of Concrete: 1. The isolation of a species of bacterium associated with the corrosion of concrete exposed to atmospheres

containing hydrogen sulphide. The Australian Journal of Experimental Biology and Medical Science, 23(2), 81-90.

[50]Parker, C. D. (1945). The corrosion of concrete: 2. The function of Thiobacillus-concretivorus (nov. spec.) in the corrosion of concrete exposd to atmospheres containing hydrogen sulphide. The Australian Journal of Experimental Biology and Medical Science, 23(2), 91-98.

[51]Parker, C. D., & Prisk, J. (1953). The Oxidation of Inorganic Compounds of Sulphur by various Sulphur Bacteria. Journal of General Microbiology, 8, 344-364.

[52]Pinheiro, S. M. M., & Silva, M. R. (2003). Alteration of the concrete microstructure promoted by biodeterioration mechanisms. Paper presented at the RILEM International Conference on Microbial Impact on Building Materials.

[53]Pinheiro, S. M. M., & Silva, M. R. (2004). Microorganisms and Aesthetic Biodeterioration of Concrete and Mortar. Paper presented at the Second International RILEM Workshop on Microbial Impact on Building Materials.

[54]Sand, W., & Bock, E. (1991). Biodeterioration of Mineral Materials by Microorganisms – Biogenic Sulfuric and Nitric Acid Corrosion of Concrete and Natural Stone. Geomicrobiology Journal, 9, 129-138.

[55]Shirakawa, M. A., Beech, I. B., Tapper, R., Cincotto, M. A., & Gambale, W. (2003). The development of a method to evaluate bioreceptivity of indoor mortar to fungal growth. International Biodeterioration & Biodegredation, 51, 83-92.

[56]Shirakawa, M. A., John, V. M., Cincotto, M. A., & Gambale, W. (2000). Concrete biodeterioration associated to diesel fuel oil contamination and selecting test attempt for repairing material. Paper presented at the First International RILEM Workshop on Microbial Impact on Building Materials.

[57]Shirakawa, M. A., John, V. M., Gaylarde, C. C., & Gambale, W. (2004). Mould and phototroph growth on masonry facades after repainting. Materials and Structures, 37(August-September 2004), 472-479.

[58]Sichel, C., Cara, M. d., Tello, J., Blanco, J., & Fernandez-Ibanez, P. (2007). Solar photocatalytic disinfection of agricultural pathogenic fungi: Fusarium species. Applied Catalysis B: Environmental, 74, 152-160.

[59]Taylor, H. F. W. (1997). *Cement Chemistry* (2nd ed.): Thomas Telford.

[60]Thomas D. Perry, I., Jaklepac-Ceraj, V., Zhang, X. V., Mcnamara, C. J., Polz, M. F., Martin, S. T., et al. (2005). Binding of Harvested Bacterial Exopolymers to the Surface of Calcite. Environmental Science and Technology, 39, 8770-8775.

[61]Tiago, I., Chung, A., & Verissimo, A. (2004). Bacterial Diversity in a Nonsaline Alkaline Environment: Heterotrophic Aerobic Populations. *Applied and Environmental Microbiology, 70*(12), 7378-7387.

[62]Torzilli, A. P., Sikaroodi, M., Chalkley, D., & Gillevet, P. M. (2006). A comparison of fungal communities from four salt marsh plants using automated ribosomal intergenic spacer analysis (ARISA). *Mycologia, 98*, 690-698.

[63]USGS. (2000). USGS Open-File Report 00-380: Droughts in Georgia. Retrieved 12/7/07, from http://pubs.usgs.gov/of/2000/0380/

[64]W. R Grace. WRDA 35 Product Information. Retrieved 12/19/07, from http://www.na.graceconstruction.com/concrete/download/DW-3E_4.pdf

[65]W.R. Grace. Darex AEA Product Information. Retrieved 12/19/07, from http://www.na.graceconstruction.com/concrete/download/AIR-5G_2.pdf

[66]Waterbury, J.B., & Stanier, R. Y. (1978). Patterns of Growth and Development in Pleurocapsalean Cyanobacteria. *Microbiological Reviews, 42*(1), 2-44.

[67]White, T. J., Bruns, T., Lee, S., & Taylor, J. (1990). Amplification and direct sequencing of fungal ribosomal RNA genes for phylogenetics. In M. A. Innis, D. H. Gelfland, J. J. Sninsky & T. J. White (Eds.), *PCR Protocols: A Guide to Methods and Applications* (pp. 315-321). San Diego, CA: Academic Press.

[68]Willey, J. D., Kieber, R. J., Eyman, M. S., & Avery Jr., G. B. (2000). Rainwater dissolved organic carbon: Concentrations and global flux. *Global biogeochemical cycles, 14*(1), 139-148.

[69]Williams, C. (March 12, 1999). Ramp opening a turn for better; Cumberland Boulevard link to I-75 --- completed a month early --- will aid commuters, developers. Atlanta Journal Constitution.

[70]Winslow, D. N. (1984). A Rockwell Hardness Test for Concrete. Cement, Concrete, and Aggregates, 6(2), 137-141.

[71]Woese CR. 1987. Bacterial Evolution. Microbiological Reviews, 51: 221-271.

APPENDIX A.TILE IMAGES

The following tiles in Figure A.1 through Figure A.105 have all been evaluated for biofilm growth according to the test method described in Chapter 4. Each tile was exposed to its respective microbial communities or pure culture for 7 days, using 20% potato dextrose broth as media and air dried for 48 hours before imaging.

Figure A.1 - Tile type A after exposure to Atlanta microbial community

Figure A.2 - Tile type B after exposure to Atlanta microbial community

Figure A.3 - Tile type C after exposure to Atlanta microbial community

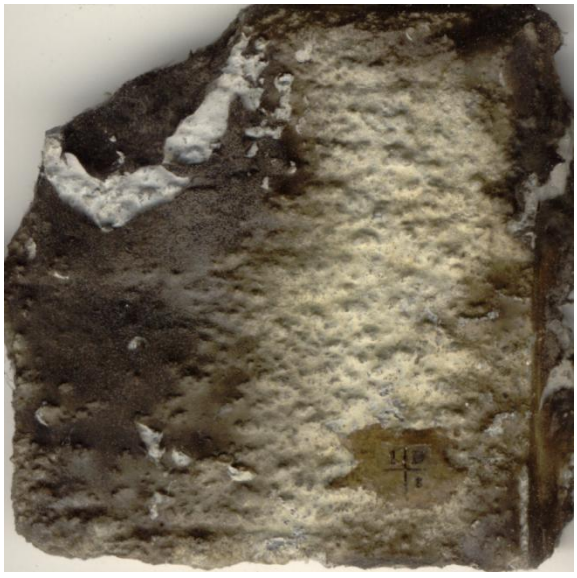

Figure A.4 - Tile type D after exposure to Atlanta microbial community

Figure A.5 - Tile type G after exposure to Atlanta microbial community

Figure A.6 - Tile type K after exposure to Atlanta microbial community

Figure A.7 - Tile type MK after exposure to Atlanta microbial community

Figure A.8 - Tile type M after exposure to Atlanta microbial community

Figure A.9 - Tile type N after exposure to Atlanta microbial community

Figure A.10 - Tile type O after exposure to Atlanta microbial community

Figure A.11 - Tile type P after exposure to Atlanta microbial community

Figure A.12 - Tile type Q after exposure to Atlanta microbial community

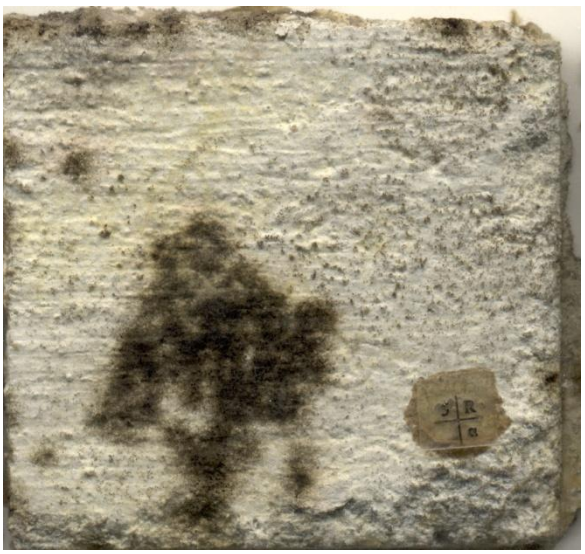

Figure A.13 - Tile type R after exposure to Atlanta microbial community

Figure A.14 - Tile type S after exposure to Atlanta microbial community

Figure A.15 - Tile type T after exposure to Atlanta microbial community

Figure A.16 - Tile type U after exposure to Atlanta microbial community

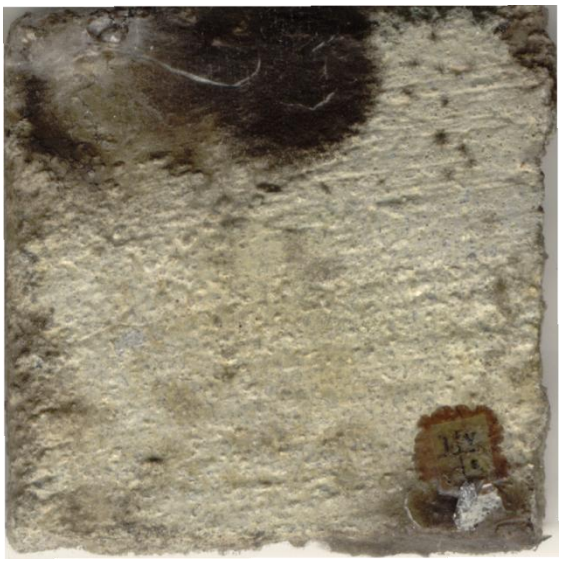

Figure A.17 - Tile type V after exposure to Atlanta microbial community

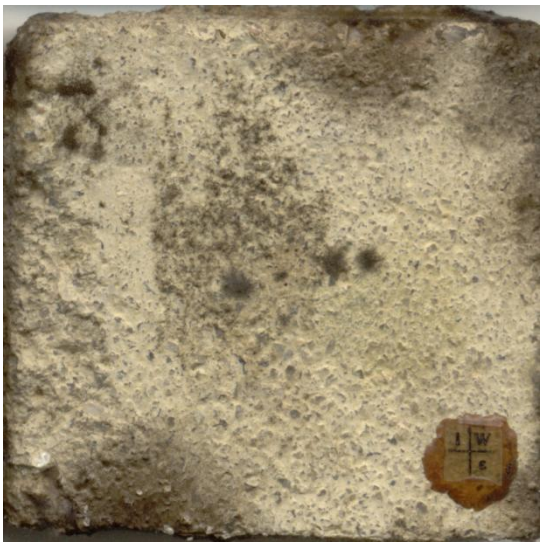

Figure A.18 - Tile type W after exposure to Atlanta microbial community

Figure A.19 - Tile type X after exposure to Atlanta microbial community

Figure A.20 - Tile type Y after exposure to Atlanta microbial community

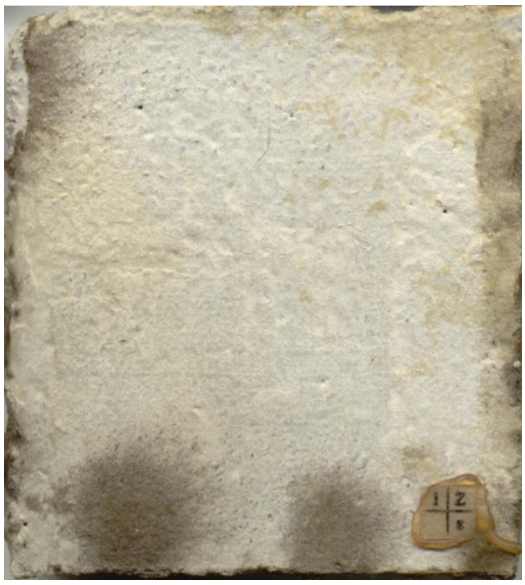

Figure A.21 - Tile type Z after exposure to Atlanta microbial community

Figure A.22 - Tile type A after exposure to Gainesville microbial community

Figure A.23 - Tile type B after exposure to Gainesville microbial community

Figure A.24 - Tile type C after exposure to Gainesville microbial community

Figure A.25 - Tile type D after exposure to Gainesville microbial community

Figure A.26 - Tile type G after exposure to Gainesville microbial community

Figure A.27 - Tile type K after exposure to Gainesville microbial community

Figure A.28 - Tile type MK after exposure to Gainesville microbial community

Figure A.29 - Tile type M after exposure to Gainesville microbial community

Figure A.30 - Tile type N after exposure to Gainesville microbial community

Figure A.31 - Tile type O after exposure to Gainesville microbial community

Figure A.32 - Tile type P after exposure to Gainesville microbial community

Figure A.33 - Tile type Q after exposure to Gainesville microbial community

Figure A.34 - Tile type R after exposure to Gainesville microbial community

Figure A.35 - Tile type S after exposure to Gainesville microbial community

Figure A.36 - Tile type T after exposure to Gainesville microbial community

Figure A.37 - Tile type U after exposure to Gainesville microbial community

Figure A.38 - Tile type V after exposure to Gainesville microbial community

Figure A.39 - Tile type W after exposure to Gainesville microbial community

Figure A.40 - Tile type X after exposure to Gainesville microbial community

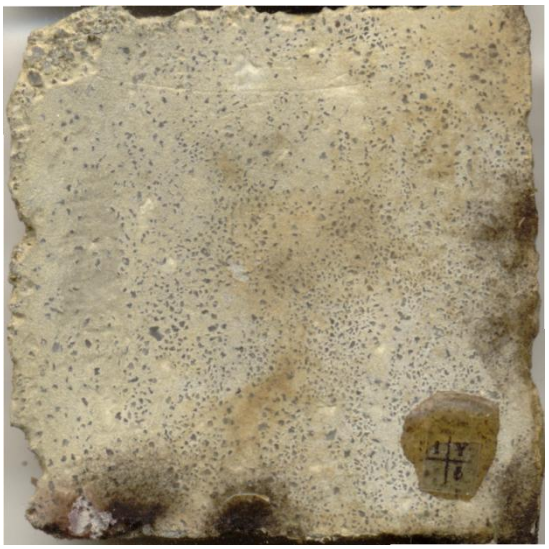

Figure A.41 - Tile type Y after exposure to Gainesville microbial community

Figure A.42 - Tile type Z after exposure to Gainesville microbial community

Figure A.43 - Tile type A after exposure to LaGrange microbial community

Figure A.44 - Tile type B after exposure to LaGrange microbial community

Figure A.45 - Tile type C after exposure to LaGrange microbial community

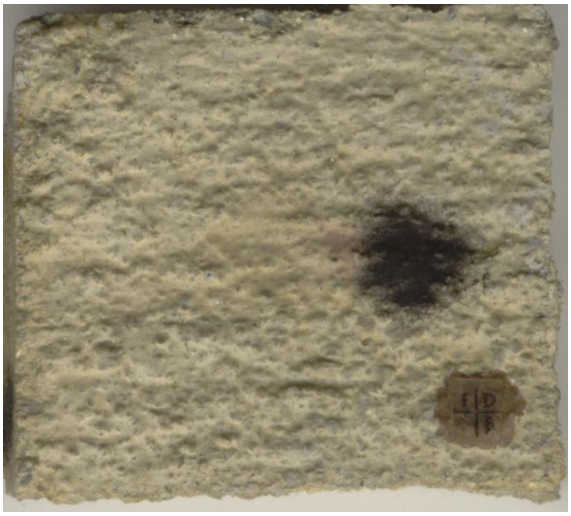

Figure A.46 - Tile type D after exposure to LaGrange microbial community

Figure A.47 - Tile type G after exposure to LaGrange microbial community

Figure A.48 - Tile type K after exposure to LaGrange microbial community

Figure A.49 - Tile type MK after exposure to LaGrange microbial community

Figure A.50 - Tile type M after exposure to LaGrange microbial community

Figure A.51 - Tile type N after exposure to LaGrange microbial community

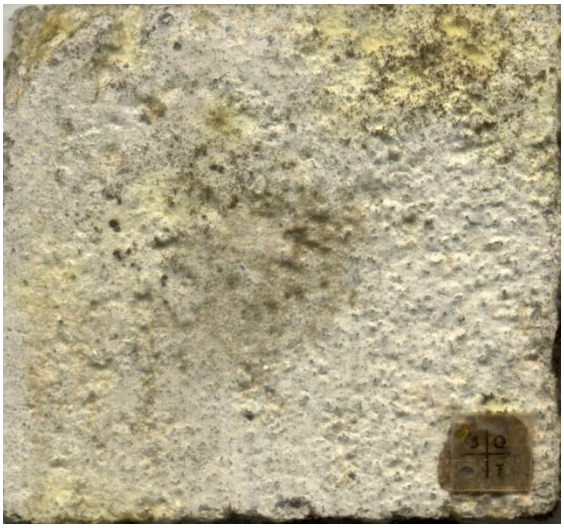

Figure A.52 - Tile type O after exposure to LaGrange microbial community

Figure A.53 - Tile type P after exposure to LaGrange microbial community

Figure A.54 - Tile type Q after exposure to LaGrange microbial community

Figure A.55 - Tile type R after exposure to LaGrange microbial community

Figure A.56 - Tile type S after exposure to LaGrange microbial community

Figure A.57 - Tile type T after exposure to LaGrange microbial community

Figure A.58 - Tile type U after exposure to LaGrange microbial community

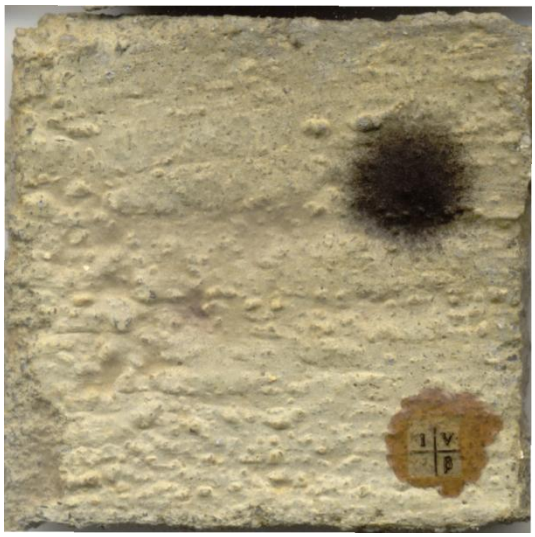

Figure A.59 - Tile type V after exposure to LaGrange microbial community

Figure A.60 - Tile type W after exposure to LaGrange microbial community

Figure A.61 - Tile type X after exposure to LaGrange microbial community

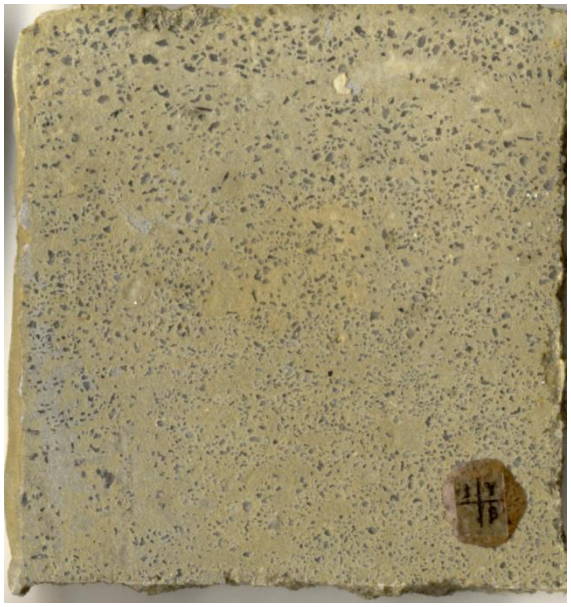

Figure A.62 - Tile type Y after exposure to LaGrange microbial community

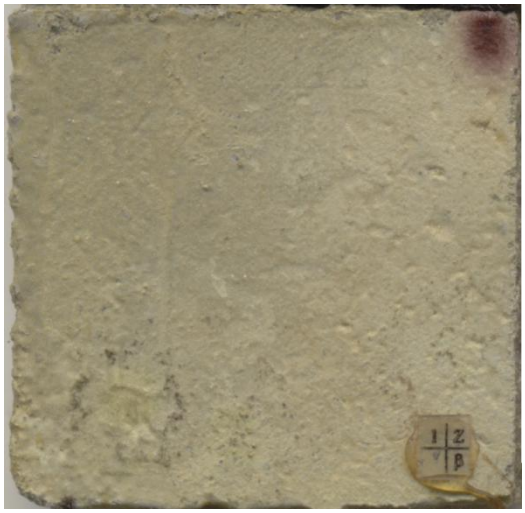

Figure A.63 - Tile type Z after exposure to LaGrange microbial community

Figure A.64 - Tile type A after exposure to Savannah microbial community

Figure A.65 - Tile type B after exposure to Savannah microbial community

Figure A.66 - Tile type C after exposure to Savannah microbial community

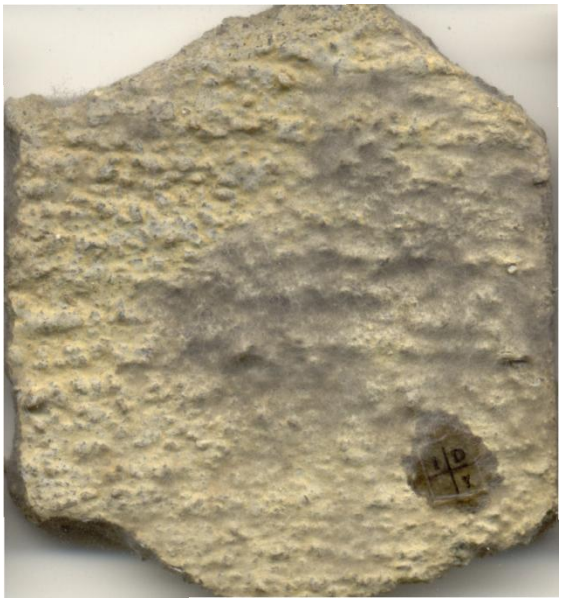

Figure A.67 - Tile type D after exposure to Savannah microbial community

Figure A.68 - Tile type G after exposure to Savannah microbial community

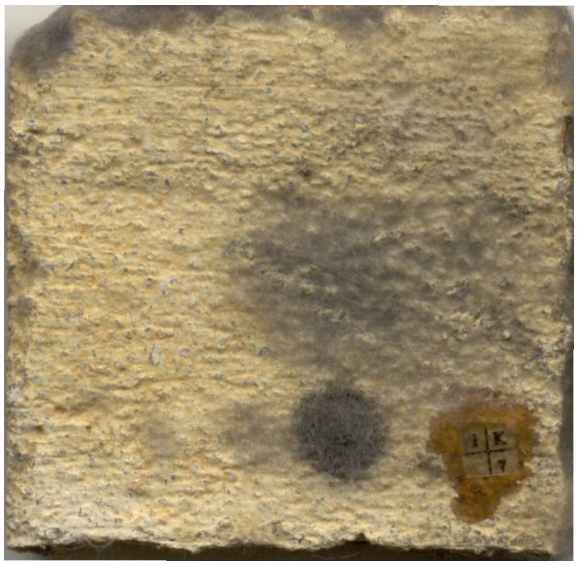

Figure A.69 - Tile type K after exposure to Savannah microbial community

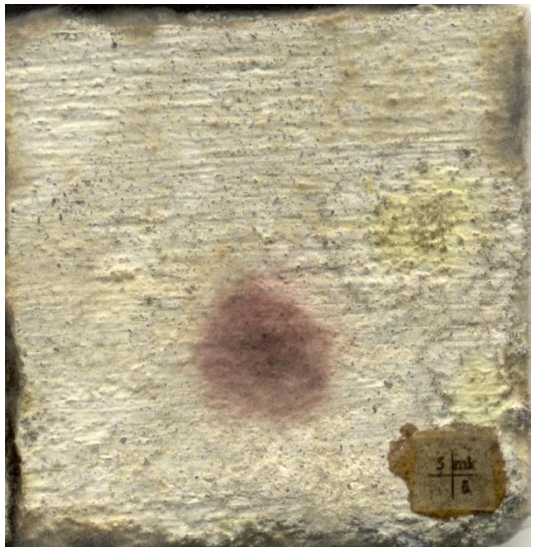

Figure A.70 - Tile type MK after exposure to Savannah microbial community

Figure A.71 - Tile type M after exposure to Savannah microbial community

Figure A.72 - Tile type N after exposure to Savannah microbial community

Figure A.73 - Tile type O after exposure to Savannah microbial community

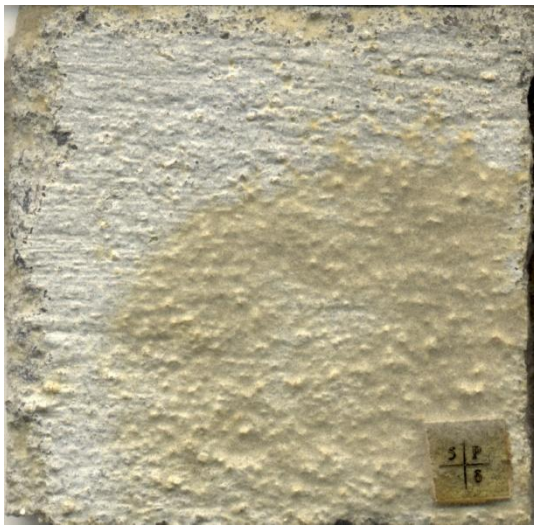

Figure A.74 - Tile type P after exposure to Savannah microbial community

Figure A.75 - Tile type Q after exposure to Savannah microbial community

Figure A.76 - Tile type R after exposure to Savannah microbial community

Figure A.77 - Tile type S after exposure to Savannah microbial community

Figure A.78 - Tile type T after exposure to Savannah microbial community

Figure A.79 - Tile type U after exposure to Savannah microbial community

Figure A.80 - Tile type V after exposure to Savannah microbial community

Figure A.81 - Tile type W after exposure to Savannah microbial community

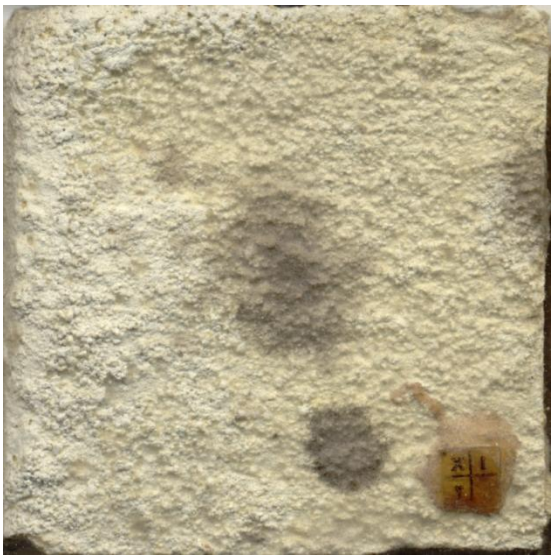

Figure A.82 - Tile type X after exposure to Savannah microbial community

Figure A.83 - Tile type Y after exposure to Savannah microbial community

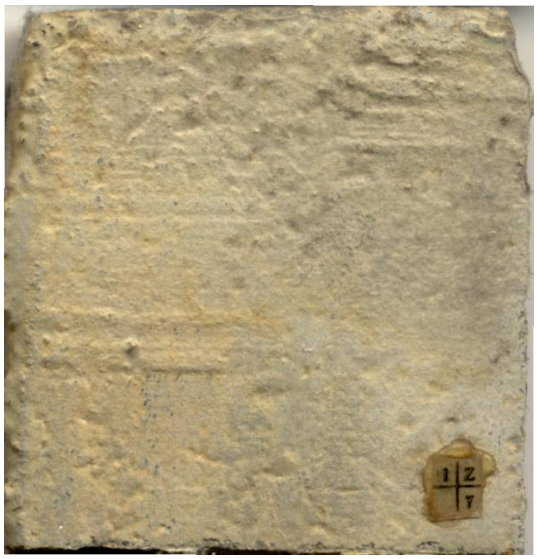

Figure A.84 - Tile type Z after exposure to Savannah microbial community

Figure A.85 - Tile type A after exposure to *Trichoderma viride* pure culture

Figure A.86 - Tile type B after exposure to *Trichoderma viride* pure culture

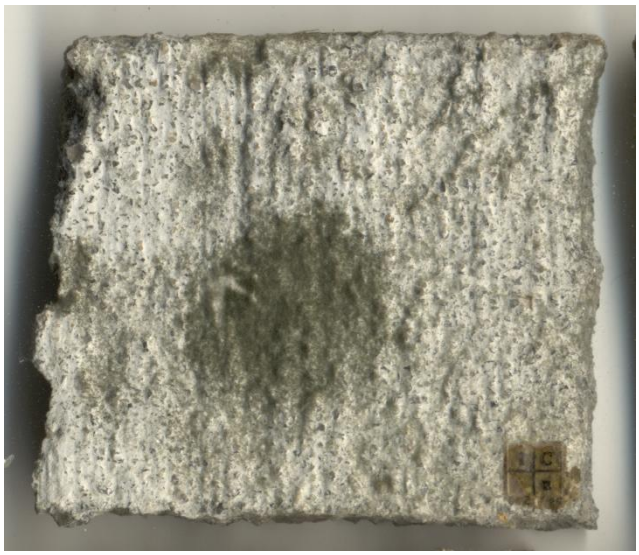

Figure A.87 - Tile type C after exposure to *Trichoderma viride* pure culture

Figure A.88 - Tile type D after exposure to *Trichoderma viride* pure culture

Figure A.89 - Tile type G after exposure to *Trichoderma viride* pure culture

Figure A.90 - Tile type K after exposure to *Trichoderma viride* pure culture

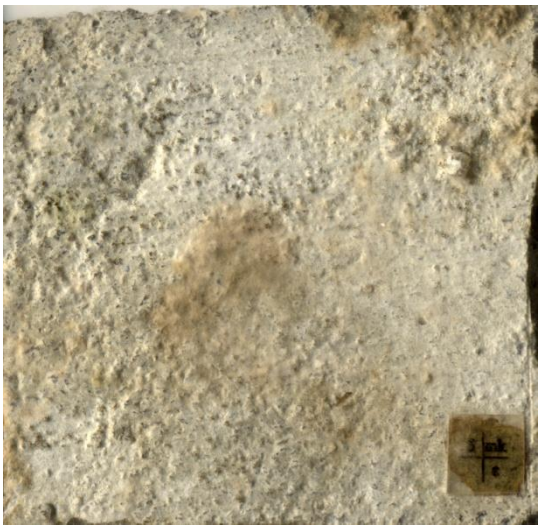

Figure A.91 - Tile type MK after exposure to *Trichoderma viride* pure culture

Figure A.92 - Tile type M after exposure to *Trichoderma viride* pure culture

Figure A.93 - Tile type N after exposure to *Trichoderma viride* pure culture

Figure A.94 - Tile type O after exposure to *Trichoderma viride* pure culture

Figure A.95 - Tile type P after exposure to *Trichoderma viride* pure culture

Figure A.96 - Tile type Q after exposure to *Trichoderma viride* pure culture

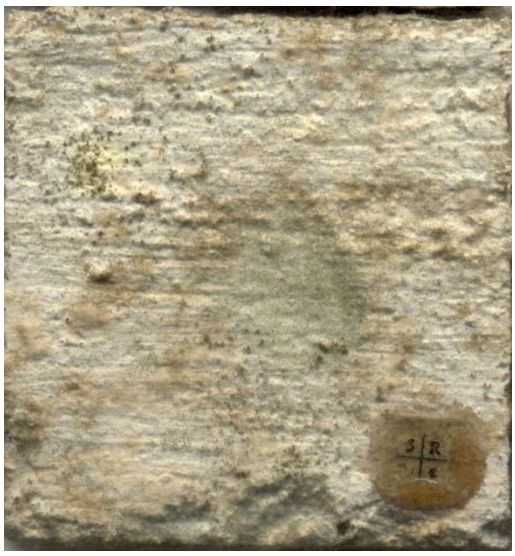

Figure A.97 - Tile type R after exposure to *Trichoderma viride* pure culture

Figure A.98 - Tile type S after exposure to *Trichoderma viride* pure culture

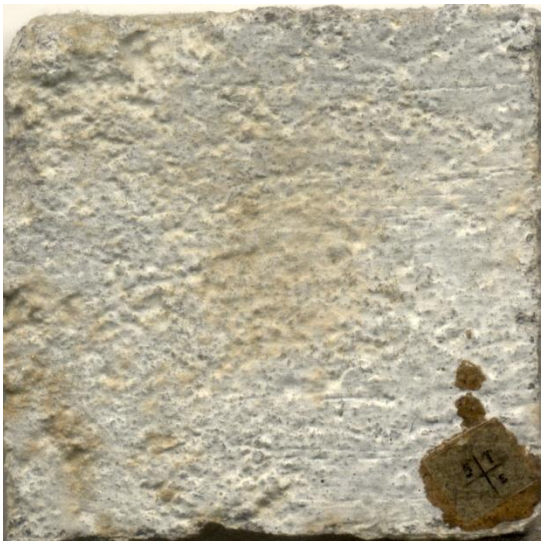

Figure A.99 - Tile type T after exposure to *Trichoderma viride* pure culture

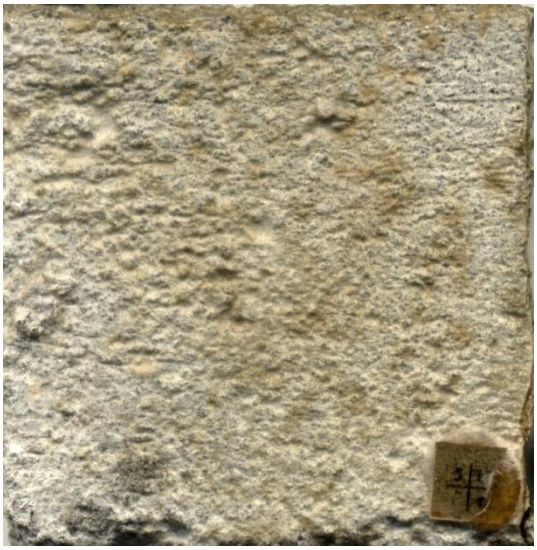

Figure A.100 - Tile type U after exposure to *Trichoderma viride* pure culture

Figure A.101 - Tile type V after exposure to *Trichoderma viride* pure culture

Figure A.102 - Tile type W after exposure to *Trichoderma viride* pure culture

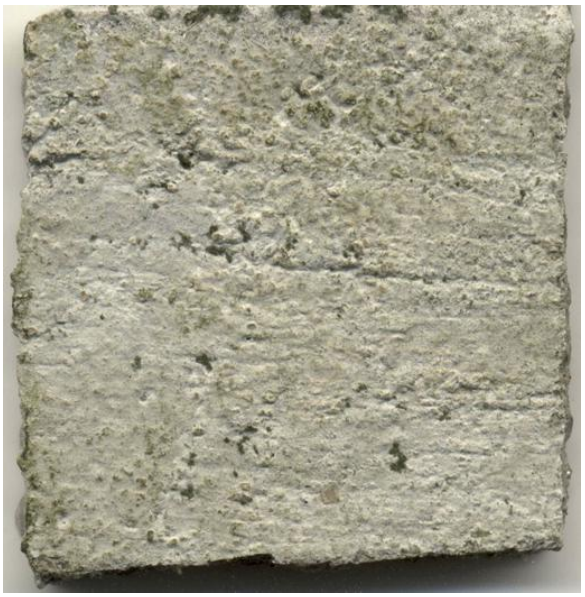

Figure A.103 - Tile type X after exposure to *Trichoderma viride* pure culture

Figure A.104 - Tile type Y after exposure to *Trichoderma viride* pure culture

Figure A.105 - Tile type Z after exposure to *Trichoderma viride* pure culture